CHARACTERISATION OF HAEMODYNAMIC AND VASCULAR DYSFUNCTION IN BICUSPID AORTIC VALVE DISEASE USING ADVANCED CARDIOVASCULAR MAGNETIC RESONANCE IMAGING TECHNIQUES

Bicuspid aortic valve disease – on the cusp of a new understanding

Malenka Mona Bissell BM, MRCPCH

Merton College

Division of Cardiovascular Medicine, Radcliffe Department of Medicine

University of Oxford

THESIS SUBMITTED FOR THE DEGREE OF DOCTOR IN PHILOSOPHY

TRINITY TERM 2015

DEDICATION

I dedicate this thesis to my daughter Leonie Ella Bissell who has been mesmerised by aortic flow patterns since 6 weeks of age.

ACKNOWLEDGEMENTS

I am immensely grateful to my academic supervisors, Prof Saul Myerson and Prof Stefan Neubauer, who gave me the freedom to develop my own interests in research, especially paediatric research, but provided guidance, time, wisdom and support whenever needed. Thank you for providing such an engaging and stimulating research environment in OCMR.

I am indebted to our collaborators from Prof Markl's group, especially Dr Alex Barker without whom I would not have established 4D flow CMR in OCMR. The frequent collaborator visits first in Freiburg and later in Chicago have been an inspiration every time and I will never forget the warm welcome and supportive collaboration I received.

I would also like to thank Dr Alex Pitcher and Jane Frances for teaching me CMR and Alison Fletcher and Jen Bryant for guiding me through the world of paediatric CMR.

I am grateful for the CMR scanning support I received from Anne Davies (otherwise I would still be scanning family members!) and the endless hours Steve Knight spent sitting with me during pregnancy allowing me to continue patient recruitment and scanning.

Many fellows have left OCMR during my time and new ones arrived all without whom OCMR would not be the same; I have been immeasurably fortunate to have developed amazing friendships with many. I am especially grateful for the support received from our physicists Dr Aaron Hess and Luca Biasiolli and the other 4D flow

fellows Dr Margaret Loudon and Dr Victoria Stoll with whom I shared endless 4D flow scans, analysis hours and cups of tea.

I am also indebted to the staff in the OCMR and CCRF: Carla Cascone, Sharon Dash, Cate Wheatley, Pauline Collier, Lucasz Owsiak, Karen Whatley, Christine Saward, Hayley Harvey, Joanna Searcey, Judith Delos Santos, Kathryn Lacey, Rachel Given, Kate Grove, Heidi Crook, Emma Heaton, Sophia Bell – all of whom helped with various admin aspects of my work along the way.

Thank you also to the two medical students Steffan Glaze and Abhishek Oswal, who I supervised. Their enthusiasm in learning inspired me to develop my passion for teaching and fostering independent thinking.

I am immensely grateful to my husband Gordon who has been there every step of the way and who is now probably a non-medical expert in bicuspid aortic valve disease, to my mother who has always been there with empathy from the far and to my amazing little girl Leonie, who spent many hours asleep in a sling while I was finishing 4D flow analysis.

My biggest thanks go to all patients and their families who have been involved in this study, especially all the paediatric participants who have helped shaping this study.

DECLARATION

I declare that the work presented in this thesis is my own. I recruited and imaged all patients and healthy volunteers and the majority of family members in this study. I analysed all CMR scans, interpreted the data, carried out the statistics and wrote the script. Our collaborators, especially Dr Alex Barker, have provided advice on the methodological aspects and post-processing tools. Dr Aaron Hess has programmed the planar fluid circulation analysis program and Dr Luca Biasiolli has programmed the MRSD and PWV analysis programme. Ms Anne Davis has helped to acquire some of the CMR data during family study visits with multiple CMR scans at the same time. Dr Margaret Loudon has performed the echocardiograms for children age 6 and younger and claustrophobic adult participants. Dr Margaret Loudon also helped with the peak flow and left ventricular volume analysis. Mr Steffan Glaze has as part of his Final Honours Project contributed to the wall shear stress analysis by drawing the circles in the flow tool. Mr Abhishek Oswal helped with the distensibility and pulse wave velocity analysis of the family members. Blood samples were sent for external analysis. Mrs Karen Whatley, Mrs Christine Saward and Mrs Rachel Given have entered the study visit demographics into the OXBAV database. I am very grateful to all these individuals, the co-investigators, our collaborating partners and especially to all study participants and their families.

I received a clinical research training fellowship from the British Heart Foundation for this study.

PAPERS ARISING FROM THIS WORK

1. Aortic dilation in bicuspid aortic valve disease: flow pattern is a major contributor and differs with valve fusion type. Bissell MM, Hess AT, Biasiolli L, Glaze SJ, Loudon M, Pitcher A, Davis A, Prendergast B, Markl M, Barker AJ, Neubauer S, Myerson SG.; Circ Cardiovasc Imaging. 2013 Jul 1;6(4):499-507 (This publication includes the data from chapter 3, manuscripts for the data from chapter 4 and 5 are in preparation).

2. 4D flow cardiovascular magnetic resonance consensus statement. Dyverfeldt P* Bissell M*, Barker AJ, Bolger AF, Carlhäll CJ, Ebbers T, Francios CJ, Frydrychowicz A, Geiger J, Giese D, Hope MD, Kilner PJ, Kozerke S, Myerson S, Neubauer S, Wieben O, Markl M.; J Cardiovasc Magn Reson. 2015 Aug 10;17(1):72.; * authors contributed equally

3. Bicuspid Aortic Valve: Identifying Knowledge Gaps and Rising to the Challenge. From the International Bicuspid Aortic Valve Consortium (BAVCon). Michelena HI, Prakash SK, Della Corte A, Bissell MM, Anavekar N, Bossee Y, Limongelli G, Bossone E, Benson DW, Lancellotti P, Isselbacher EM, Enriquez-Sarano M, Sundt III TM, Pibarot P, Evangelista A, Milewicz DM, Body SC, on behalf of the BAVCon investigators; Circulation 2014 Jun 24;129(25):2691-704.

4. Aortic 4D flow: Quantification of signal-to-noise ratio as a function of field strength and contrast enhancement for 1.5T, 3T, and 7T.Hess AT, Bissell

MM, Ntusi NA, Lewis AJ, Tunnicliffe EM, Greiser A, Stalder AF, Francis JM, Myerson SG, Neubauer S, Robson MD; Magn Reson Med. 2015 May;73(5):1864-71

5. Aortic relative pressure components derived from 4D flow cardiovascular magnetic resonance. Lamata P, Pitcher A, , Krittian S, Nordsletten D, Bissell MM, Cassar TE, Barker AJ, Markl M, Neubauer S, Smith N; Magn Reson Med. 2014 Oct;72(4):1162-9

6. 4D Flow MRI in aortic valve disease demonstrates altered distribution of aortic blood flow helicity. Lorenz R, Bock J, Barker A, von Knobelsdorff-Brenkenhoff F, Bissell MM, Korvink JG, Wallis W and Markl M; Magn Reson Med. 2014 Apr;71(4):1542-53

ABSTRACTS ARISING FROM THIS WORK

Oral presentations at conferences

1. Bissell MM et al.; Improvement of haemodynamic flow abnormalities after aortic valve replacement in bicuspid aortic valve disease. Cardiol Young May 2015 **Young investigator award winner**

2. Bissell MM et al.; Cusp fusion pattern – a predictor for aortic dilation in bicuspid aortic valve disease. British Heart Valve Society Annual Meeting (2013) **Young investigator award finalist**

3. Bissell MM et al.; Bicuspid Aortic Valve Disease: Effect of Cusp Fusion Pattern on Aortic Flow Abnormalities. Society of Heart Valve disease Biannual Meeting, Venice (2013)

4. Bissell MM et al.; Aortic flow abnormalities contribute to the aortopathy in bicuspid aortic valve disease. Cardiol Young 2013, 23 (S1): O10-7

5. Bissell MM et al.; Cusp fusion pattern in bicuspid aortic valve disease predicts severity of aortic flow abnormalities. Journal of Cardiovascular Magnetic Resonance 2013, 15(Suppl 1):O69 (30 January 2013) **Early Career award – clinical finalist**

6. Bissell MM et al.; Familial Bicuspid Aortic Valve Disease Frequently Shows Discordance of Leaflet Fusion Pattern and Extent: Insights from Cardiovascular Magnetic Resonance. Circulation. 2012;126:A16060

7. Bissell MM et al.; Partial leaflet fusion forms part of familial bicuspid aortic valve disease. British Congenital Cardiac Association annual meeting (BCCA); Belfast (2012) **Young investigator award finalist**

8. Bissell MM et al.; Bicuspid aortic valve disease: Helical flow patterns in the ascending aorta; Bissell MM, Pitcher A, Prendergast B, Markl M, Myerson SG, Neubauer S. Paediatricians with Expertise in Cardiology Specialist Interest Group (PECSIG) Meeting, Oxford (2012)

9. Gedicke MM et al.; Aortic flow patterns in bicuspid aortic valve disease visualised with 4D flow imaging. Arch Dis Child 2012;97:Suppl 1 A129-A130doi:10.1136/archdischild-2012-301885.309

10. Gedicke MM et al.; Flow patterns in bicuspid aortic valve disease. British Congenital Cardiac Association annual meeting (BCCA); London (2011) **Young investigator award winner**

POSTERS AT CONFERENCES

1. Bissell MM et al.; Haemodynamic flow abnormalities in bicuspid aortic valve disease improve with aortic valve replacement. Journal of Cardiovascular Magnetic Resonance 2015, 17(Suppl 1):P330 (3 February 2015)

2. Bissell MM et al.; Pulmonary artery dilation with a bicuspid pulmonary valve – similar haemodynamic flow patterns to bicuspid aortic valve disease. British Congenital Cardiac Association annual meeting (BCCA); Edinburgh (2013)

3. Bissell MM et al.; Is cusp fusion pattern a predictor for aortic dilation in bicuspid aortic valve disease? – haemodynamic insights. British Congenital Cardiac Association annual meeting (BCCA); Edinburgh (2013)

4. Bissell MM et al.; Severity of aortic flow abnormalities in bicuspid aortic valve disease is predicted by cusp fusion pattern. British Cardiovascular Society (BCS); London 2013

5. Bissell MM et al.; Aortic valve replacement reduces helical flow pattern in bicuspid aortic valve disease. British Congenital Cardiac Association annual meeting (BCCA); Belfast (2012)

ABBREVIATIONS

4D	4 dimensional
AA	Ascending Aorta
AHA	American heart association
AP-BAV	Anterior-posterior BAV
AVR	Aortic valve replacement
BAV	Bicuspid aortic valve disease
BSA	Body surface area
cm	Centimetre
CMR	Cardiovascular Magnetic Resonance
CT	Computed tomography
DDA	Distal descending aorta
ECG	Electrocardiogram
EDTA	Ethylenediaminetetraacetic acid
ESC	European Society of Cardiology
HV	Healthy volunteer
LN-BAV	Left-non coronary cusp fusion pattern BAV
LP	Left posterior
LV	Left ventricle
m	Metre
mm	Millimetre
MMP	Matrix Metalloproteinase
MRI	Magnetic Resonance Imaging
MRSD	Maximum rate of systolic distension
ms	Millisecond
N	Newton
OCMR	Oxford centre for clinical magnetic resonance research

p	Probability
PDA	Proximal descending aorta
PWV	Pulse wave velocity
RA	Right anterior
RL-BAV	Right-left coronary cusp fusion pattern BAV
RN-BAV	Right-non coronary cusp fusion pattern BAV
s	second
SD	Standard deviation
SSFP	Steady-state free precession
STJ	Sinotubular junction
WSS	Wall shear stress
WSS_{syst}	Circumferentially averages systolic wall shear stress

TABLE OF CONTENTS

THESIS ABSTRACT

Bicuspid aortic valve disease (BAV) is known to be heritable and often shows a concomitant aortopathy with increased risk of aortic dissection. This may also be present in family members. The underlying pathophysiology was largely believed to be an intrinsic aortopathy. However, recent advances in cardiovascular magnetic resonance imaging now allow in-depth haemodynamic and functional assessment of the aorta to further delineate the underlying pathophysiology.

This thesis explored the association of haemodynamic and functional aortic changes with aortic dilation in BAV patients, first degree relatives and healthy volunteers. Patients with a bicuspid aortic valve were found to have an abnormal degree of helical flow in the ascending aorta with predominantly right-handed helical flow. Compared to healthy volunteers patients with a bicuspid aortic valve had larger ascending aortas, higher rotational (helical) flow, systolic flow angle and systolic wall shear stress. There were also differences between the cusp fusion patterns in BAV, with right-non coronary cusp fusion showing more severe flow and aortic abnormalities than those with a right-left coronary cusp fusion pattern: higher rotational flow, higher in-plane wall sheer stress and larger aortas respectively. BAV patients with normal flow patterns had similar aortic dimensions and wall shear stress to healthy volunteers and younger BAV patients showed abnormal flow patterns but no aortic dilation, both further supporting the importance of flow pattern in the aetiology of aortic dilation.

However, aortic function measures (distensibility, aortic strain and pulse wave velocity) were similar between healthy volunteers, patients with a bicuspid aortic valve and first degree relatives with a tricuspid aortic valve.

Aortic valve replacement (AVR) significantly changed the ascending aortic flow pattern in patients with a bicuspid aortic valve. The majority of patients with mechanical AVR or Ross procedure showed normal flow patterns with near normal rotational flow values post operatively and reduced in-plane wall shear stress. By contrast, all subjects with bioprosthetic AVR had residual abnormal helical flow patterns (mainly marked right-handed helical flow), with similar rotational flow values to native BAV. Wall shear stress post-bioprosthetic AVR showed a similar pattern.

These findings point towards the importance of haemodynamic factors in the bicuspid aortic valve aortopathy rather than additional haemodynamic-independent mechanisms. Haemodynamic classification may allow better risk prediction and selection of patients for earlier surgical intervention. Changes in abnormal flow pattern after valve replacement could have important implications for future aortic growth, and may influence the future choice of prosthetic valves.

1 ST CHAPTER: GENERAL INTRODUCTION

1.1 BICUSPID AORTIC VALVE DISEASE

Bicuspid aortic valve disease (BAV) is the most common congenital heart disease with a prevalence of around 1-2% in the general population and is more common in males than females (1). A normal tricuspid aortic valve is formed of three semilunar cusps, which originate from the endocardial cushions in the embryological outflow tract.

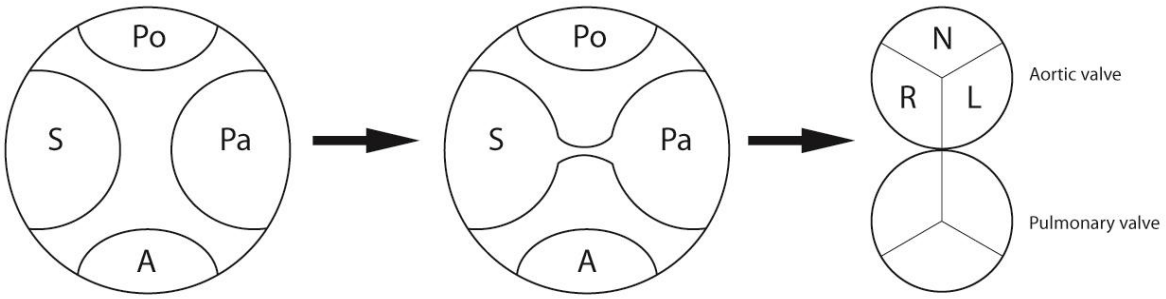

Figure 1-1: Embryological development of the tricuspid aortic valve: 4 endocardial cushions: S = septal, Pa = parietal, A = anterior, Po = posterior

A bicuspid aortic valve forms during embryological development through a fusion or lack of separation of these endocardial cushions, leading to two uneven sized cusps (2). The bicuspid aortic valve is more prone to aortic stenosis and regurgitation during a patient's lifetime. Recent retrospective studies estimate that up to 25% of adult patients experience serious complications over 10 years of follow up (3) creating a considerable health burden. The average age for aortic valve replacement in bicuspid aortic valve disease is around 40 ±20 years. (4). Even throughout childhood approximately 3-10% of children with bicuspid aortic valves already need treatment (5) with severe aortic stenosis in some cases already occurring in utero requiring fetal interventions (4).

1.1.1 Genetics in bicuspid aortic valve disease

Bicuspid aortic valve disease is known to cluster in some families (6,7) but the underlying genetic factors are still largely unknown. In family screening studies using echocardiography, only 9-25% of family members were found to have a bicuspid aortic valve (6,8,9). This suggests either an autosomal dominant inheritance pattern with reduced penetrance (not all family members have detectable signs and symptoms of the disease) or a polygenetic background. Genes that have been identified in a small number of individuals include NOTCH1, ACTA2, TGFBR2, TGFB1 and KCNJ2 (10) but no universal "BAV gene" has been found so far. This favours the polygenetic theory where an interplay of several genes causes a bicuspid aortic valve. Due to the increased incidence in BAV in some family members many clinicians will screen first degree family members but this is contentious and is not done routinely in the UK and Europe (11). To date, all family screening data was published using echocardiography. I therefore decided to use cardiovascular magnetic resonance imaging to assess whether this imaging modality would have a higher pick-up rate of a BAV in family members.

1.1.2 Leaflet fusion pattern in bicuspid aortic valve disease

Recent animal studies have suggested that BAV may in fact represent at least two different entities, defined on the basis of pattern of leaflet fusion. Bicuspid aortic valve with a right-left coronary leaflet fusion pattern (RL-BAV) is the more common variant (70% of cases) and is almost always the fusion pattern seen when BAV co-exists with structural vascular anomalies, such as coarctation of the aorta or Turner syndrome (12). It is also the fusion pattern associated with the aortic root phenotype (involving dilation of the aortic sinuses at

the ‘root’ of the aorta only) (13,14). Furthermore, inbred Syrian hamsters only display this fusion pattern (2). Right-non-coronary leaflet fusion pattern (RN-BAV) may be a risk factor for progressive valve dysfunction, with a higher rate of intervention demonstrated in a retrospective study of 310 children (15). In animal models this fusion pattern is specifically associated with abnormalities of eNOS signalling in mice and with abnormal endothelial function in humans (2). Left-non-coronary leaflet fusion (LN-BAV) is extremely rare (<1%) (16).

As part of the family screening element of this thesis I aimed to investigate the inheritance of fusion patterns among human families, to assess whether different fusion patterns were distinct genetic entities in humans, too.

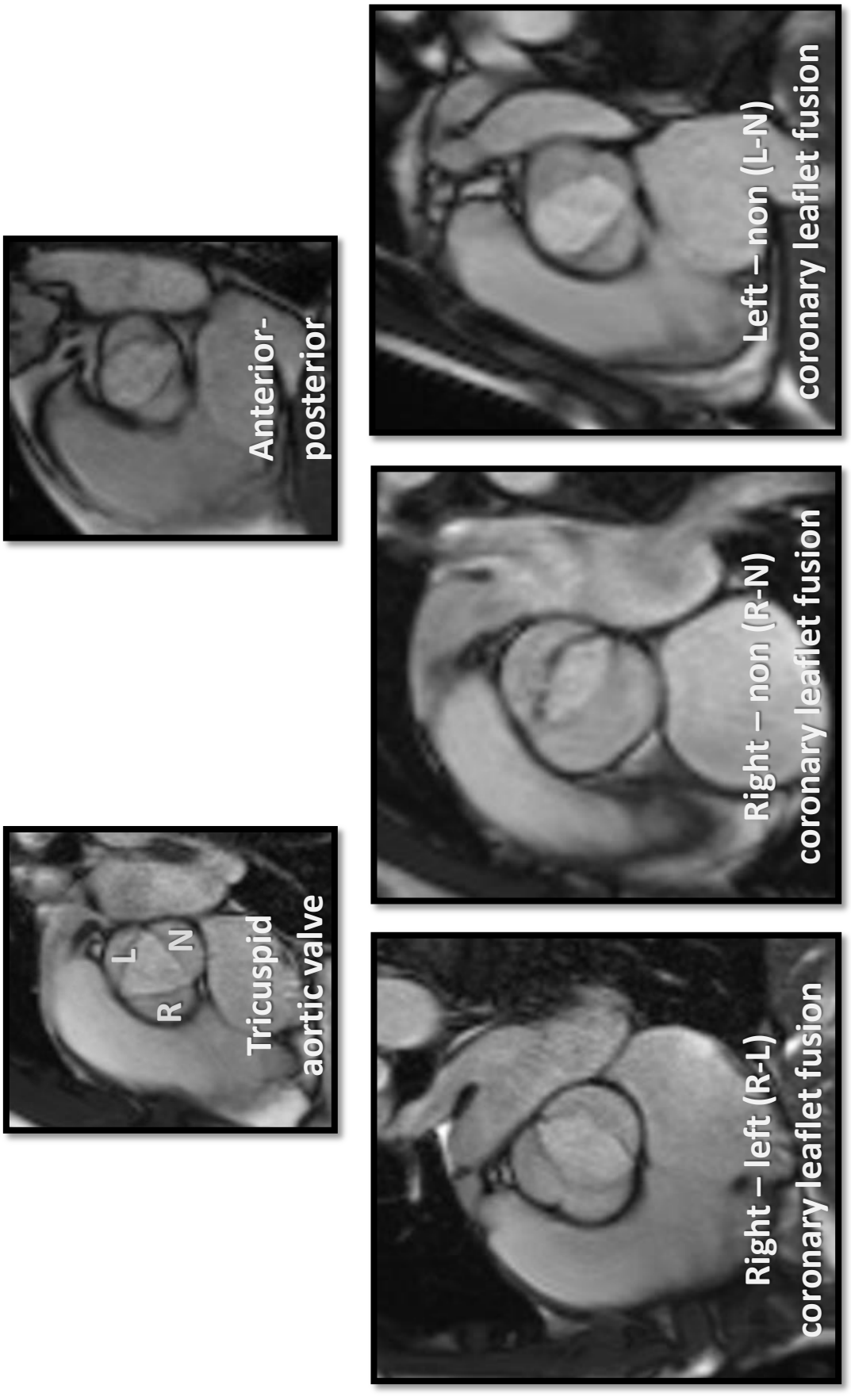

Figure 1-2: Different fusion pattern in bicuspid aortic valve disease (17)

1.2 AORTOPATHY IN BICUSPID AORTIC VALVE DISEASE

Bicuspid aortic valve disease is commonly associated with aortic dilation with a 10 fold increased risk of aortic dissection (18). To date the following risk factors for progressive aortic dilation have been identified: aortic size, male sex, aortic regurgitation and a positive family history (19).

Della Corte et al suggested (13,14) that the aortopathy in BAV can be subdivided into subgroups. They especially identified the aortic root phenotype as a distinct separate entity with no ascending aortic dilation which mainly occurs in young males with RL-BAV and has an increased incidence of aortic regurgitation.

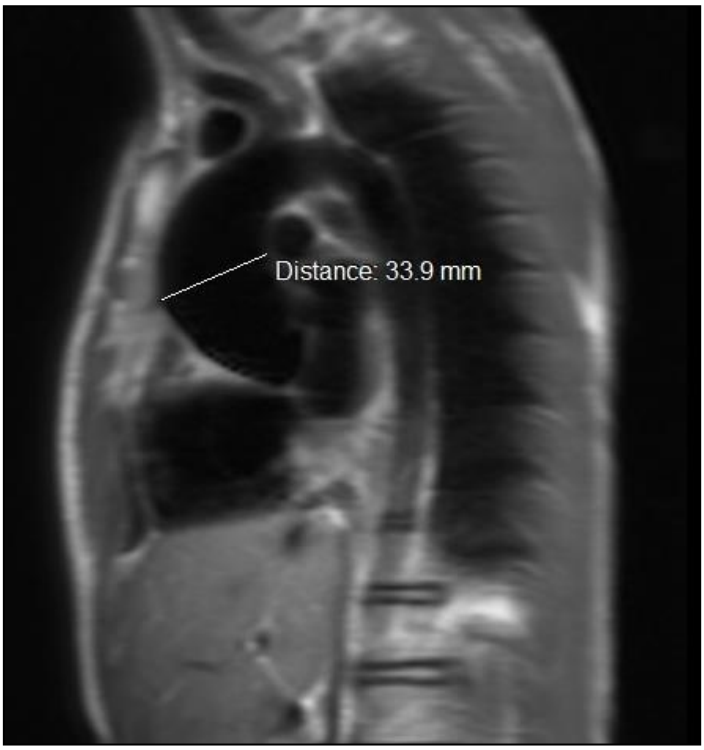

Figure 1-3: Dilated ascending aorta in an 8-year old patient with a bicuspid aortic valve

The underlying pathophysiology for the aortopathy was traditionally believed to be an intrinsic aortopathy similar to Marfan syndrome. This has been supported by the finding

that aortic dilation can be present even in normal functioning bicuspid aortic valves (20). Aortic dilation can also continue after aortic valve replacement (21). Furthermore, aortic elastic properties such as distensibility, pulse wave velocity and the maximum rate of aortic distension have been shown to be abnormal in BAV patients (22-24). Abnormal aortic elastic properties and enlarged aortic dimensions with a tricuspid aortic valve have also been observed in relatives of patients with BAV (8), further suggesting an underlying genetic cause for an intrinsic aortopathy. This intrinsic aortopathy histopathologically manifests as a cystic medial degeneration caused by abnormal regulatory pathways of the vascular smooth muscle cells. A reduction of fibrillin 1 activates matrix metalloproteinases (MMPs) (25) and alters transforming growth factor β expression which leads to the degrading of structural support of the aorta with a reduction in elastin (19). Especially MMP2 has been shown to be increased in tissue excised from dilated aortas (26-28) but also MMP9 was increased in one study (29). Furthermore Tzemos et al showed that even circulating MMP2 was increased in BAV patients while MMP 9 was normal (22).

These limited data have been the basis for the recent change in the 2010 American College of Cardiology (ACC) and the American Heart Association (AHA) guidelines in favour of a recommendation for prophylactic surgery at an aortic diameter of 4.5-5cm in BAV patients, similar to Marfan patients. Furthermore any first-degree relative of a patient with BAV should be screened for aortic dilation (30). This would theoretically involve cascade screening of an estimated 2 million people in the UK alone. However, the assumptions of a similar aortopathy to Marfan syndrome are not supported by strong evidence, and the BAV aortopathy may be a different entity. The far-reaching clinical and health economic consequences of this recommendation mean that our limited knowledge and understanding

of the prevalence, extent and clinical relevance of BAV aortopathy needs urgently to be addressed.

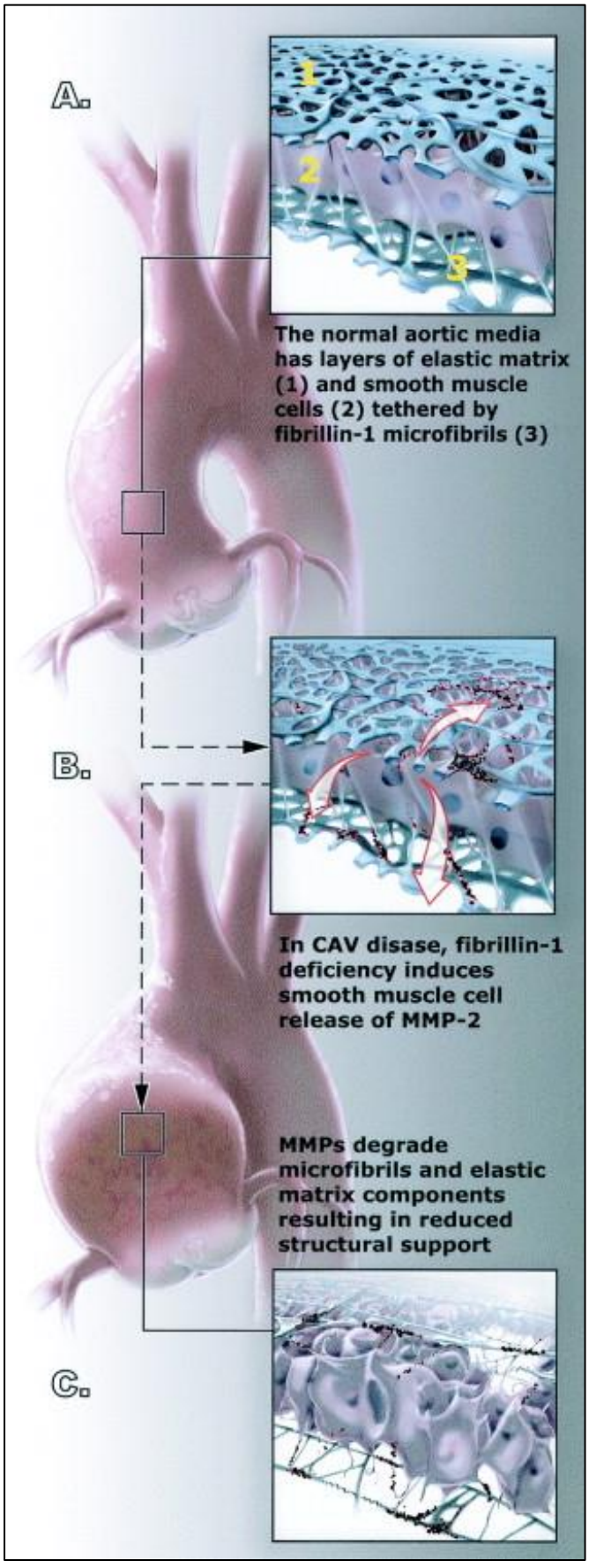

Figure 1-4: Pathophysiology of the intrinsic aortopathy in BAV by Fedak et al (26)**; CAV = congenital BAV aortopathy**

1.2.1 Blood flow pattern

A bicuspid aortic valve is thought to give rise to abnormal aortic flow patterns (31), although whether these were a consequence of the dilated aorta, or a haemodynamic component in the development of the BAV aortopathy is less clear. Recent advances in cardiovascular magnetic resonance imaging (CMR) now enable 3-dimensional imaging of the blood flow in the aorta (4D flow MRI) (32). This new technique was used in a pilot study (n = 20) examining flow pattern in bicuspid aortic valve disease with striking results. BAV patients were found to have a marked helical flow pattern in the ascending aorta with distinct differences between the leaflet fusions patterns: the RL-BAV group showed a marked right-handed helical flow pattern and the RN-BAV group a left-handed helical flow pattern (33). 4D flow MRI is a new and evolving technique with the opportunity for the first time to examine haemodynamic factors in bicuspid aortic valve disease in detail.

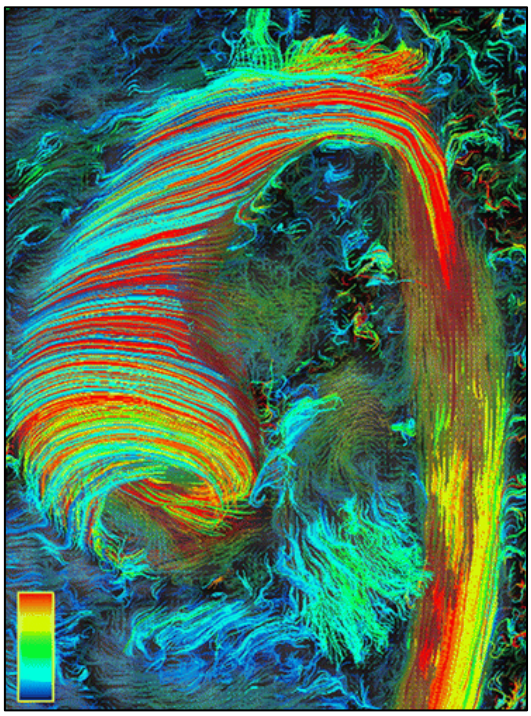

Figure 1-5: Helical flow pattern in the ascending aorta in a patient with BAV by Hope at al (33)

1.2.2 Wall shear stress

Wall shear stress within a vessel is described as the force per unit area created by blood flow acting on a vessel endothelium. Shear stress exists wherever flow occurs (34). This leads to mechanotransduction, a conversion of mechanical stresses to biochemical responses through nitrovasodilators, prostaglandins, lipoxygenases and other molecules (34).

Wall shear stress near the wall is known to influence vessel growth and architecture. To date this has mainly been observed in animal models or in vitro experiments. In hypertension animal models showed an increase in especially circumferential shear stress in the initial phase. However, as vascular remodelling has taken place such as wall hypertrophy, shear stress levels decreased to near normal levels again suggesting that remodelling may occur to "normalise" the increased shear stress in hypertension (35). Wall shear stress has also been postulated as an important determinant of a developing vessel size as wall shear stress values are consistent throughout the animal kingdom within the arterial network (36). Low wall shear stress is thought to play a role in atherosclerosis development (37). This is the first area where 4D flow MRI wall shear stress assessment was used. Markl's group demonstrated relatively lower wall shear stress in the areas where plaque formation was identified (38,39). Limitations in spatial resolutions and partial volume effects in this new 4Dflow MRI approach make definition of the exact vessel lumen boundary difficult suggesting that this new method is an estimation of the true in vivo wall shear stress (40).

The observed helical blood flow in BAV by Hope et al (33) is likely to be disorganised and at the start of the DPhil thesis there were no data available to suggest how this would influence the wall shear stress at the vessel wall.

1.3 CARDIOVASCULAR MAGNETIC RESONANCE IMAGING

1.3.1 Aortic anatomy

Cardiovascular magnetic resonance (CMR) imaging provides a highly accurate and precise modality to assess the structure of the aortic valve and aorta. It allows an accurate distinction to be drawn between bicuspid valves of differing morphologies and confident ascertainment of the presence or absence of aortic coarctation, with which some BAV morphologies are associated. Furthermore, accurate measures of aortic size and shape can be made in any plane, which is an important advantage over echocardiography, given the frequent asymmetry of flow jets arising from the abnormal valve (41), which is perhaps contributing to asymmetric aortic dilation.

1.3.2 Aortic elastic function

Global aortic stiffness is an important marker of the presence and severity of aortic disease. CMR can provide unique insights into the regional and local biophysical properties of the vasculature (42). Aortic stiffness can be assessed over regions of the aorta by measuring the pulse wave velocity between any two points, or can be assessed locally at any point in the aorta using aortic distensibility quantification. The new oscillatory sphygmomanometer-based technology (Vicorder, Smart medical, UK), which is both magnet-safe and non-

invasive, enables calculations of central pulse pressure, during CMR acquisition. This is likely to represent a further improvement of the accuracy of distensibility measures.

1.3.3 Aortic flow abnormalities assessed by 4D flow

Novel complex CMR flow sequences now provide a promising platform to study the effects of aortic valve and intrinsic aortic pathology on aortic flow patterns and, in turn, the impact of these flow patterns on the vascular structure. This state-of-the-art phase contrast technique can encode velocities along all three planes in the aorta, whilst three-dimensional structural information is also acquired. These data are time-resolved, i.e. available throughout the cardiac cycle with a temporal resolution of 40 ms. These data sets are pre-processed, visualised in 3D and then quantified. Quantitative parameters, such as flow rate, peak flow, peak velocity, wall shear stress and oscillatory shear index, can be derived in any location of the aorta. Our collaborators from Prof Markl's group have led the field in this area and published case reports and feasibility studies in small cohorts of patients with aortic disease (32,38,43-55).

1.4 AIMS OF THIS THESIS

This thesis aims to examine in more detail the links between flow patterns, aortic dilation and measures of aortic vascular function using CMR to 1) understand the pathophysiological mechanisms of aortic dilation in BAV and 2) identify novel markers for disease progression and the risk of aortic dilation. I chose a prospective cross-sectional design for this study, with a longitudinal follow-up. The cross-sectional study will give insight into the role haemodynamic factors may play in the pathophysiology of BAV aortopathy. The longitudinal element will follow on from my thesis work and will assess the potential of imaging biomarkers for risk stratification of rapid aortic growth in bicuspid aortic valve disease.

1.4.1 Hypothesis

I hypothesised that right-left coronary leaflet fusion and right-non-coronary leaflet fusion bicuspid aortic valves are two distinct phenotypes with distinct inheritance patterns in family members, different underlying pathological aortopathy pathways and haemodynamic profiles, with distinct patterns of abnormality of regional vascular stiffness and endothelial function. Some of these pathological aortopathy pathways may also be seen in first degree family members. Furthermore, I hypothesised that the leaflet fusion pattern and degree of haemodynamic and endothelial dysfunction have prognostic significance and can together predict future aortic dilation with implications for follow-up, imaging strategy, intervention and family screening.

2 ND CHAPTER: GENERAL METHODS

2.1 STUDY APPROVALS & GENERAL ASPECTS

2.1.1 Ethical approval

The entire study was approved by the West Berkshire ethics committee (Ref: 10/H0505/100). All participants or their guardians gave written informed consent and the study was conducted in accordance with the principles of the declaration of Helsinki.

2.1.2 General exclusion criteria

Exclusion criteria for the cardiovascular magnetic resonance imaging protocol of the study include:

1. Female who is pregnant (patients who plan or may plan to become pregnant during the 5 year study will not be excluded, unless they plan to become pregnant at the time of the initial study visit).
2. Lactating mothers will not be automatically excluded.
3. Contra-indications to magnetic resonance imaging (pacemaker, cranial aneurysm clips, metallic ocular foreign bodies, severe claustrophobia).
4. Presence of complex congenital cardiac disease. (Patent foramen ovale, mitral valve prolapse, atrial septum defect, ventricular septum defect, coarctation of the aorta will not exclude the participant from inclusion, although the presence or severity of one or more of these lesions may represent an exclusion under point 6 of the exclusion criteria).
5. Patient is terminally ill.

6. Any other significant disease or disorder which, in the opinion of the investigator, may either put the participant at risk because of participation in the study, or may influence the result of the study, or the participant's ability to participate in the study.
7. Participants who have participated in another cardiac research study involving an investigational product in the past 3 months.

2.1.3 Power calculation

There were no data available for 4D flow MRI measurements in bicuspid aortic valve disease at the start of this study. Therefore the sample size was calculated to detect a 1/3 clinically meaningful difference in proximal ascending aortic distensibility. The mean distensibility measurement in healthy volunteers (SD) was 5.6 (3.0) $10^{-6}cm^2dyne^{-1}$ (56). To detect a 1/3 difference and assuming a power of 0.9 at a significance level of $\alpha = 0.05$, a sample size of 54 would be required in each group.

2.2 DATA ACQUISITION

2.2.1 Cardiovascular magnetic resonance 1.5 Tesla acquisition

For anatomical and aortic function imaging a 1.5 Tesla system (Avanto, Siemens, Erlangen, Germany) with a 32-channel cardiac coil was used. All images were electrocardiogram (ECG)-gated. Steady-state free-precession (SSFP) cine sequences acquired during a single breath-hold were used for aortic dimension measurements, left ventricular volume assessment and aortic valve morphology. Short axis planes of the aorta were acquired perpendicular to the long axis at the sinuses of Valsalva, sinotubular junction, ascending and proximal descending aorta at the level of the pulmonary artery, and a further plane in the descending aorta 12cm below the first plane. For aortic function measures (distensibility and maximal rate of systolic distension), free-breathing SSFP images with a high temporal resolution (10ms) (23) were acquired in the same short axis aortic planes as for dimensions (latter three above). Through-plane phase contrast velocity mapping images with a high temporal resolution were acquired perpendicular to the ascending and descending aorta at the level of the pulmonary artery for pulse wave velocity (PWV) calculations.

2.2.2 Cardiovascular magnetic resonance 3 Tesla acquisition - 4D flow assessment

For the 4D flow MRI assessment, a 3.0 Tesla system (Trio, Siemens, Erlangen, Germany) with a 32-channel cardiac coil was used. All images were electrocardiogram (ECG)-gated. Flow-sensitive gradient-echo pulse sequence CMR was used to characterize and quantify flow haemodynamics in the thoracic aorta. Datasets were acquired with prospective ECG-gating

during free-breathing, using a respiratory navigator. The image acquisition volume was placed in an oblique sagittal plane encompassing the whole thoracic aorta. 1 set of anatomical and 3 sets of flow images are acquired during a 20 min scan phase. Sequence parameters were: echo time 2.5ms, repetition time 5.1ms, flip angle 7°, voxel size 1.9-2.0x1.5-1.7x2.0-2.2mm^3, temporal resolution 40ms. The velocity encoding range was determined using the lowest non-aliasing velocity on scout measurements (healthy volunteers 1-1.5m/s; BAV patients 1.5-4.5m/s).

2.2.3 Echocardiographic acquisition

Children younger than 6-8 years old are unable to lie still long enough and comply with breath-holding instructions sufficiently to perform a CMR scan. In the clinical setting these children would undergo a CMR scan under general anaesthetic. Therefore in this study participants under the age of 6 years and claustrophobic adult participants underwent basic echocardiography assessment on a Phillips iE33 system (Andover, MA, USA). Aortic valve morphology was assessed from a standard, focused short axis image of the valve. Datasets were analysed using Xcelera reporting software (Philips, MA, USA).

2.3 DATA ANALYSIS

2.3.1 Valve morphology and function

Valve morphology was classified by leaflet fusion type using CMR short axis anatomical images or short axis echocardiographic images. The bicuspid aortic valve morphology was defined as per Sievers et al (17) and Buchner et al (57).

The velocity across the aortic valve was measured using through-plane phase contrast velocity mapping in an image slice placed perpendicular to the ascending aorta, just above the valve tips. Aortic stenosis was defined as absent or mild if peak velocity was <3m/s, and moderate-severe if ≥3m/s. Peak velocity and flow volume were analysed using CMR42 (Circle Cardiovascular Imaging Inc., Calgary, Canada; Figure 2-1). The aortic valve flow was manually identified in each time frame of the cardiac cycle. Flow volumes were used to calculate regurgitant fraction.

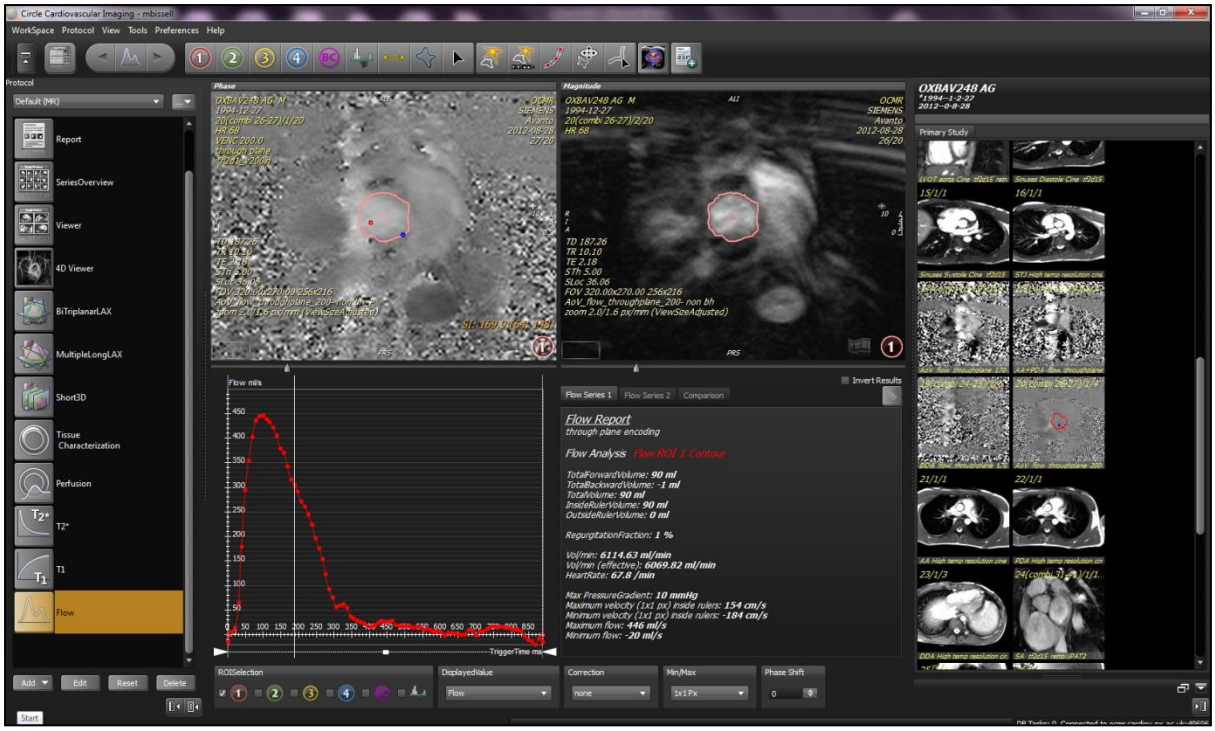

Figure 2-1: Peak velocity and regurgitant fraction analysis using CMR42 (Circle Cardiovascular Imaging Inc., Calgary, Canada)

2.3.2 Aortic diameters

Aortic diameters were measured (Figure 2-2) as per AHA guidelines (30) from inner edge to inner edge at end-diastole. Measurement planes were acquired with CMR perpendicular to the aortic lumen (to ensure true short axis diameters) in the middle of the sinuses of Valsalva, at the sinotubular junction, the ascending and proximal descending aorta at the level of the pulmonary artery and at the descending aorta 12 cm below the measurement plane of the proximal descending aorta. The sinuses were measured in diastole from cusp to commissure as described by Burman et al (58). All aortic diameters were indexed for body surface area (BSA) using the Haycock formula (59) to account for the wide range of body size and relatively smaller diameters in the paediatric subjects.

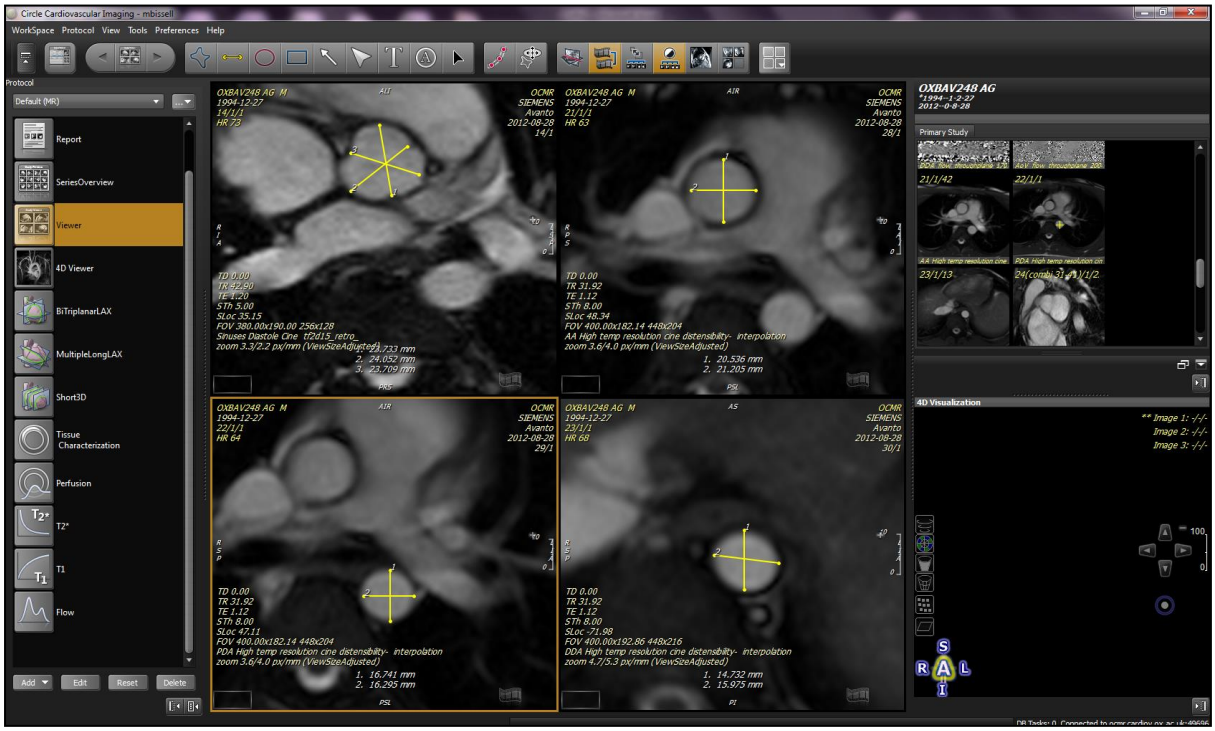

Figure 2-2: Measurement of aortic diameters using CMR42 (Circle Cardiovascular Imaging Inc., Calgary, Canada)

2.3.3 Left ventricular function

Left ventricular function was measured by the standard technique using a stack of multiple short axis cine images, and analysed using the semi-automated CMR42 software (Figure 2-3). Departmental ranges for normal values were used as references. For the paediatric population z-scores were calculated.

Figure 2-3: Analysis of left ventricular function using CMR42 (Circle Cardiovascular Imaging Inc., Calgary, Canada)

2.3.4 Vascular function measurements

Vascular function measurements were examined to determine any differences in the elastic properties of the aorta consistent with an underlying intrinsic aortopathy.

Central blood pressure (for aortic distensibility) was measured during the CMR scan using the Vicorder device (Smart Medical, Moreton in Marsh, United Kingdom), calibrated to brachial cuff pressures (60).

2.3.4.1 Distensibility and maximum rate of systolic distension (MRSD)

Distensibility (the fractional increase in aortic area as a function of pressure change) was calculated using automated measurements of aortic luminal area (61) in an automated Matlab tool (The Mathworks, Inc, Natick, MA) designed by our working group (Figure 2-4).

Measurements are defined as followed (61):

- Compliance [mm^2 / mmHg] = (max_area - min_area) / pulse_pressure
- Arterial strain [arbitrary units] = (max_area - min_area) / min_area
- Distensibility [1 / mmHg] = arterial_strain / pulse_pressure

While starting this thesis, Donato Aquaro et al published a new measure of intrinsic wall function called maximum rate of systolic distension (MRSD) which is defined as the maximum positive slope (rate of increase) of the normalized lumen area measurements during systole (23). This measure is blood pressure independent and is possibly more reproducible. It might also be a better indicator for subtle changes in intrinsic wall function. I therefore liaised with our physics team to incorporate this novel measurement into the distensibility tool (Figure 2-4).

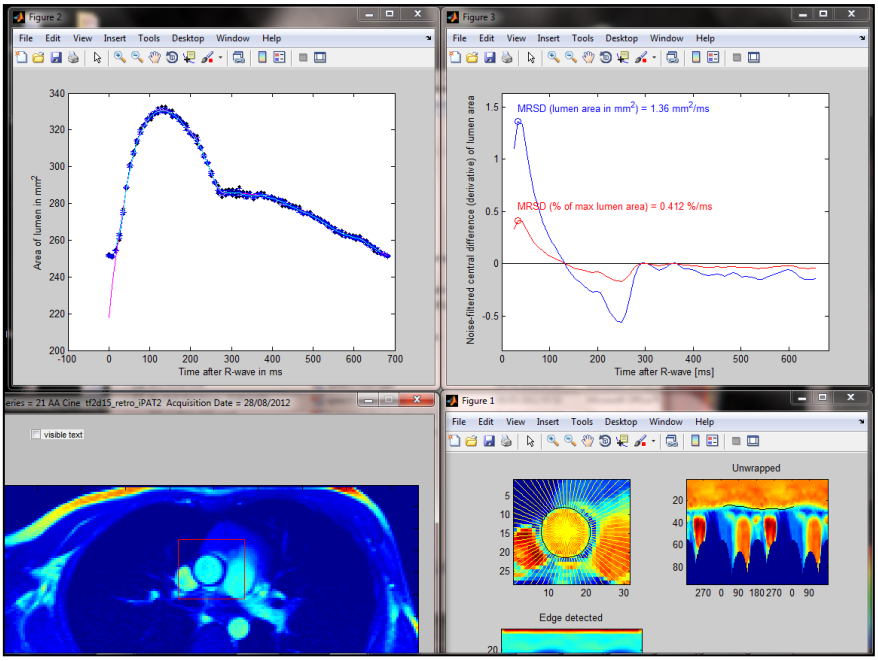

Figure 2-4: Distensibility and MRSD analysis using our Matlab tool (The Mathworks, Inc, Natick, MA)

2.3.4.2 Pulse wave velocity

Pulse wave velocity was computed using the same in-house software based on widely accepted active contour models (62) which automatically segmented 2D phase contrast images, previously validated by Herment et al (63). The length of the aortic centreline was measured manually on an oblique-sagittal slice through the aorta (half-Fourier single-shot turbo spin-echo [HASTE] scan sequence), while transit time between normalized flow velocity curves was estimated using the half-maximum of the linear fit on the systolic upslope.

2.3.5 Cardiovascular magnetic resonance 4D flow assessment

Flow through the ascending aorta in normal subjects is usually cohesive, with a slight helical spiral, though in bicuspid aortic valve patients the flow has been shown to be highly

deranged with markedly accentuated helical flow (33). Helical flow is composed of a forward component (along the long axis of the aorta) and a rotational component (rotating around the long axis in a circumferential direction). The 3-dimensional flow patterns were measured in a short axis slice at the sinotubular junction, ascending and proximal descending aorta both at the level of the pulmonary artery. Measurements were averaged over a period at peak systole (one time frame before and three after peak systolic flow) to mitigate measurement noise (64).

The 4D flow tools for data processing are a combination of EnSight (CEI Inc, Apex, NC) Version 9.1.2 and Matlab plug- ins (The Mathworks, Inc, Natick, MA) designed by our collaborators, Michael Markl's group (40). The datasets were corrected for eddy current and noise reduction, aliasing removal and static tissue subtraction were applied. Pathlines, indicating flow direction over time were used for visualisation (Figure 2-5). This initial post-processing of the data takes 30-60min and is important to achieve optimal data quality for the quantification processes below. Overcorrecting can lead to artefacts in the data. I assessed my initial 10 datasets in detail with our collaborator Dr Alex Barker from Prof Markl's group to ensure accurate optimisation of the datasets. This also enabled me to optimise acquisition of the 4D flow MRI datasets.

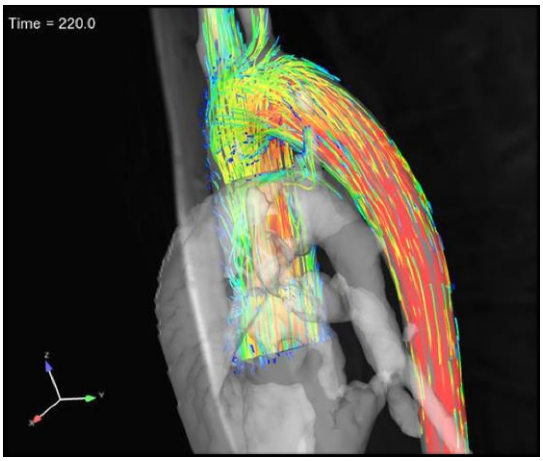

Figure 2-5: Pathlines indicating flow direction over time

Analysis planes were placed at pre-defined anatomical position for further quantitative analysis (Figure 2-6). In this thesis planes 1 and 7 were analysed as well as plane 0 (at the level of the sinotubular junction). Flow in the sinuses suffers from a large amount of eddy currents and is therefore not easily analysed with current correction methods.

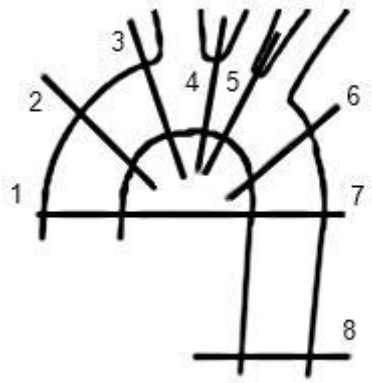

Figure 2-6: Position of analysis planes

2.3.5.1 Wall shear stress analysis

The 4D flow images can also be utilized to measure wall shear stress (WSS). Altered wall shear stress can act as a stimulus for vascular remodelling by inducing expression of transcriptional factors (36).

Wall shear stress quantifies the shearing force of the moving blood against the vessel lumen and is defined as:

$$WSS\ magnitude = 2\eta\dot{\varepsilon} \cdot \vec{n}$$

η = viscosity of the blood

$\dot{\varepsilon}$ = deformation tensor (which includes the velocity components and spatial dimensions as part of the three-directional velocity field of the acquired CMR data)

$\vec{n}$ = inward unit normal (which describes the direction towards the centre of the vessel)

WSS magnitude is the combination vector of the circumferential (in-plane) shear stress vector and the axial (through-plane) shear stress vector (Figure 2-7) (49):

$$WSS\ magnitude = \sqrt{a^2 + t^2}$$

a = circumferential shear stress vector

t = axial shear stress vector

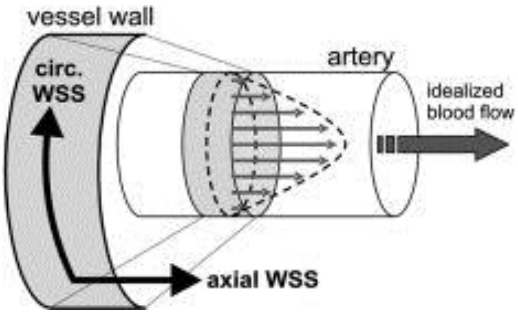

Figure 2-7: Components of wall shear stress by Frydrychowicz et al (49)

Wall shear stress was calculated using the flow tool in Matlab (The Mathworks, Inc, Natick, MA) (40) where the planes were contoured manually for each time frame (Figure 2-8). Systolic wall shear stress was measured in eight anatomical positions within the aortic

lumen. The circumferentially averaged systolic wall shear stress ($WSS_{circavg}$) was averaged over these eight anatomical positions using the combined vector magnitude of both through-plane and in-plane (rotational) wall shear stress.

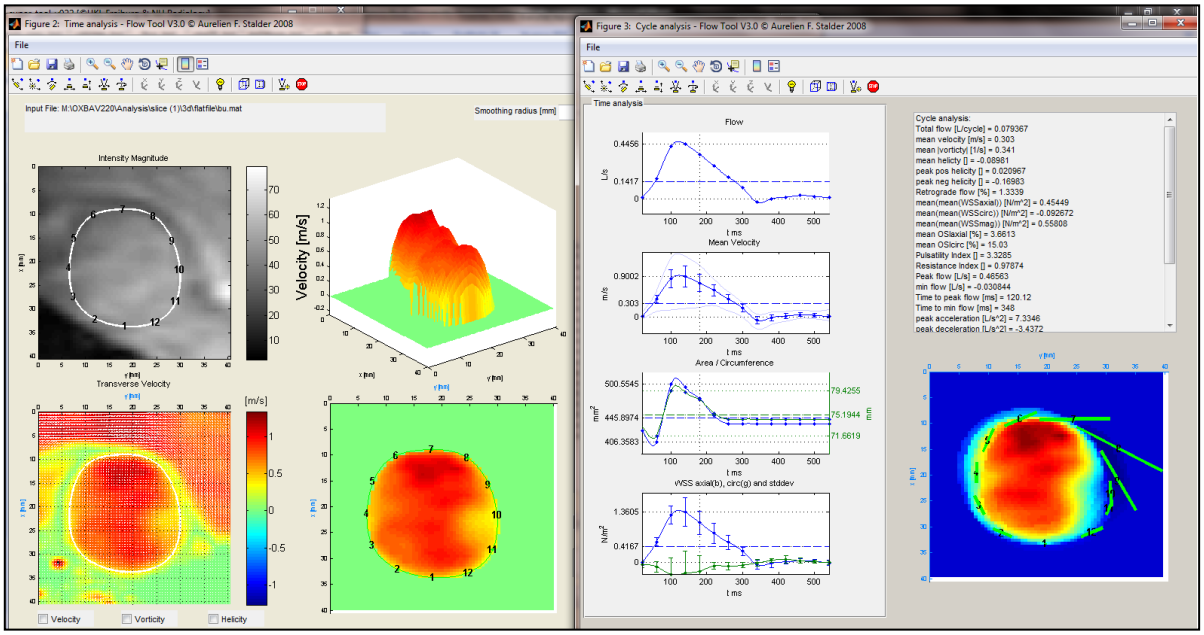

Figure 2-8: Wall shear stress analysis using the flow tool

Limitations in spatial resolutions and partial volume effects make definition of the exact vessel lumen boundary difficult. This together with the numerical derivation of velocity fields as the only current option to quantify wall shear stress are likely contributing to an underestimation of the actual in vivo wall shear stress in humans (40). However, to date this is the only analysis tool available for wall shear stress analysis from 4D flow MRI data. Markl et al (65) assessed reproducibility, inter (between two observers) and intra (the same observer doing the same analysis twice) observer variability for this method of 4D flow analysis. Inter observer variability for wall shear stress showed a Pearson's correlation coefficient = 0.84 and Bland-Altman mean difference -0.02 with limits of agreement ± 0.09.

Intra observer variability for wall shear stress showed a Pearson's correlation coefficient = 0.87 and Bland-Altman mean difference 0 with limits of agreement ± 0.07. For reproducibility healthy volunteers had a 4D flow MRI assessment 1 year apart. Pearson's correlation coefficient was 0.55 and Bland-Altman mean difference -0.03 with limits of agreement ± 0.14.

I completed intra observer assessment on 5 healthy volunteer datasets. Pearson's correlation coefficient was 0.99 and Bland-Altman mean difference 0 with limits of agreement ± 0.02.

2.3.5.2 Rotational (helical) flow

Initial helical flow assessment was qualitative. Mr Steffan Glaze assessed his and my inter-observer variability of qualitative assessment as part of this final honours project and concluded that especially in the "mild right-handed helical flow" group, definition of normal or abnormal was very inconsistent. He furthermore assessed the helicity measure that I was involved in implementing with our collaborators from Prof Markl's group (66). However, this measure was unable to distinguish between clearly seen right and left-handed helical flow and I therefore decided against using this for quantitative analysis of the rotational (helical) flow. Together with Dr Aaron Hess from our physics team I implemented the 'circulation' measure to accurately quantify the helical/rotational flow we already assessed visually.

The 'circulation' measure is the integral of vorticity with respect to the cross-sectional area of the aorta (67) based on the definition of Farthing and Peronneau in 1979 (68). The vector perpendicular to the transverse plane determines the handedness as well as the magnitude

of the helix (Figure 2-9). For quantification the in-house Matlab tool (The Mathworks, Inc, Natick, MA) was used. To establish normal values, I calculated two standard deviations from the mean from 50 healthy volunteer datasets: -5 to +11 mm^2/s. Abnormal (increased) right-handed helical flow (an anti-clockwise rotation viewed from left-anteriorly) was defined as rotational flow values >11 mm^2/s and abnormal left-handed helical flow (clockwise rotation) as <-5 mm^2/s. Complex flow was defined as a lack of an observable coherent helical flow pattern.

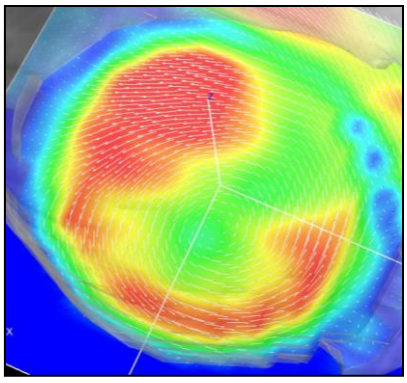

Figure 2-9: Velocity vectors in a patient with bicuspid aortic valve disease

2.3.5.3 Flow angle and displacement

Another parameter I was keen to quantify was the angle with which the blood flow leaves the bicuspid aortic valve. Our collaborators from Prof Markl's group integrated flow angle and displacement measurements into their tools. The flow angle represents the angle between the line perpendicular to the short axis analysis plane of the aorta and the instantaneous mean flow vector at peak systole (69). However, the flow displacement measure was not indexed to aortic diameter. I therefore decided to contact another research group who had developed a normalised displacement tool which did take the

aortic diameter into consideration and use this for the analysis. Here, flow displacement was calculated as the distance from the vessel centre line centroid to the velocity-weighted centroid (the centre of the flow jet) as described by Sigovan et al (70) and normalized to aortic diameters.

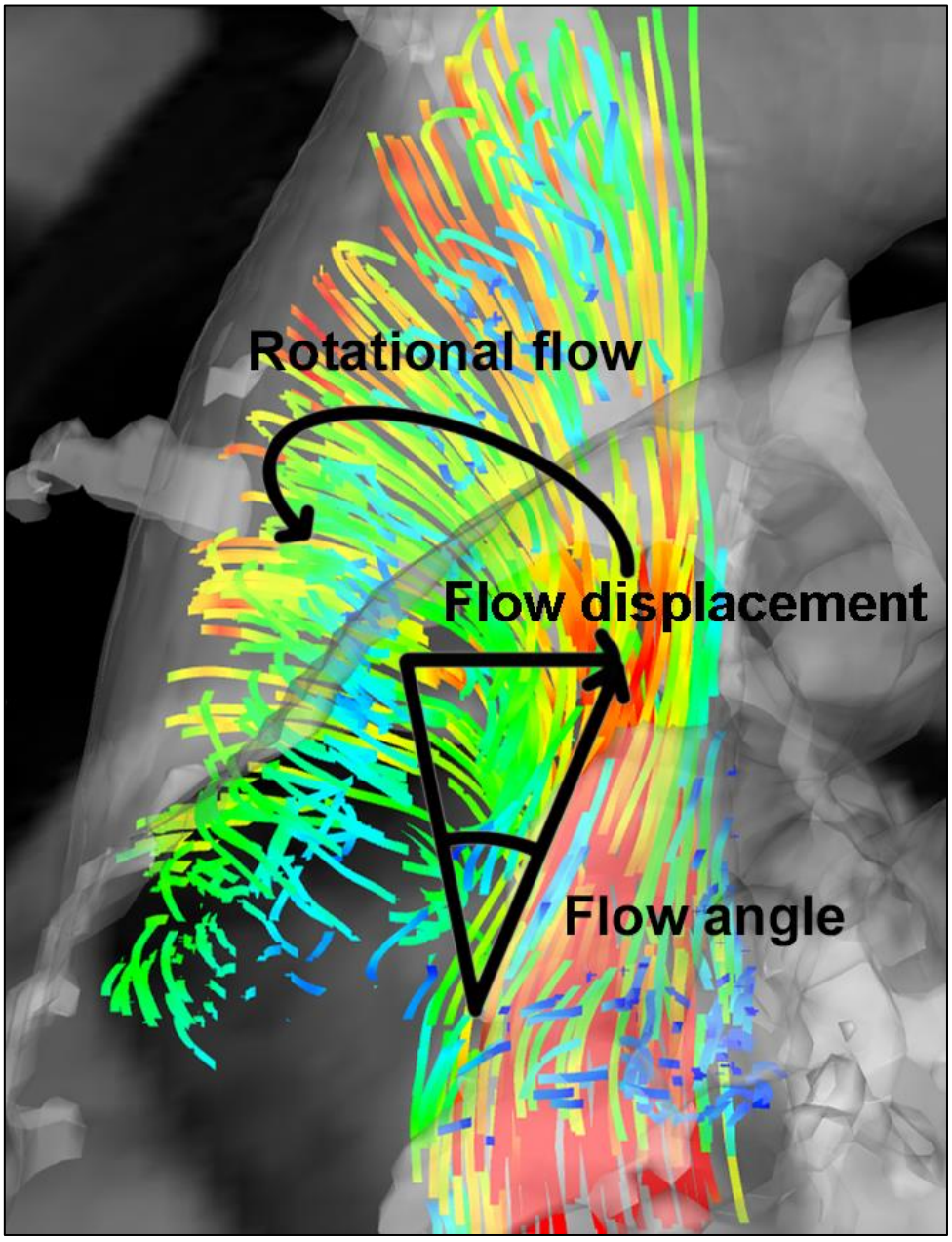

Figure 2-10: Depiction of flow angle and rotational flow in a patient with bicuspid aortic valve disease

2.4 BLOOD SAMPLE ANALYSIS

Fasting peripheral venous EDTA (Ethylenediaminetetraacetic acid) blood samples were taken and immediately spun at 3000rpm for 10min followed at 10000rpm for 10min. Blood samples were then frozen for analysis at -80 degrees Celsius. Blood samples were analysed for matrix metallo-proteinases 2 and 9 using the commercially available R&D Systems MMP-9 and MMP-2 ELISA kits. I chose MMP-2 and MMP-9 as both of these have been reported to be abnormal in BAV previously (26-29).

2.5 STATISTICAL ANALYSIS

SPSS Statistics Version 21 (IBM Cooperation, New York, USA) was used for statistical analysis. Data were tested for normal distribution with the Kolmogorov-Smirnov test. Normally distributed data were analysed using the Students t-test for two group comparison. One-way ANOVA with post-hoc Games-Howell analysis was used for multiple group comparison (e.g. different flow patterns). Correlation was assessed using the Pearson correlation coefficient. Non-normally distributed data were analysed using non-parametric testing: Mann - Whitney U test for comparison of two groups and Kruskal-Wallis H for multiple group comparison. For categorical data the Chi-square test was performed. A p-value < 0.05 was considered significant.

3 RD CHAPTER: HAEMODYNAMIC AND FUNCTIONAL AORTIC ASSESSMENT IN BICUSPID AORTIC VALVE DISEASE

3.1 ABSTRACT

3.1.1 Background

Ascending aortic dilation is important complication in bicuspid aortic valve disease (BAV) which has an increased risk of aortic dissection. We used cardiovascular magnetic resonance (CMR) to understand the pathophysiology better by examining the links between 3-dimensional flow abnormalities, aortic function and aortic dilation.

3.1.2 Methods and Results

142 subjects underwent CMR (mean age 40 years; 95 with BAV, 47 healthy volunteers [HV]). BAV patients had predominantly abnormal right-handed helical flow in the ascending aorta, larger ascending aortas (18.3 ±3.3 vs. 15.2 ±2.2 mm/m^2, p<0.001), and higher rotational (helical) flow (31.7 ±15.8 vs. 2.9 ±3.9 mm^2/s, p<0.001), systolic flow angle (23.1 ±12.5 vs. 7.0 ±4.6°, p<0.001) and systolic wall shear stress (0.85 ±0.28 vs. 0.59 ±0.17 N/m^2, p<0.001) compared to HV. BAV with right-handed flow and right-non coronary cusp leaflet fusion (n= 31) showed more severe flow abnormalities (rotational flow 38.5 ±16.5 vs. 27.8 ±12.4 mm^2/s, p<0.001; systolic flow angle 29.4 ±10.9 vs. 19.4 ±11.4°, p<0.001; in-plane wall shear stress (0.64 ±0.23 vs. 0.47 ±0.22 N/m^2, p<0.001) and larger aortas (19.5 ±3.4 vs. 17.5 ±3.1 mm/m^2, p<0.05) than right-left cusp leaflet fusion (n=55). BAV patients with normal flow patterns had similar aortic dimensions and wall shear stress to healthy volunteers and younger BAV patients showed abnormal flow patterns but no aortic dilation, both further supporting the importance of flow pattern in the aetiology of aortic dilation. Aortic function measures (distensibility, aortic strain and pulse wave velocity) were similar across all groups.

3.1.3 Conclusions

Flow abnormalities may be a major contributor to aortic dilation in BAV. Fusion type affects the severity of flow abnormalities, and may allow better risk prediction and selection of patients for earlier surgical intervention.

3.2 INTRODUCTION

This chapter aims to examine the relationships between flow patterns in the proximal aorta of patients with bicuspid aortic valves (BAV) and the associated aortopathy. As described in detail in chapter 1 (section 1.2), this aortopathy was largely believed to be intrinsic. However, one study using advanced CMR 4D flow suggested that haemodynamic factors may also play a role (33). The true relationship between proximal aortic flow and the aortopathy has not been well defined however, and there are good theoretical reasons why flow may have a causal relationship with the aortopathy. Animal models, for example, have shown that increased shear stress and pressure can induce vessel dilation by activating many intracellular pathways including matrix metalloproteinase activation (36).

Now for the first time technology has advanced sufficiently to enable assessment of intraluminal flow in vivo. Although there has been an explosion in the field since the start of this study, with several studies assessing similar patient cohorts, this cohort remains the largest to date, allowing meaningful subgroup assessment and a stronger examination of the related factors.

This chapter examines ascending aortic flow pattern and aortic vascular function in a large cohort of BAV patients. It will assess the differences in flow abnormalities as well as any differences between the RL-BAV and RN-BAV groups. It will also compare normal functioning bicuspid aortic valve disease with stenotic bicuspid aortic valve disease to further assess the haemodynamic impact. A subgroup of paediatric patients will give insight into the early stages of the disease process.

3.3 METHODS

3.3.1 Study design and patient recruitment

This arm of the study recruited BAV patients and healthy volunteers to provide a comparison of aortic function and flow dynamics. In addition, there was a specific aim to include sufficient subjects with both of the commoner types of leaflet fusion pattern (RL-BAV and RN-BAV). Patients with bicuspid aortic valves were recruited prospectively from cardiology clinics and CMR lists between January 2011 and January 2013. Healthy volunteers were recruited from posters within the hospital and University buildings, and were free from any known significant medical problems. The healthy volunteers were age and sex-matched to the BAV patients at time of recruitment.

A standard study visit for both groups is detailed in Table 3-1.

Table 3-1: Standard study visits

	BAV	Healthy Volunteers
Check for eligibility	✓	✓
Obtain written informed consent	✓	✓
Baseline characteristics (height, weight, systolic and diastolic blood pressure, heart rate, current medication)	✓	✓
Medical history and physical examination	✓	✓
Electrocardiogram	✓	
Fasting blood sample (optional for children)	✓	✓
1.5 Tesla MRI scan: anatomical imaging, valvular function, left ventricular function, distensibility and pulse wave velocity or echocardiogram	✓	✓
3 Tesla MRI scan: 4D flow assessment of the aorta	✓	✓

3.3.2 Eligibility criteria

3.3.2.1 Inclusion Criteria

Bicuspid aortic valve patients:

i) Documented anatomically or functionally bicuspid aortic valve spectrum disease, shown on any prior imaging study (such as echocardiography, CMR, CT)

Healthy volunteers

ii) No evidence of cardiovascular disease.

All:

iii) Participant (or legal representative) has capacity and is willing to give informed consent to the research protocol.

iv) Able (in the investigator's opinion) and willing to comply with the main study requirements.

3.3.2.2 Exclusion criteria

See Chapter 2 (section 2.1.2.2).

3.3.3 Patient enrolment

One hundred patients with BAV were identified of whom 95 completed the assessment (5 withdrew due to claustrophobia). All 47 healthy volunteers (HV) completed the study protocol successfully. Three patients with fully repaired coarctation of the aorta and one patient with an incidental small atrial septal defect were included. All participants underwent CMR assessment at 1.5 and 3 Tesla as detailed in chapter 2.

3.3.4 Patient demographics

Demographic characteristics and aortic dimensions of the healthy volunteers and BAV groups are shown in Table 3-2. The BAV group had larger aortic diameter indexed to BSA at the sinotubular junction and ascending aorta, as expected. There was no difference in size at the sinuses of Valsalva, the proximal descending aorta or the distal descending aorta.

Table 3-2: Demographics and aortic dimensions of healthy volunteers and patients with bicuspid aortic valve disease

	Healthy volunteers	Bicuspid aortic valve patients
Male (%)	68%	76%
Age (years)	40.2±17.7	39.5±16.9
Mean arterial pressure (mmHg)	87.9±11.1	89.2±12.0
Aortic diameters/BSA (mm/m^2):		
Aortic sinuses	16.7±2.2	17.2±2.7
Sinotubular junction	15.1±2.1	16.6±3.1*
Mid ascending aorta	15.2±2.2	18.2±3.7*
Proximal descending aorta	11.0±1.6	11.2±1.8
Distal descending aorta	9.8±1.5	9.8±1.6

Values are mean ±standard deviation; *p<0.001; BSA = body surface area

3.4 RESULTS

3.4.1 Flow patterns in the ascending aorta

Examples of ascending aortic flow patterns in BAV patients are shown in Figure 3-1, and the distributions among BAV groups in Figure 3-2.

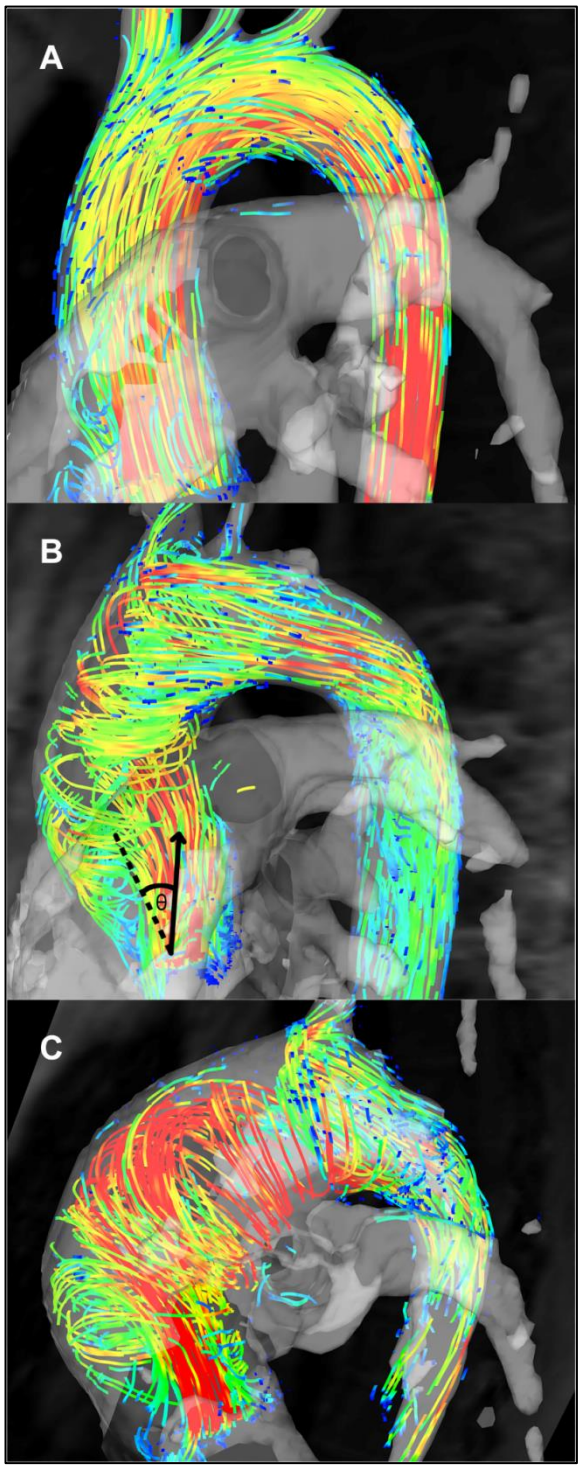

Figure 3-1: Flow patterns in bicuspid aortic valve disease; (A) Normal flow pattern; (B) Right-handed helical flow; (C) Left-handed helical flow. The systolic flow angle (θ) is demonstrated on figure B - the angle between the aortic mid-line (dashed) and the instantaneous mean flow vector at peak systole (arrow).

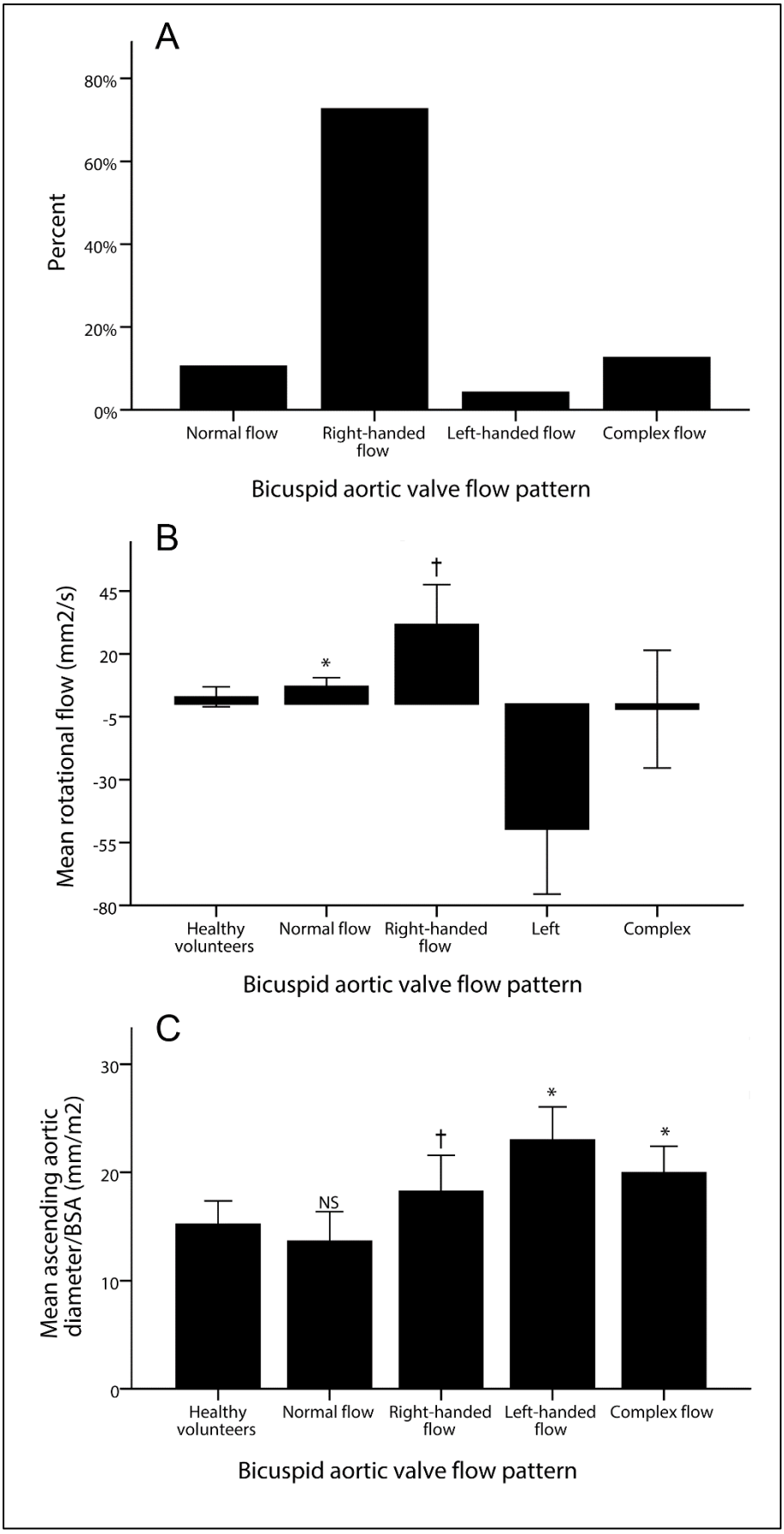

Figure 3-2: (A) Incidence of flow patterns in bicuspid aortic valve disease (BAV); (B) Mean rotational flow values in the different BAV flow patterns; (C) Mean ascending aortic diameter in the different flow patterns; Error bars indicate standard deviation; * p<0.05 compared to healthy volunteers (HV); † p<0.001 compared to HV

The most common flow pattern was right-handed helical flow, which occurred in 72% of patients (n=69). Normal flow patterns were observed in 11% (n=10), complex flow in 13% (n=12) and left-handed helical flow in 4% (n=4). Aortic dimensions and flow dynamic data are shown in Table 3-3. BAV patients with right-handed flow patterns had larger ascending aortic diameters, higher systolic flow angles and higher rotational flow values than healthy volunteers. Those with left-handed flow had even higher values, but the group was too small for meaningful comparison. In contrast, BAV patients with normal flow had similar aortic diameters and systolic flow angles to the healthy volunteers, but mildly increased rotational flow. The complex flow group had higher ascending aortic diameters and systolic flow angles, but rotational flow values were similar to the healthy volunteers group, due to the lack of a clearly helical flow pattern.

Table 3-3: Aortic dimensions and flow haemodynamics in bicuspid aortic valve disease and healthy volunteers.

	Healthy volunteers	**Bicuspid aortic valve patients (all fusion types)**			
	(n=47)	Normal flow (n=10)	Right-handed flow (n=69)	Left-handed flow (n=4)	Complex flow (n=12)
Aortic diameter/BSA (mm/m^2)					
Sinotubular junction	15.1±2.1	14.2±2.0	16.5±3.1*	19.1±1.6	18.2±2.9*
Mid ascending aorta	15.2±2.2	13.6±2.7	18.3±3.3**	23.0±3.1*	20.0±2.5**
Systolic flow angle (°)	7.0±4.6	9.7±5.9	23.1±12.5**	30.0±16.1	30.0±11.6**
Rotational flow (mm^2/m)	2.9±3.9	7.0±3.5*	31.7±15.8**	-49.7±25.8	-2.0±23.4
Systolic $WSS_{circavg}$ (N/m^2)	0.59±0.17	0.74±0.11*	0.85±0.28**	1.18±0.29	0.76±0.25
Systolic in-plane WSS (N/m^2)	0.01±0.12	0.08±0.10	0.53±0.24**	-0.84±0.35	-0.01±0.40
max systolic through-plane WSS (N/m^2)	0.75±0.20	1.02±0.22*	1.02±0.45**	1.31±0.53	1.05±0.49
Anterior - posterior eccentricity (N/m^2)	-0.18±0.17	-0.13±0.47	0.32±0.44**	0.40±0.48	0.26±0.51
Peak velocity (m/sec)	n/a	1.9±0.6	2.5±0.8	3.7±0.5	3.2±1.0
Age (years)	40.2±17.7	24.1±11.5*	42.2±17.1	20.2±5.3**	42.7±17.5

Values are mean ±standard deviation; *p<0.05, ** p<001 vs. healthy volunteers; BSA = body surface area; max= maximum

3.4.1.1 Wall shear stress

$WSS_{circavg}$ was significantly increased in both the right and left-handed flow groups, predominantly as a result of increased in-plane (rotational) wall shear stress, which contributed over 50% to $WSS_{circavg}$ (<2% in healthy volunteers). The maximum through-plane wall shear stress was also significantly higher in BAV patients compared to healthy volunteers, and the right-handed flow group demonstrated marked anterior-posterior eccentricity (difference in wall shear stress between the outer and inner aortic curvature, Figure 3-3). The normal flow group had similar in-plane (rotational) wall shear stress values to the HV group, but $WSS_{circavg}$ and maximum through-plane wall shear stress were marginally higher, possibly due to the slightly increased peak velocity from mild aortic valve restriction.

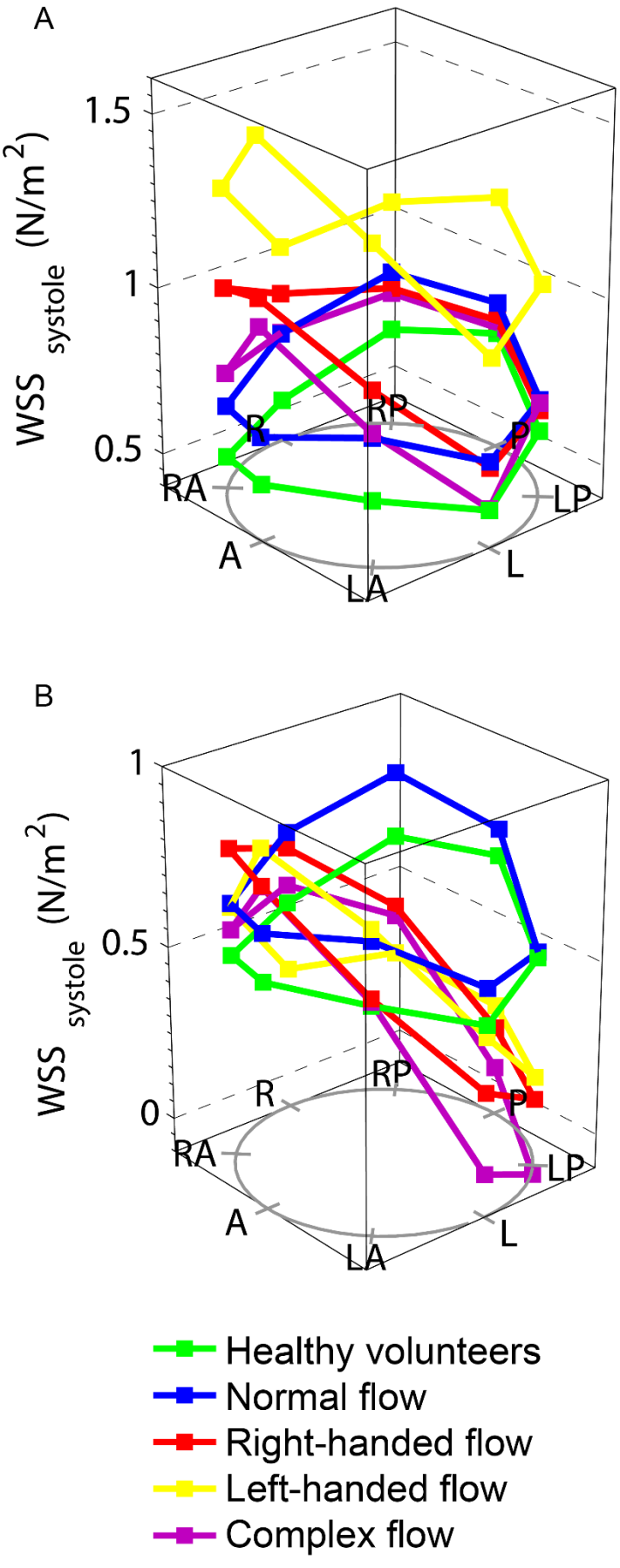

Figure 3-3: Wall shear stress (WSS) at all locations in the ascending aorta, in different bicuspid aortic valve flow patterns; (A) systolic WSS; (B) through-plane systolic WSS. A= anterior, LA= left anterior, L= left, LP= left posterior, P= posterior, RP= right posterior, R= right, RA= right anterior

Since wall shear stress is affected by aortic diameter, we attempted to account for this by dividing the group into aortic diameter tertiles: < 15 mm/m^2, 15 – 22 mm/m^2 and > 22 mm/m^2. When comparing these tertiles, the right-handed flow group had significantly higher rotational flow and $WSS_{circavg}$ values throughout compared to the HV group (Figure 14). In the healthy volunteer group, $WSS_{circavg}$ decreased as the aortic diameter enlarged (p=0.005) and rotational flow remained at the same low level, whereas $WSS_{circavg}$ remained constant in the right-handed flow group with a slight increase in rotational flow (Figure 3-4).

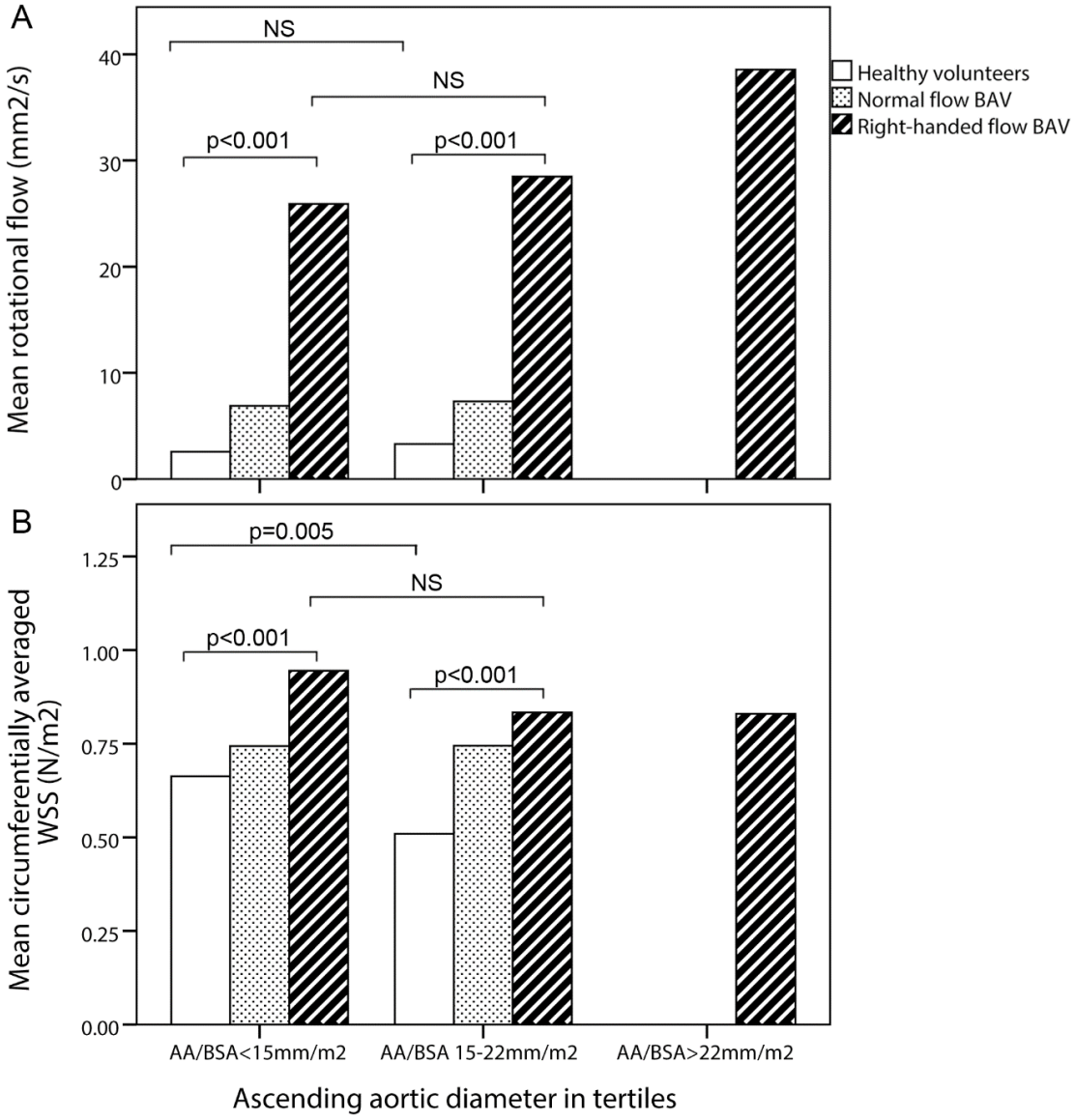

Figure 3-4: Mean rotational flow (a) and peak systolic circumferentially-averaged wall shear stress (WSS) (b) in ascending aortic diameter tertiles; NS = not significant; AA/BSA = ascending aortic diameter/Body surface area

3.4.2 Aortic flow patterns in the paediatric population

Comparing the 18 BAV patients aged <18 separately, all forms of flow disturbance were already present and right-handed flow remained the most prevalent pattern (56%), followed by normal flow pattern (28%), left-handed helical flow (11%) and complex flow (5%). One third already had enlarged ascending aortic diameters (z-score >2) and all of these had an abnormal flow pattern despite some having normal aortic valve function. Of the remaining two thirds with normal aortic diameters, 50% already had a right-handed helical flow pattern, even though aortic valve function was normal (n=7) or only mildly stenosed (n=4), suggesting that abnormal flow patterns predate aortic dilation.

3.4.3 Effect of fusion type

The recruited frequency of BAV fusion type was as followed: RL-BAV 58%, RN-BAV, 33%. LN-BAV 3%, true anterior-posterior cusp type 3% and unicuspid 3%. The RN-BAV group showed greater flow abnormalities than the RL-BAV group with a normal flow pattern in only 1/31 (3%), left handed helical flow in 10% and complex flow in 23% (Figure 3-5).

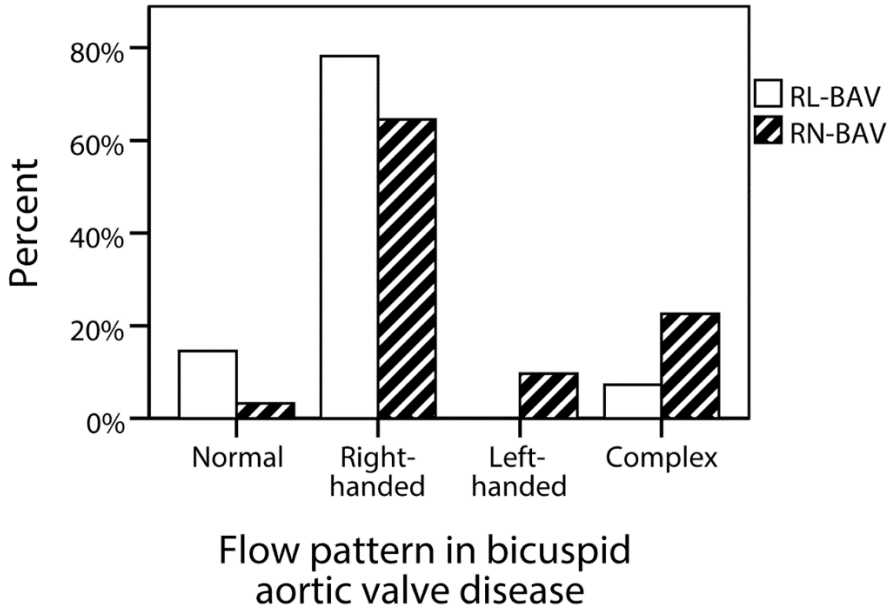

Figure 3-5: Proportion of patients with each ascending aortic flow pattern in the two main bicuspid aortic valve fusion sub-groups (RL-BAV and RN-BAV)

The quantitative comparison of haemodynamic flow measures between RL-BAV and RN-BAV was restricted to only those with the most common flow abnormality (right-handed flow), in order to minimise the influence of different flow patterns. Both sub-groups were comparable in age, peak velocity, regurgitant fraction and left ventricular function. However the RN-BAV group had larger aortic diameters with more severe haemodynamic flow abnormalities (Table 3-4). RL-BAV and RN-BAV had a similar systolic wall shear stress profile and eccentricity, but RN-BAV had higher in-plane (rotational) wall shear stress, whereas RL-BAV had a trend towards higher maximum through-plane wall shear stress and higher anterior-posterior eccentricity (Figure 3-6). These differences remained significant when patients with aortic stenosis were excluded.

Table 3-4: Aortic dimensions and flow haemodynamics in bicuspid aortic valve fusion subtypes.

	BAV fusion sub-types (right-handed flow only)	
	RL-BAV (n=43)	RN-BAV (n=20)
Aortic diameter/BSA (mm/m^2)		
Sinotubular junction	16.2±3.4	17.4±2.4
Mid ascending aorta	17.5±3.1	19.5±3.4*
Systolic flow angle (°)	19.4±11.4	29.4±10.9**
Rotational flow (mm^2/m)	27.8±12.4	38.5±16.5**
Systolic $WSS_{circavg}$ (N/m^2)	0.85±0.25	0.84±0.31
Systolic in-plane WSS (N/m^2)	0.47±0.22	0.64±0.23**
max systolic through-plane WSS (N/m^2)	1.05±0.38	0.88± 0.49
Anterior - posterior eccentricity (N/m^2)	0.30±0.57	-0.07±0.56*
Peak velocity (m/sec)	2.4 ±0.7	2. 5 ±0.8
Age (years)	42.0±15.5	43.9±17.2

Values are mean ±standard deviation; * p<0.05, ** p<0.001; BSA = body surface area; max= maximum

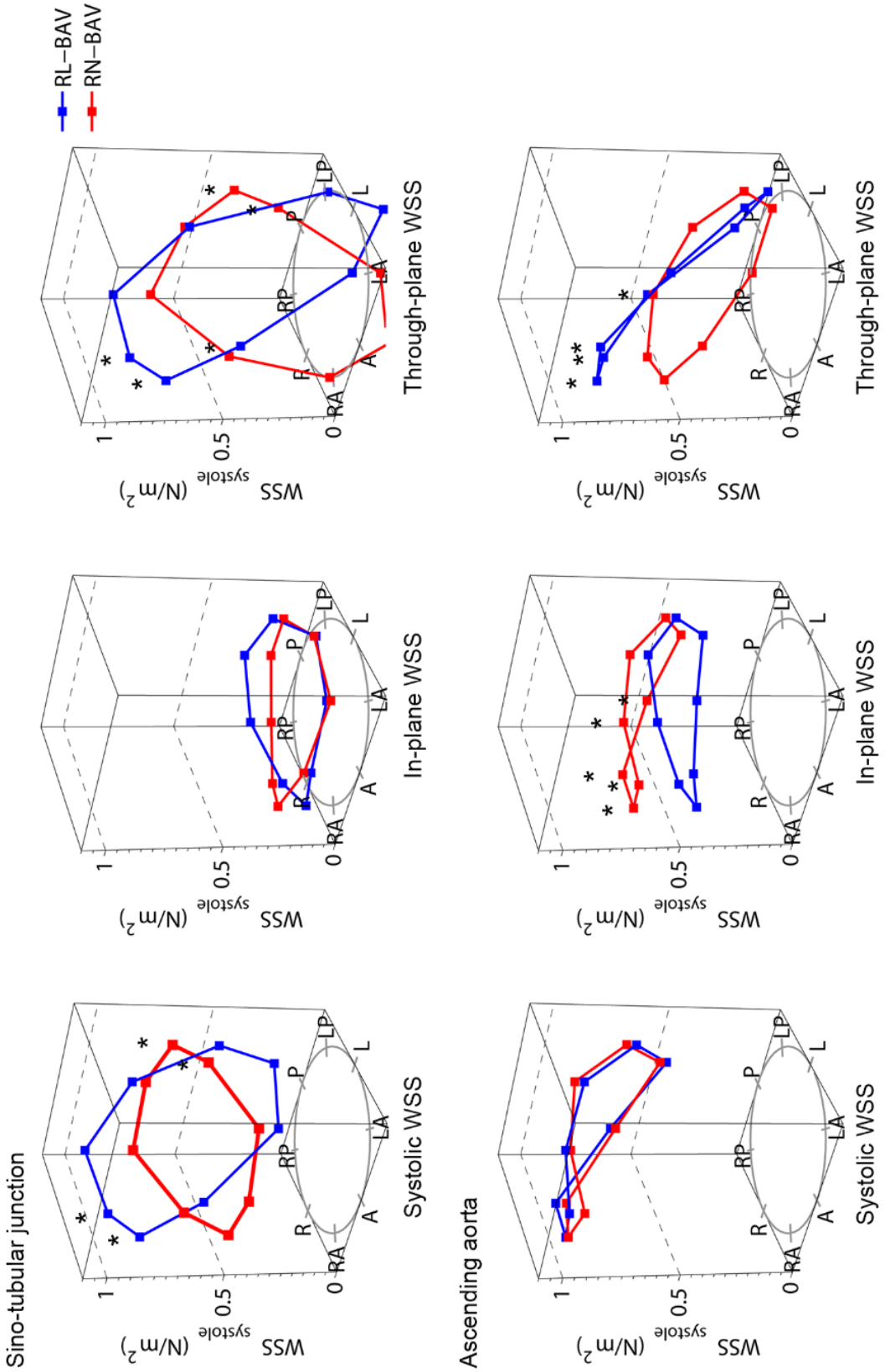

Figure 3-6: Wall shear stress (WSS) profiles in the leaflet fusion groups (RL-BAV and RN-BAV) with right-handed helical flow; A= anterior, LA= left anterior, L= left, LP= left posterior, P= posterior, RP= right posterior, R= right, RA= right anterior; *= p<0.05

3.4.4 Effect of aortic stenosis on flow abnormalities

Bicuspid aortic valve patients with moderate-severe aortic stenosis had larger ascending aortic diameters, higher absolute rotational flow and higher wall shear stress values with more pronounced eccentricity compared to the group with normal valve function or mild aortic stenosis (Table 3-5). When comparing stenotic right-handed and left-handed flow patterns, left-handed flow still showed a trend towards higher values.

Table 3-5: Aortic dimensions and flow haemodynamics in stenotic bicuspid aortic valve disease

	Aortic stenosis (n=24)	No aortic stenosis (n=71)
Aortic diameter/BSA (mm/m^2)		
Sinotubular junction	17.3±2.4	16.3±3.3
Mid ascending aorta	19.9±2.1	17.6±3.9*
Systolic flow angle (°)	27.1±11.3	21.7±13.5
Rotational flow (mm^2/m)	41.1±23.5	23.4±13.5*
Systolic $WSS_{circavg}$ (N/m^2)	1.09±0.28	0.76±0.21*
Systolic in-plane WSS (N/m^2)	0.65±0.35	0.41±0.23*
max systolic through-plane WSS (N/m^2)	1.47±0.48	0.89±0.31*
Anterior - posterior eccentricity (N/m^2)	0.70±0.48	0.12±0.36*
Peak velocity (m/sec)	3.9 ±0.5	2.1±0.4*
Age (years)	39.5±18.9	39.4 ±16.3

Values are mean ±standard deviation; * p<0.001; BSA = body surface area; max= maximum

3.4.5 Flow pattern in the descending aorta

The majority of BAV patients (64%) had a normal flow pattern in the proximal descending aorta (right-handed flow 28%, left-handed flow 8%). There was no difference in diameter of the proximal descending aortic diameter according to flow pattern.

3.4.6 Vascular measures in bicuspid aortic valve disease

There was no statistically significant difference between the BAV and HV group in all measures of vascular function as well as MMP 2 and MMP 9 concentrations (Table 3-6). There were also no significant differences in vascular function measures between any of the BAV sub-groups, and no significant association between vascular function measures and flow patterns when aortic dimensions were taken into account. MRSD was mildly decreased in the BAV group in both the ascending and proximal descending aorta, though with borderline statistical significance for both.

Table 3-6: Aortic vascular function measures in healthy volunteers and patients with bicuspid aortic valve disease.

	Healthy volunteers	Bicuspid aortic valve patients
Distensibility (1 / mmHg):		
Ascending aorta	4.65±3.21	4.06±3.07
Proximal descending aorta	4.86±2.05	4.98±2.28
Distal descending aorta	7.31±3.49	7.65±4.12
Arterial strain:		
Ascending aorta	0.21±0.13	0.19±0.13
Proximal descending aorta	0.23±0.09	0.24±0.10
Distal descending aorta	0.33±0.13	0.37±0.18
Maximum rate of systolic distension (%/ms):		
Ascending aorta	0.20±0.11	0.16±0.10*
Proximal descending aorta	0.21±0.09	0.18±0.08*
Distal descending aorta	0.27±0.07	0.24±0.08
Median pulse wave velocity arch (range) (m/s)	4.74 (13.05)	4.54 (29.67)
Median central pulse pressure (range) mmHg	47 (37)	51 (43)*
Mean matrix metalloproteinase 2 (ng/mL)	3.64	3.62
Mean matrix metalloproteinase 9 (ng/mL)	3.63	4.07

Values are mean ±standard deviation or median (range); SE = standard error; *p=0.04

3.5 DISCUSSION

3.5.1 Flow abnormalities in bicuspid aortic valve disease

In the largest study to date of 3-dimensional flow patterns in BAV, the most common flow abnormality in the ascending aorta was increased right-handed helical flow, irrespective of the BAV fusion type. Flow abnormalities were most pronounced in the ascending aorta, with a large proportion normalizing in the proximal descending aorta.

3.5.2 The association between flow patterns, wall shear stress and aortic dilation

Even a normally functioning BAV has an asymmetric orifice and increased flow angle compared to healthy volunteers (71). This study has shown that the increased flow angle is associated with higher rotational (helical) flow values - the asymmetric jet hits the aortic wall at a more acute angle, resulting in a larger amount of the jet rotating along the aortic wall increasing the in-plane component of the wall shear stress. It also causes asymmetric and locally increased through-plane wall shear stress, which contributes to the increased $WSS_{circavg}$ in BAV. Increased $WSS_{circavg}$ in BAV (particularly with more pronounced helical flow patterns in the ascending aorta) was associated with higher ascending aortic diameters, suggesting that $WSS_{circavg}$ (particularly in-plane [rotational] wall shear stress) may be a causative factor in aortic dilation. While it is not possible to exclude the possibility that the larger ascending aorta leads to increased $WSS_{circavg}$, this would conflict with the findings of previous studies showing reduced wall shear stress in patients with aortic dilation and a tricuspid aortic valve (72). One hypothesis may be that flow abnormalities initiate the

aortopathy as a compensatory response to maintain constant wall shear stress - increased wall shear stress can trigger matrix metalloproteinases and other cellular mechanisms involved in aortic dilation (36,73), and this may be a protective mechanism by which a constant wall shear stress is maintained (36). This is supported by this study's findings showing lower $WSS_{circavg}$ with increasing aortic diameters in the healthy volunteer group, but a constant high $WSS_{circavg}$ with increasing aortic diameters in the right-handed flow BAV group.

The concept of abnormal flow patterns and increased wall shear stress occurring prior to aortic dilation (and inferred causal relationship) is also supported by the findings in our paediatric population - several children already showed increased rotational flow values but normal ascending aortic diameters suggesting that the increased rotational flow is involved in the pathophysiology of developing aortic dilation. This is in keeping with a recent study showing increased (visually graded) helical flow in BAV patients without significant valve disease and normal ascending aortic diameters (74). In contrast to BAV patients, patients with Marfan syndrome and known intrinsic aortopathy have essentially normal wall shear stress values in normal sized aortas (75).

3.5.3 The importance of in-plane (rotational) wall shear stress in aortic dilation and differences between bicuspid aortic valve fusion types

The high proportion of in-plane (rotational) wall shear stress (>50%) in BAV patients seemed to be strongly associated with increased rotational flow and differed between BAV fusion types. The RN-BAV sub-group had increased aortic diameters, systolic flow angles, rotational flow and in-plane wall shear stress, while the RL-BAV group had smaller aortic diameters,

and higher maximum through-plane wall shear stress. This might suggest that the higher rotational flow and in-plane wall shear stress contribute to aortic dilation to a greater extent than through-plane wall shear stress and eccentricity.

The RN-BAV group exhibited more severe flow abnormalities (outlined above, and also including a higher proportion of left-handed flow), and was associated with larger ascending aortic diameters, compared to RL-BAV. While the cause of the dilation in this group is not confirmed (and may reflect either a different intrinsic aortopathy or increased in-plane wall shear stress as discussed above), it suggests that RN-BAV is at higher risk of ascending aortic dilation than the more common RL-BAV, and might be regarded as a marker of poor prognosis. Other studies examined only small numbers of the RN-BAV sub-group (33,64,74) and the degree of difference in flow patterns between fusion types and association with aortic dimensions had not hitherto been well characterized.

3.5.4 The effect of aortic stenosis

Ascending aortic diameters and degree of stenosis increase with time in subjects with BAV (3). Our study suggests that aortic stenosis further worsens the $WSS_{circavg}$ by:

1) Increasing rotational flow and in-plane (rotational) wall shear stress;

2) Increasing the maximum through-plane wall shear stress and eccentricity.

This is supported by a recent small retrospective study showing higher annual ascending aortic growth rate in BAV subjects with eccentric flow jet compared to those with central flow jets (76). However, aortic stenosis does not appear to be the only factor, as high systolic flow angles and rotational flow values were already seen in patients with normally functioning BAV.

3.5.5 Left-handed helical flow

Two other studies have reported a higher incidence of left-handed flow (10-20%) in young patients with RN-BAV, though numbers were small (n≤5) (33,74). This study reports a similar incidence in the paediatric group, though there was a paucity of left-handed flow patterns in the older BAV population (all cases were < 26 years old). In all studies, left-handed flow has not been reported in RL-BAV. The group with left-handed flow in this study was small for meaningful comparison (n=4), but showed a trend towards worse aortopathy, with increased aortic diameters, systolic flow angle, rotational flow and wall shear stress. This may be confounded by coexisting moderate-severe aortic stenosis although flow and wall shear stress values in this group were still increased compared to those with right-handed flow and moderate-severe aortic stenosis. This and the paucity of left-handed flow in the older population might indicate that a left-handed flow pattern is a more severe abnormality, which may necessitate ascending aortic replacement at a younger age. A larger cohort would be necessary to examine this question in more detail.

3.5.6 Aortic function measures

All measures of aortic function and MMP measurements were similar in BAV and healthy volunteers groups suggesting little evidence of an intrinsic aortopathy, in keeping with one previous echocardiography study (77). This is, however, in contrast to four other echocardiography studies which showed differences in ascending aortic function (e.g. elasticity, distensibility) in mainly younger and smaller BAV cohorts (56,78-80). These studies also showed larger sinuses of Valsalva, suggesting that these BAV cohorts may have included the aortic root (sinus) dilation phenotype (thought to involve a genetic intrinsic

aortopathy (81) and not prevalent in our study). This might explain the differences observed. To date, only one study assessed ascending aortic distensibility using CMR in a much younger population (mean age 16 ± 4 years) and showed reduced distensibility and MRSD in BAV patients compared to healthy volunteers (23). Subtle differences may be easier seen in a younger population with high distensibility values than in this study's cohort which included much older participants with naturally reduced distensibility values as well.

3.5.7 Limitations

This study was cross-sectional in design, and cannot identify causative factors with confidence. The longitudinal follow-up study will be more helpful in determining which parameters are predictors for aortic growth and could be used in clinical practice.

The measurement of wall shear stress with 4D flow CMR has relatively low temporal (40ms) and spatial (~2mm^3) resolution (40) and may underestimate the degree of wall shear stress. However, acceptable inter and intra-observer variability were reported in a recent reproducibility study (65) and Barker et al have shown significant results even after adjusting for a maximum error of 10% (64).

Recruitment specifically targeted the RN-BAV sub-type aiming for equal numbers in each group. The proportion of the different fusion types in this cohort does not therefore reflect the distribution in the general BAV population.

3.5.8 Conclusion

Results from this chapter suggest that haemodynamic flow abnormalities caused by BAV are strongly associated with ascending aortic dilation and may be an important aetiological factor in the pathogenesis of this condition. It cannot provide conclusive evidence for a causative effect of flow abnormalities on aortic dilation however, and the longitudinal follow-up study would provide further insight. This study also demonstrated variation in the severity of flow abnormalities and aortic dilation among different BAV fusion types, and this may facilitate risk stratification in BAV aortopathy. These findings further our understanding of the aortopathy associated with BAV, and may allow future selection of patients who benefit from intensified follow-up and earlier surgical intervention.

4 TH CHAPTER: THE EFFECT OF AORTIC VALVE REPLACEMENT ON ASCENDING AORTIC FLOW PATTERNS

4.1 ABSTRACT

4.1.1 Background

Abnormal aortic flow patterns in bicuspid aortic valve disease may be partly responsible for the associated aortic dilation. Aortic valve replacement (AVR) may therefore slow the growth of concomitant aortic dilation via normalisation of flow patterns.

4.1.2 Methods and Results

90 participants underwent 4D flow cardiovascular magnetic resonance: 30 BAV patients with prior AVR (11 mechanical, 10 bioprosthetic, 9 Ross procedure), 30 BAV patients with a native aortic valve and 30 healthy volunteers. The majority of subjects with mechanical AVR or Ross showed normal flow pattern (73% and 67% respectively) with near normal rotational flow values (7.2 ± 3.9 and 10.6 ± 10.5 mm^2/s respectively vs 3.8±3.1 mm^2/s for normal volunteers; both $p>0.05$); and reduced in-plane wall shear stress (0.19 ± 0.13 N/m^2 for mechanical AVR vs. 0.40 ± 0.28 N/m^2 for native BAV, $p<0.05$). By contrast, all subjects with bioprosthetic AVR had abnormal flow patterns (mainly marked right-handed helical flow), with similar rotational flow values to native BAV (20.7±8.8 mm^2/s and 26.6 ± 16.6 mm^2/s respectively, $p>0.05$). Wall shear stress post bioprosthetic AVR showed a similar pattern. Data before and after valve replacement (n=16) supported these findings: mechanical AVR showed a significant reduction in rotational flow (30.4 ± 16.3 $\rightarrow$ 7.3 ± 4.1 mm^2/s; $p<0.05$) and in-plane wall shear stress (0.47 ± 0.20 $\rightarrow$ 0.20 ± 0.13 N/m^2; $p<0.05$), whereas these remained unchanged in the bioprosthetic AVR group.

4.1.3 Conclusion

Abnormal flow patterns in bicuspid aortic valve disease are significantly reduced after mechanical AVR or Ross procedure, though remain similar after bioprosthetic AVR. The type of valve replacement may thus influence post-operative flow patterns, and could have important implications for future aortic growth.

4.2 BACKGROUND

As described in Chapter 1, many BAV patients will undergo aortic valve replacement (AVR) in their lifetime for either aortic regurgitation or aortic stenosis. Chapter 3 describes the haemodynamic impact that helical blood flow may have on aortic growth. Aortic valve replacement may result in more laminar proximal aortic flow. If the haemodynamic flow theory from chapter 3 is correct, straightening the flow through aortic valve replacement may reduce the aortic growth rate. Existing results in the literature are, however, inconclusive. All are retrospective, mostly echocardiographic, studies and included either mainly or only mechanical aortic valve replacement (21,82-86). The rate of aortic aneurysm development after AVR (defined as ascending aortic diameter >4.5cm) during long term follow up is 10-22% (82,86), though the need for ascending aorta replacement after 15 years of follow-up remains low at 1 - 3% (83,84,86). As aortic replacement was a very rare event, it does not give much information about the aortic growth rate of the remainder of the study population. Unsurprisingly, aortic dilation was more likely in patients with enlarged aortas at the time of surgery (86). To date there are few longitudinal studies examining aortic growth rate in BAV patients after valve replacement, with conflicting results (21,85,87,88).

Given the possible pathophysiological effects of the abnormal helical flow on aortic growth in BAV disease, examining the flow patterns in the proximal aorta after valve replacement may provide novel insights. A recent pilot study examined these in mainly tricuspid aortic valve disease (89), and suggested that different types of valve replacement may result in different flow patterns. To date however, no study has assessed the impact of valve replacement on the flow abnormalities specifically in bicuspid aortic valve disease. I

therefore hypothesised that aortic valve replacement may favourably alter flow patterns in the ascending aorta in patients with a bicuspid aortic valve, with the potential consequence of a reduction in future aortic expansion. I also sought to examine the flow patterns after different types of valve replacement (bioprosthetic versus mechanical) to determine if these differ and which therefore might be the preferred type of valve replacement in BAV.

4.3 METHODS

4.3.1 Patient recruitment

This arm of the study aimed to recruit patients with bicuspid aortic valve disease who had undergone or were about to undergo aortic valve replacement. These were identified prospectively from the BAV patient cohort in chapter 3 (any who underwent valve replacement during the course of the study), from cardiology clinics and CMR lists between January 2011 and August 2015. An age and sex-matched sub-set of healthy volunteers from the recruited cohort in chapter 3 were used to provide a comparison. As second control group we also used naïve un-operated bicuspid aortic valve patients matched to the post-operative peak velocity values of the surgical group from the cohort in chapter 3.

4.3.2 Eligibility criteria

4.3.2.1 Inclusion Criteria

Bicuspid aortic valve patients:

i) Patients with previous aortic valve replacement for bicuspid aortic valve disease, or subjects with documented bicuspid aortic valve disease scheduled for aortic valve replacement.

Healthy volunteers:

i) No evidence of cardiovascular disease.

All:

ii) Participant (or legal representative) has capacity and is willing to give informed consent to the research protocol.

iii) Able (in the investigator's opinion) and willing to comply with the main study requirements.

4.3.2.2 Exclusion criteria

See Chapter 2.

4.3.3 Patient enrolment

This arm of the study prospectively enrolled 105 participants:

- AVR group: 45 bicuspid aortic valve patients due for or having previously undergone aortic valve replacement.
- Healthy volunteers: 30 age- and sex-matched healthy volunteers from the cohort in chapter 3
- Native BAV: 30 un-operated bicuspid aortic valve patients matched to the post-operative peak velocity values of the surgical group from the cohort in chapter 3

Any bicuspid aortic valve patients with other complex heart disease such as atrioventricular septal defect, hypoplastic left heart syndrome were excluded and none of the BAV patients were known to have coarctation of the aorta.

From the 45 patients in the AVR group, 7 patients were excluded from the main analysis who underwent concomitant aortic root replacement, 5 patients who underwent aortic valve repair and 3 patients who had MRI contraindications after aortic valve replacement. Prosthetic valve types in the remaining 30 patients were mechanical bileaflet (n=11), bioprosthetic (n=10) or a Ross procedure (n=9). A sub-group of 16 patients also had CMR assessment both pre- and post-operatively allowing comparison of flow patterns before and

after valve replacement. All participants underwent anatomical and haemodynamic CMR assessment as detailed in chapter 2.

4.3.4 General demographics and valve characterisation

The 11 patients with mechanical aortic valve replacement (AVR-mechanical) all had bileaflet tilting disc types - either an ATS Medical valve (23-25mm), n=5; or an ON-X ACE aortic valve (21-27mm), n=6. Valve models in the bioprosthetic aortic valve replacement group (AVR-tissue) were Perimount Magna Ease (23-27mm), n=4; Trifecta (23-27mm) n=4; Hancock II porcine (27mm), n=1 and Mitroflow pericardial (21mm), n=1. General demographics of the different BAV groups and controls are summarised in Table 4-1. The Ross procedure (Ross) group was younger as expected and had a higher regurgitant fraction after surgery. They also had a longer time interval between operation and imaging study. The AVR-tissue group was older. Both the AVR-mechanical and AVR-tissue had significantly higher ascending aortic diameters compared to healthy volunteers (35.9 ± 6.7 and 35.9 ± 4.4 vs 28.6 ± 4.3 mm $p < 0.05$), whereas the Ross group's ascending aortic diameters were similar to the healthy volunteer group.

Table 4-1: Ascending aortic flow pattern parameters by aortic valve replacement subgroup.

	Healthy Volunteers	BAV-native	AVR-mechanical	AVR-tissue	Ross
Total number (male)	30 (23)	30 (23)	11 (10)	10 (9)	9 (8)
Age in years	43±17	42±16	42±12	58±11 *,#	24±12 *,#
Time after operation in months (range)			6 (3-14)	9 (1-37)	126 (1-268)
Indicator for AVR:					
Aortic stenosis			4	7	8
Aortic regurgitation			5	1	1
Both			2	2	
Fusion pattern pre-AVR:					
RL-BAV			7	5	
RN-BAV			2	5	
other			2		

Values are mean ±standard deviation except where indicated; *=p<0.05 compared to healthy volunteers; #=p<0.05 compared to native BAV

4.4 RESULTS

4.4.1 Flow patterns after aortic valve replacement

The distribution of flow patterns is illustrated in Figure 4-2. BAV patients with a mechanical AVR and those who had a previous Ross procedure had a much higher proportion of normal aortic flow patterns (73% and 67% respectively) compared to patients with a native BAV (17%). In contrast, the AVR-tissue group demonstrated abnormal flow patterns in all cases: 8 patients (80%) had a right-handed helical flow pattern, 1 (10%) had a left-handed helical flow pattern and 1 (10%) had a complex flow pattern, showing a similar incidence of abnormal flow pattern compared to the native BAV group.

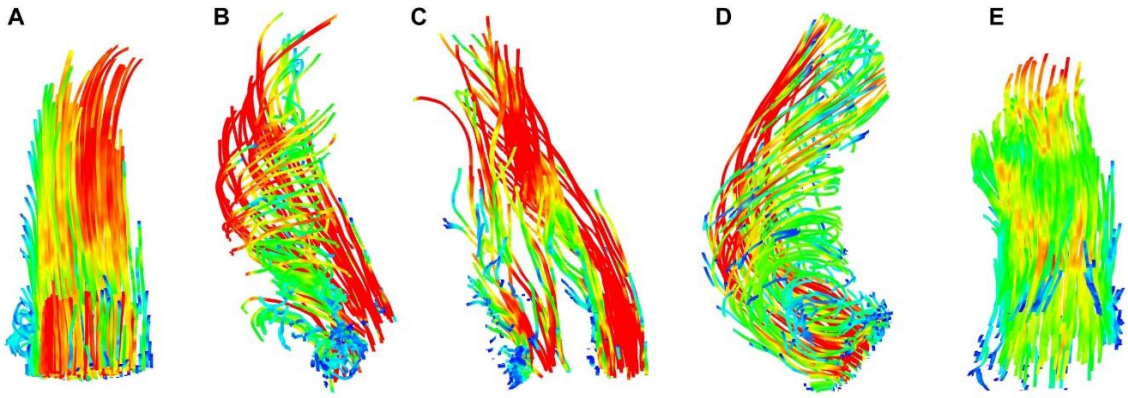

Figure 4-1: Typical ascending aortic flow patterns after aortic valve replacement (AVR); A – healthy volunteer with a laminar flow pattern ; B – native bicuspid aortic valve disease with a right-handed helical flow pattern; C – AVR-mechanical with 2 laminar jets; D – AVR-tissue with a right-handed helical flow pattern; E – AVR-Ross with a laminar flow pattern

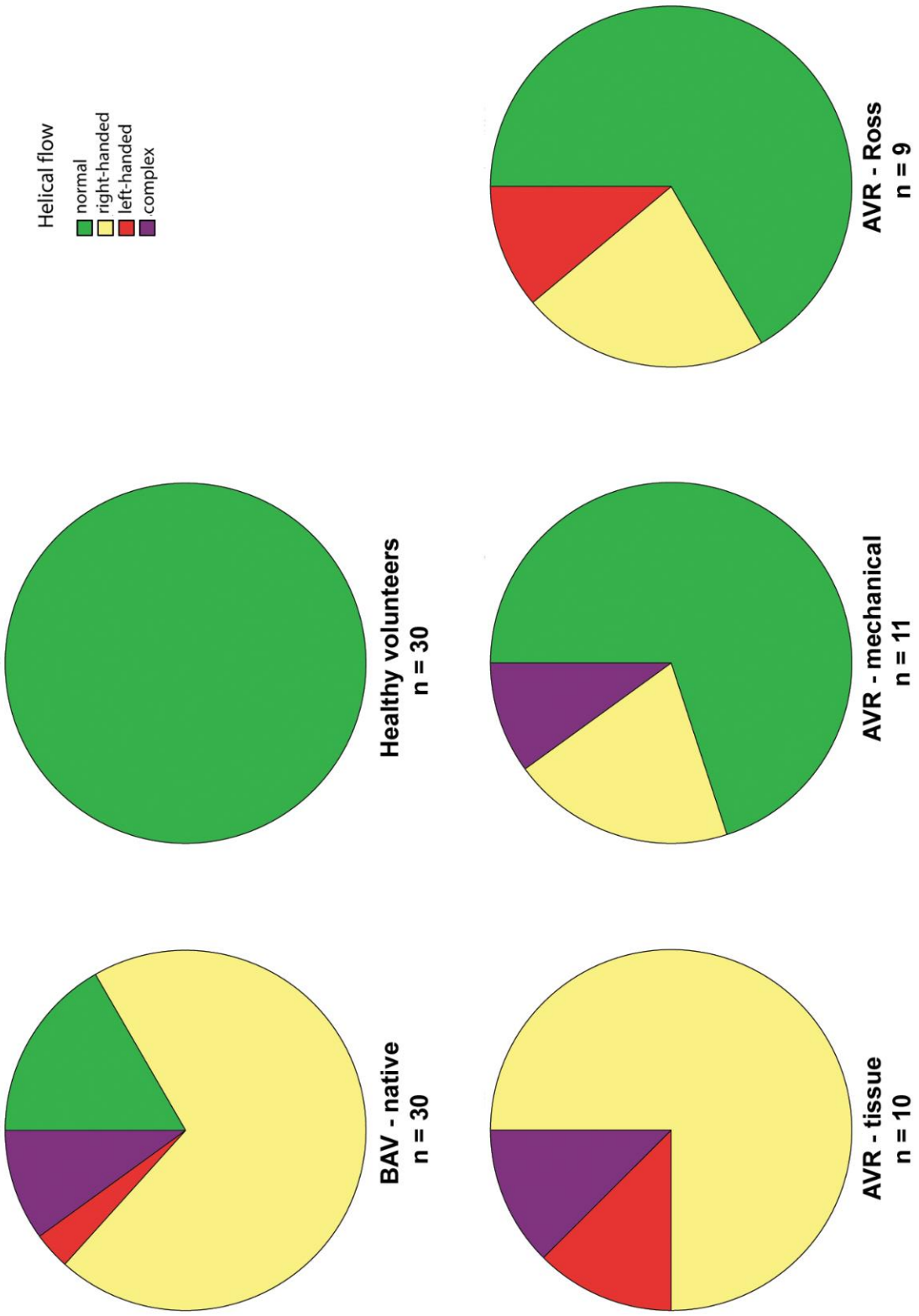

Figure 4-2: Ascending aortic flow patterns after three types of aortic valve replacement, compared to un-operated BAV disease and healthy volunteers

Table 4-2: Ascending aortic flow pattern parameters by aortic valve replacement subgroup.

	Healthy Volunteers	BAV- native	AVR-mechanical	AVR-tissue	Ross
Systolic flow angle (°)	7.5±5.3	25.6±13.3*	16.5±9.6	16.2±8.5	9.8±4.9$^{\#}$
Normalised flow displacement	0.038±0.036	0.133±0.072*	0.083±0.076	0.163±0.064*	0.096±0.067
Absolute rotational flow (mm^2/s)	3.8±3.1	26.6±16.6*	7.2±3.9$^{\#}$	20.7±8.8*	10.6±10.5$^{\#}$
Mean systolic $WSS_{circavg}$ (N/m^2)	0.58±0.15	0.77±0.23*	0.67±0.20	0.68±0.20	0.80±0.35
Absolute systolic in-plane (rotational) WSS (N/m^2)	0.07±0.06	0.40±0.28*	0.19±0.13$^{\#}$	0.38±0.19*	0.21±0.17
Max systolic through-plane WSS (N/m^2)	0.76±0.21	0.95±0.44	0.91±0.38	0.78±0.215	1.03±0.65
RA-LP systolic $WSS_{circavg}$ (N/m^2)	-0.12±0.13	0.22±0.31*	0.27±0.22*	0.36±0.26*	0.24±0.67
Mean peak velocity (m/s)	-	2.3±0.8	2.1±0.5	2.1±0.3	1.9±0.8
Ascending aortic diameter (mm)	28.6±4.3	35.0±6.7*	35.9±4.4*	37.9±5.2*	30.4±8.3
Mean aortic regurgitant fraction (%)	-	8.8±9.9	3.7±2.8	5.8±7.5	22.8±20.6$^{\#}$
Left ventricular ejection fraction (%)	-	68±6	67±15	70±8	65±10

Values are mean (standard deviation) except where indicated; *=p<0.05 compared to healthy volunteers; $^{\#}$=p<0.05 compared to native BAV

The degree of rotational (helical) flow was significantly lower in the AVR-mechanical group, compared to the BAV-native group (7.2 ± 3.9 vs 26.6 ± 16.6 mm^2/s; $p<0.05$), in keeping with the higher proportion of normal flow patterns. Both flow angle and displacement calculation assume that the "normal" flow is along the midline which is not the case after mechanical valve replacement therefore these may be less meaningful parameters in this group.

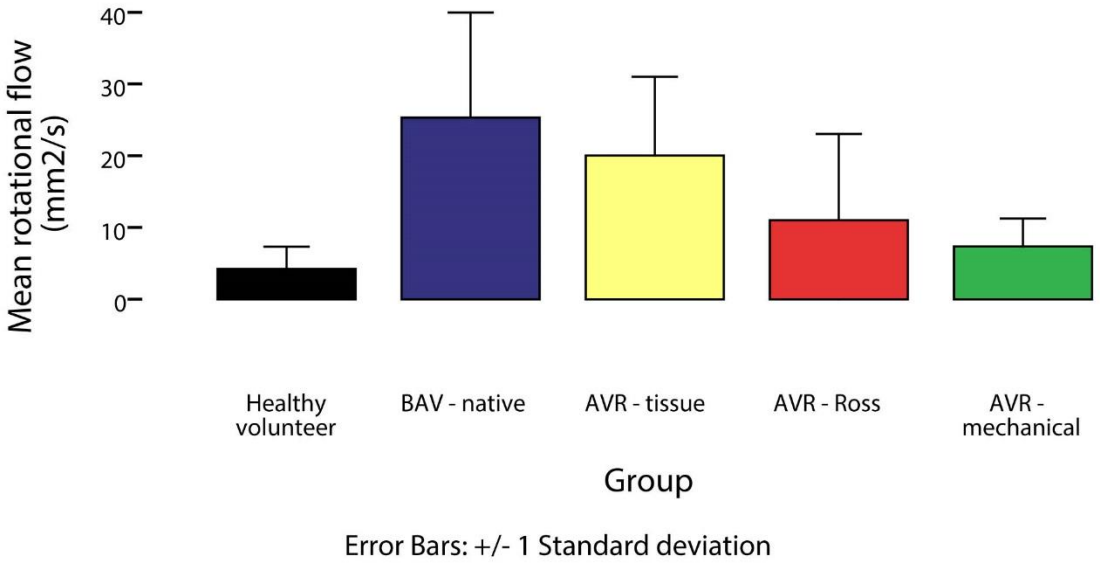

Figure 19: Mean rotational flow – comparison of the different aortic valve replacement groups;

The AVR-tissue group showed higher rotational (helical) flow values, which were similar to the BAV-native group and significantly higher than in healthy volunteers (AVR tissue 20.7 ± 8.8 vs healthy volunteers 3.8 ±3.1 mm^2/s; $p<0.05$). Flow displacement was also increased compared to the healthy volunteer group (0.163±0.064 vs 0.038±0.036; $p<0.05$) and systolic flow angle showed a trend towards higher values compared to the healthy volunteer group.

The Ross group had significantly lower rotational flow values compared to the native BAV-group (10.6 ± 10.5 vs 26.6 ± 16.6 mm^2/s; $p<0.05$) and the flow angle was significantly reduced (10.1 ± 5.7 vs 22.3 ± 13.2°; $p<0.05$). Normalised flow displacement showed a trend towards lower values.

4.4.2 Wall shear stress after aortic valve replacement

In all 3 AVR groups the circumferentially averaged systolic wall shear stress ($WSS_{circavg}$) showed similar values compared to the native BAV group but failed to reach a statistically significant difference from the healthy volunteer group (Table 4-2). The marked right-anterior left-posterior asymmetry in wall shear stress as observed in patients with BAV in chapter 3 was again seen in all BAV groups in this study (Figure 4-3). The AVR-tissue group showed higher in-plane (rotational) wall shear stress, in keeping with the higher degree of helical flow in this group. In-plane (rotational) systolic wall shear stress was significantly *lower* in the AVR-mechanical group, compared to native BAV patients (0.19 ± 0.13 N/m^2 vs 0.40 ± 0.28 N/m^2; $p<0.05$). This is in keeping with the lower degree of helical flow in this group. Through-plane wall shear stress was similar across groups.

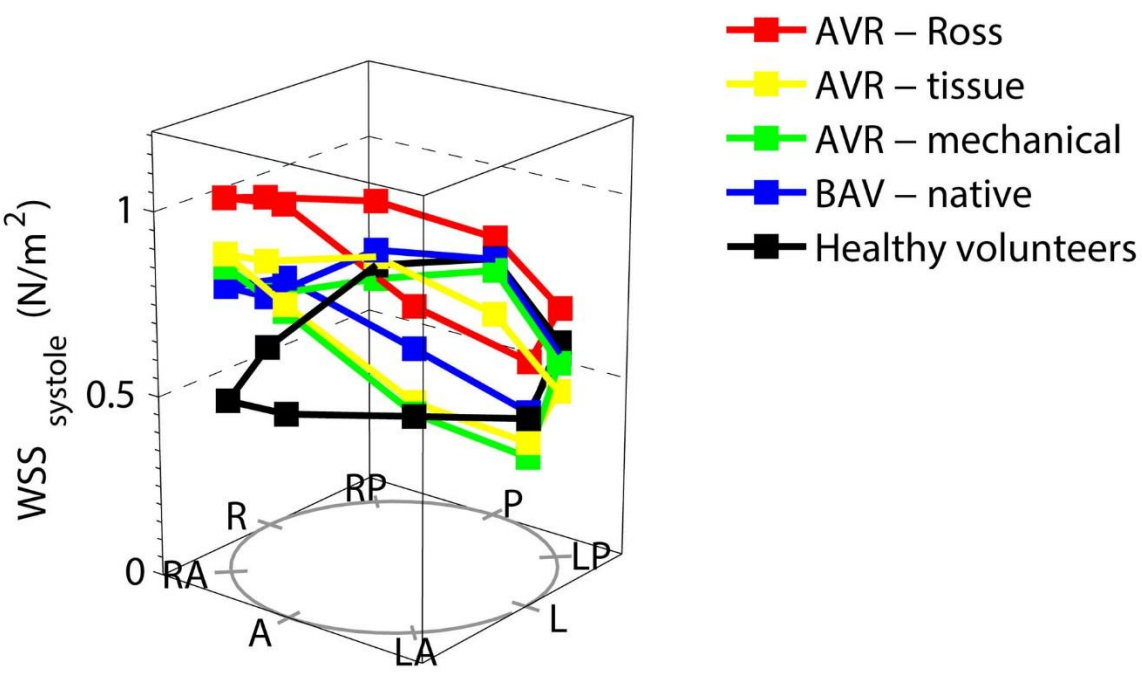

Figure 4-3: Systolic wall shear stress (WSS) after AVR: The anatomical positions are shown at the bottom of the figure. A = anterior (outer curvature); LA= left anterior, L= left, LP= left posterior, P= posterior, RP= right posterior, R= right, RA= right anterior; the height of the dots indicates the WSS value

4.4.3 Changes in flow pattern and wall shear stress after aortic valve replacement

Data was available both pre- and post-aortic valve replacement in 16 out of the 30 patients who attended one study visit before and one study visit after valve replacement (10 patients with mechanical AVR, 6 with a bioprosthetic AVR).

The AVR-mechanical group all had abnormal flow patterns at baseline (7/10 with right-handed helical flow; 3/10 with complex flow), but after aortic valve replacement all flow patterns either normalised (7/10) or showed marked reduction in the helical (rotational) component of flow (3/10). On average the group showed a significant reduction in mean rotational flow values after valve replacement ($30.4 \pm 16.3 \rightarrow 7.3 \pm 4.1$ mm^2/s; $p<0.05$). The

reduction in systolic flow angle and normalised flow displacement did not reach statistical significance. This was accompanied by a reduction in $WSS_{circavg}$ (1.02 ± 0.21 → 0.68 ± 0.21 N/m^2; $p<0.05$), as well as both the individual components, in-plane (rotational) (0.47 ± 0.20 → 0.20 ± 0.13 N/m^2; $p<0.05$) and through-plane wall shear stress (1.43 ± 0.54 → 0.92 ± 0.39 N/m^2; $p<0.05$), and a trend towards reduced right-anterior left-posterior asymmetry.

By contrast, all 6 patients who received a bioprosthetic valve had a residual right-handed helical flow pattern after valve replacement, with no significant change in mean rotational flow, normalised flow displacement or systolic flow angle. Pre-valve replacement these patients had right-handed (n=4) or complex flow patterns (n=2). There was a similar reduction in $WSS_{circavg}$ (1.04 ± 0.20 → 0.70 ± 0.21 N/m^2; $p<0.05$), through-plane wall shear stress (1.47 ± 0.34 → 0.75 ± 0.21 N/m^2; $p<0.05$), and right-anterior left-posterior asymmetry (0.77 ± 0.29 → 0.25 ± 0.27 N/m^2; $p<0.05$), compared to the AVR-mechanical group, but the in-plane (rotational) wall shear stress component was unchanged.

Table 4-3: Comparison ascending aortic flow pattern parameters before and after valve replacement

	AVR-mechanical		AVR-tissue	
	Pre-AVR	Post-AVR	Pre-AVR	Post-AVR
Number	10	10	6	6
Absolute rotational flow (mm^2/s)	30.4±16.3	7.3±4.1*	35.6±23.1	22.2±6.0
Systolic $WSS_{circavg}$ (N/m^2)	1.02±0.21	0.68±0.21*	1.04±0.20	0.70±0.21*
Absolute systolic in-plane WSS (N/m^2)	0.47±0.20	0.20±0.13*	0.56±0.32	0.44±0.19
max systolic through-plane WSS (N/m^2)	1.43±0.54	0.92±0.39*	1.47±0.34	0.75±0.21*
RA-LP systolic $WSS_{circavg}$ (N/m^2)	0.55±0.66	0.28±0.23	0.77±0.29	0.25±0.27*
Systolic flow angle (°)	26.5±9.3	17.1±9.8	23.8±9.4	20.2±7.2
Normalised flow displacement	0.126±0.093	0.069±0.065	0.166±0.053	0.141±0.068
Peak velocity (m/sec)	3.4±1.5	2.0±0.5*	3.7±0.8	2.1±0.4*
Regurgitant fraction (%)	38±19	3±2*	12±14	2±2
Left ventricular ejection fraction (%)	71±9	68±16	75±9	75±5

Values are mean (standard deviation); * = p<0.05 compared to pre-AVR; AVR = aortic valve replacement, RL-BAV = right-left coronary cusp fusion pattern bicuspid aortic valve, RN-BAV = right-non-coronary cusp fusion pattern bicuspid aortic valve

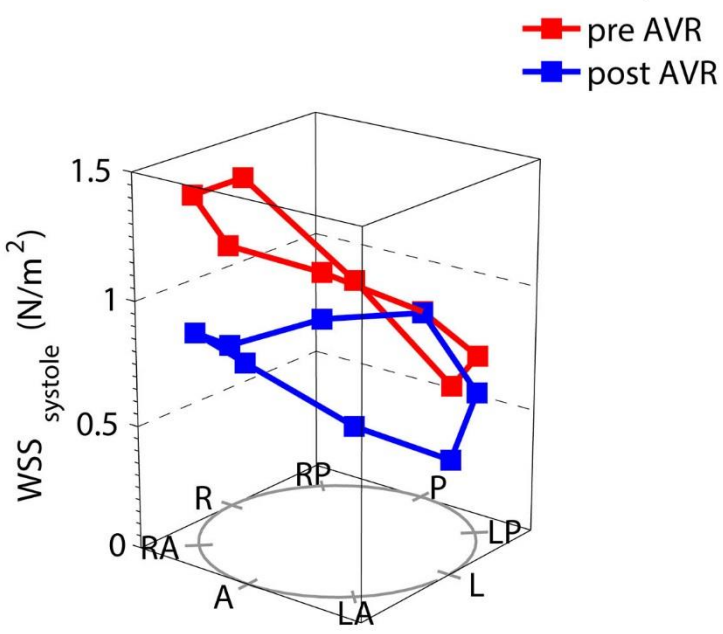

Figure 4-4: Systolic wall shear stress (WSS) before and after mechanical aortic valve replacement: The red line is pre AVR (before aortic valve replacement) and the blue post AVR (after aortic valve replacement). The anatomical positions are shown at the bottom of the figure. A = anterior (outer curvature); LA= left anterior, L= left, LP= left posterior, P= posterior, RP= right posterior, R= right, RA= right anterior; the height of the dots indicates the WSS value

4.5 DISCUSSION

4.5.1 Flow pattern after aortic valve replacement

Abnormal helical flow in bicuspid aortic valve disease is significantly reduced after mechanical valve replacement or Ross procedures - most of the BAV patients in these groups had a normal flow pattern post-operatively. This was supported by the patients in whom pre-operative flow data was available, who demonstrated normalisation or major reduction in abnormal flow after valve replacement. Most patients in the AVR-tissue group still had a pronounced helical flow pattern however, including those with pre-operative flow data who showed little change in rotational flow values post-operatively. The greater reduction in rotational flow and in-plane wall shear stress in the AVR-mechanical (but not the AVR-tissue group) was an interesting finding. One recent pilot study looking at flow patterns after tricuspid aortic valve replacement was supportive of this, and showed that bioprotheses had a higher degree of qualitatively assessed helical (rotational) flow (89). In this study, the 2 patients in the AVR-tissue group with complex flow patterns before valve replacement showed a more organised right-handed helical flow pattern post-operatively, which may reflect in the impact of the bioprosthetic valve. The AVR-tissue group also still had high systolic flow angle and normalised flow displacement values after valve replacement. It is possible that over time the ascending aorta remodels in response to the increased wall shear stresses into the “typical” anteriorly bulging shape (90) and therefore even despite a normalisation of the aortic valve opening with a trileaflet bioprosthetic valve, the orientation of the now asymmetrically angled aorta to the aortic valve annulus continues to contribute to an asymmetric jet resulting in helical flow. By contrast, a

mechanical valve replacement introduces a non- physiological flow of two parallel flow jets arising off centre which reduces the overall rotational (helical) flow, even in the presence of a dilated aorta. The orientation of the bileaflet valve in the AVR-mechanical group may also play a role. However, in this cohort all patients had their mechanical AVR implanted in a R-L orientation in relation to the ascending aorta.

The Ross group also showed significantly reduced helical flow post-operatively but normal ascending aortic diameters, whereas the AVR-mechanical and AVR-tissue groups had diameters similar to the un-operated BAV group. This may be due to the timing of operation, as most of the Ross procedures were completed in childhood and ascending aortic diameter in BAV increases with age. The Ross group also retained more normal aortic flow geometry in the form of lower normalised flow displacement values and near normal flow angles suggesting that a normalisation of flow in childhood/adolescence may prevent the development of a BAV aortopathy.

4.5.2 Wall shear stress after aortic valve replacement

Both the AVR-mechanical and Ross groups showed reduced in-plane (rotational) wall shear stress, likely due to the reduction in rotational flow. In contrast the in-plane (rotational) wall shear stress in the AVR-tissue group remained high. $WSS_{circavg}$ also reduced after valve replacement in the subjects with pre- and post-operative flow data, which is partly due to the reduction in peak velocity leading to a reduction in through-plane WSS, but also be due to the reduced in-plane wall shear stress in the AVR-mechanical group. The asymmetry in wall shear stress values remained post AVR, with highest wall shear stress values in the right anterior (outer) curvature, as is typically seen in un-operated BAV patients, suggesting that

even after valve replacement some of the haemodynamic asymmetry remains. In the group with pre- and post-operative data however, there was a reduction in this wall shear stress asymmetry which is likely mainly due to the reduction in peak velocity leading to a reduction in through-plane wall shear stress.

4.5.3 Clinical implication

The normalisation of flow patterns post AVR seen in some groups in this study may result in reduced future ascending aortic growth. There are few longitudinal studies examining aortic growth after AVR in BAV patients, with differing results. A recent retrospective study of 360 BAV patients after the Ross procedure showed no difference in aortic growth compared to the general population (87). This is the largest follow-up study to date and further supports the hypothesis that haemodynamic flow disturbances drive aortic dilation. The Ross procedure tends to be used in childhood or young adulthood, so the ascending aorta has had fewer years of increased wall shear stress before normalisation of flow. One small echocardiography study of 13 BAV patients after mechanical valve replacement showed a similar growth rate of the ascending aorta post AVR compared to un-operated BAV patients (21); However, two larger studies showed a reduction in aortic growth rate after aortic valve replacement: One involving 70 BAV (type of valve replacement not mentioned) patients showed a reduced aortic growth rate on echocardiography (85). The other study (n=192) with a larger proportion of bioprosthetic valve replacement showed similar aortic growth in BAV and tricuspid aortic valve patients after valve replacement assessed by computed tomography (CT) or CMR (88). The larger studies may be more representative of the general BAV population and CT/CMR measurements of the ascending aorta may be more reproducible.

The differing flow patterns according to prosthetic valve type in this study, with persistent flow displacement and abnormal helical flow in some groups (especially the AVR-tissue group) but normalisation in others, may explain this discrepant findings in the literature regarding progressive aortic dilation after valve replacement in patients with BAV. However, this study cannot rule out, that the majority of patients have an additional underlying intrinsic aortopathy. This could also explain the continued aortic dilation in patients after AVR despite normalisation of flow profiles. As no patient in these studies underwent 4D flow assessment, one cannot comment how the ascending aortic flow profiles correlated with continued growth in one study but not in others.

In keeping with the suggestion that mechanical AVR provides greater normalisation of flow patterns, the 5 patients in this cohort that underwent aortic valve repair/valvotomy did not show any changes in flow patterns post-operatively. A further 5 patients in this cohort who underwent mechanical aortic valve replacement with concomitant ascending aortic replacement showed a similar normalisation of flow abnormalities to the mechanical AVR group, suggesting that the valve replacement introduces a more pronounced change in flow pattern than a change in aortic diameter resulting from aortic root replacement. This is further supported by the finding in two recent small studies, examining flow patterns in BAV patients post valve-sparing root replacement, showing that significant abnormal rotational flow remains (91,92).

4.5.4 Limitations

Patient numbers in this study were relatively small and not all patients, particularly the Ross group, had data available both before and after aortic valve replacement. In the mechanical

and bioprosthetic groups different models of aortic valve prosthesis were used and it is feasible that there are differing flow patterns associated with different valve models. However, both mechanical valve models were of a very similar design (bileaflet tilting disc type). In addition, almost all bioprosthetic valves have a similar shaped valve, which is designed to be as close as possible to the native trileaflet valve.

The interval between valve replacement and CMR assessment also varied between 1 month and 22 years in the Ross group, and up to 3 years in other AVR groups. The AVR groups had different age ranges - very young patients tend to undergo a Ross operation whereas older patients more often opt for a bioprosthetic rather than a mechanical valve, and age may influence flow patterns through differences in aortic shape and stiffness.

4D flow MRI is a new imaging technique but measures such as wall shear stress have been validated, even though the true wall shear stress is likely to be higher than the measured value, due to limited spatial resolution, as discussed in chapter 3 (section 3.5.7). This cross-sectional study is unable to assess the impact of flow normalisation on aortic growth rate, for which further longitudinal follow-up will be necessary.

4.5.5 Conclusion

Abnormal helical flow in bicuspid aortic valve disease is significantly reduced after mechanical valve replacement or Ross procedures. Following bioprosthetic valve replacement, however, the degree of helical flow pattern remained similar to un-operated and pre-operative values. These findings suggest for the first time that the type of valve replacement influences aortic flow patterns in BAV. The type of valve replacement could potentially affect future aortic growth rate post-surgery.

5 TH CHAPTER: HEREDITARY PATTERNS IN BICUSPID AORTIC VALVE DISEASE

5.1 ABSTRACT

5.1.1 Background

Bicuspid aortic valve (BAV) is known to be heritable and often shows a concomitant aortopathy which was thought to also be present in some family members. Little is known about aortic function in such family members.

5.1.2 Methods

253 participants were prospectively enrolled: 57 patients with BAV, 142 of their first degree relatives and 54 healthy volunteers. Participants over 6 years of age underwent CMR, and those under 6 years echocardiography. Advanced aortic assessment included aortic diameters, pulse wave velocity, arterial stiffness, maximum rate of systolic dysfunction (MRSD) and distensibility by CMR, total peripheral resistance (TPR) by Vicorder© as well as circulating matrix metalloproteinase (MMP) 2 and 9 from a peripheral blood sample. A subset of 10 family members also underwent comprehensive 4D flow MRI assessment.

5.1.3 Results

12% family members were found to have a BAV. 101 family members with a normal functioning tricuspid aortic valve underwent further CMR assessment. Compared to sex, age and blood-pressure matched healthy volunteers all family members had significantly smaller sinus, ascending and descending aortic diameters (Sinuses: healthy volunteers 16.8±2.2 vs relatives 15.5±1.9 mm, $p<0.05$; sinotubular junction: healthy volunteers 15.1±2.1 vs relatives 13.8±1.8 mm, $p<0.05$; ascending aorta: healthy volunteers 15.3±2.2 vs relatives

14.4±2.1 mm, $p<0.05$). There was no difference in pulse wave velocity, ascending, proximal and distal descending aortic strain, MRSD and distensibility, TPR as well as circulating MMP2 and MMP9. In the subset of family members undergoing advanced 4D flow MRI assessment, there was no difference in flow angle, rotational flow and wall shear stress compared to healthy volunteers.

5.1.4 Conclusion

Family members with (normal) trileaflet aortic valves of patients with a bicuspid aortic valve have normal aortic size and function. These findings point towards the importance of haemodynamic factors rather than an additional haemodynamics-independent mechanisms in bicuspid aortic valve patients' aortopathy.

5.2 BACKGROUND

Aortic dilation is very common in patients with BAV and increases with age, affecting up to 80% of patients with BAV (1). As described in chapter 1 (section 1.2), there has also been concern that first-degree family members of BAV patients have a tendency towards aortic dilation, despite an apparently normal valve, which is in keeping with the intrinsic aortopathy theory. Biner et al (8) showed in a recent echocardiographic study including 54 BAV patients and 48 of their first-degree relatives with tricuspid valves, that 1 in 3 relatives manifested an aortic dilation phenotype. Loscalzo et al (93) identified at least one family member with a thoracic aortic aneurysm (despite an apparently normal, tricuspid valve) in all of 13 families of patients with BAV associated with aortic dilation. Therefore the American College of Cardiology (ACC) and the American Heart Association (AHA) guidelines are suggesting screening in first-degree relative of a patient with BAV especially if an aortopathy is present in the patient (11). This could have far-reaching clinical and health economic consequences as aortic dilation develops with age and potentially repeated screening of all first-degree relatives would be necessary. Therefore characterisation of a potential aortopathy and identification of potential makers for risk stratification in BAV relatives is as an important arm of this thesis.

5.3 METHODS

5.3.1 Patient recruitment

Family members were recruited indirectly via the patient cohort from chapter 3. During the study visit the patient was invited to pass on the information about family screening in this study. If the family members were interested in taking part in the study, they contacted myself directly. Healthy volunteers were taken from the cohort in chapter 3 and additionally recruited from posters within the hospital and University buildings, and were free from any known significant medical problems. The healthy volunteers were age and sex-matched at time of recruitment.

5.3.2 Eligibility criteria

5.3.2.1 Inclusion Criteria

Relatives:

i) Have a tricuspid aortic valve.

ii) A family member has bicuspid aortic valve spectrum disease

Healthy volunteers:

iii) No evidence of cardiovascular disease

All:

iv) Participant (or legal representative) has capacity and is willing to give informed consent to the research protocol.

v) Able (in the investigator's opinion) and willing to comply with age appropriate main study requirements.

5.3.2.2 Exclusion Criteria

See chapter 2.

5.3.3 Patient enrolment

142 first degree relatives from 57 families were prospectively enrolled. 117 underwent CMR assessment at 1.5 Tesla. The remaining 25 underwent echocardiography assessment as they were either children less than six years of age or were adults unable to tolerate the MRI scan due to claustrophobia as discussed in chapter 2. As patients with BAV have shown significant haemodynamic flow abnormalities, a subset 10 relatives with a tricuspid aortic valve also underwent advanced 4D flow MRI assessment. These relatives were from families enriched with BAV. Nine family members completed the 4D flow assessment. One elderly family member did not complete the 4D flow assessment as the 2nd CMR scan was too long for her to complete.

5.4 RESULTS

5.4.1 Bicuspid aortic valve inheritance patterns

Of 142 relatives 17 (12 %) were found to have a BAV. This was diagnosed with CMR in 15 cases and echocardiography in 2 cases (child age < 6 years and claustrophobic adult). These 17 relatives spread over 10 families.

5.4.2 Bicuspid aortic valve fusion pattern

In 5 of 10 families there was a concordant pattern of cusp fusion seen in all affected members (RL-BAV in 4 families, RN-BAV in 1 family). In the remaining 5 families, there was discordance in the spatial arrangement of leaflets (Figure 5-1) including RL-BAV, RN-BAV and a unicuspid aortic valve in one family.

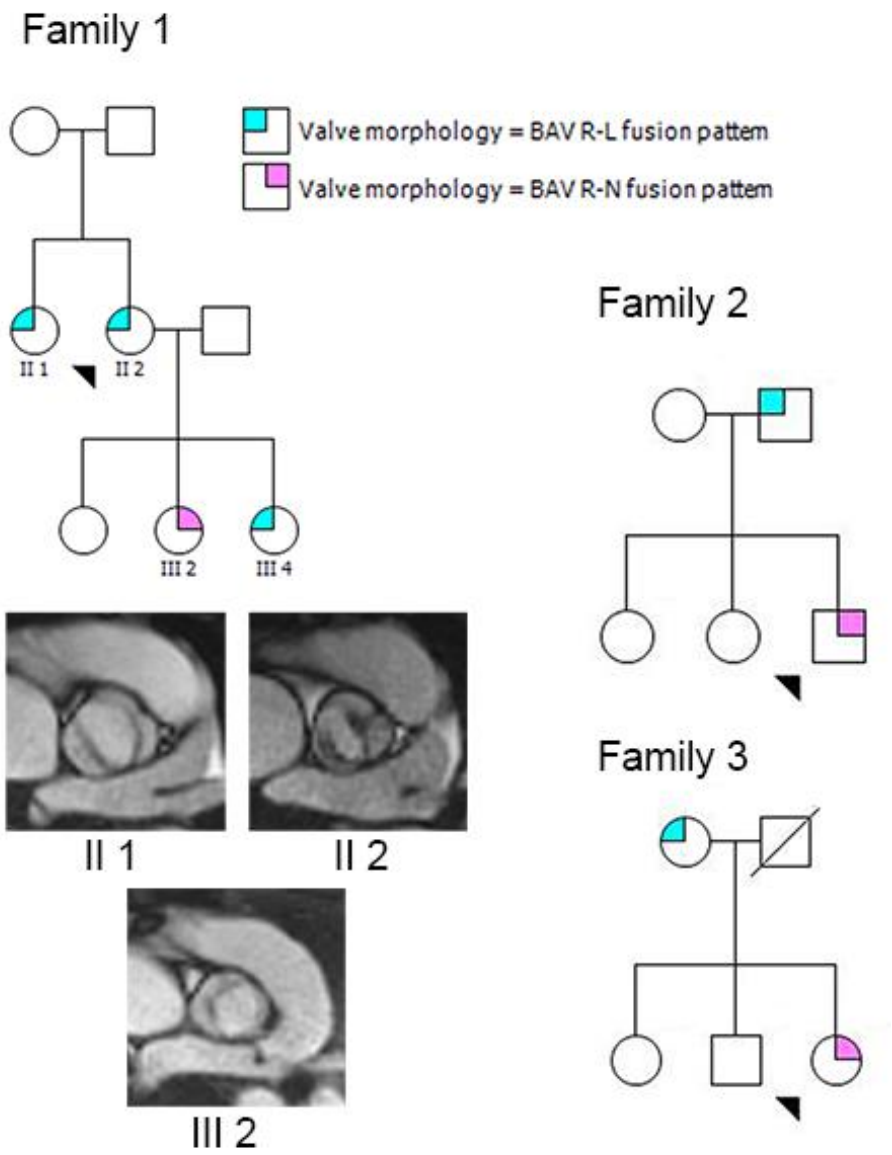

Figure 5-1: Discordant inheritance of bicuspid aortic valve fusion type

When looking at the frequency of fusion pattern, RL-BAV was observed in 77% of cases and RN-BAV in 19% of cases. This was similar to the incidence seen in the general BAV population. Interestingly, we also observed variability in the extent of leaflet fusion in two families (Figure 5-2). In the remaining families the fusion was complete.

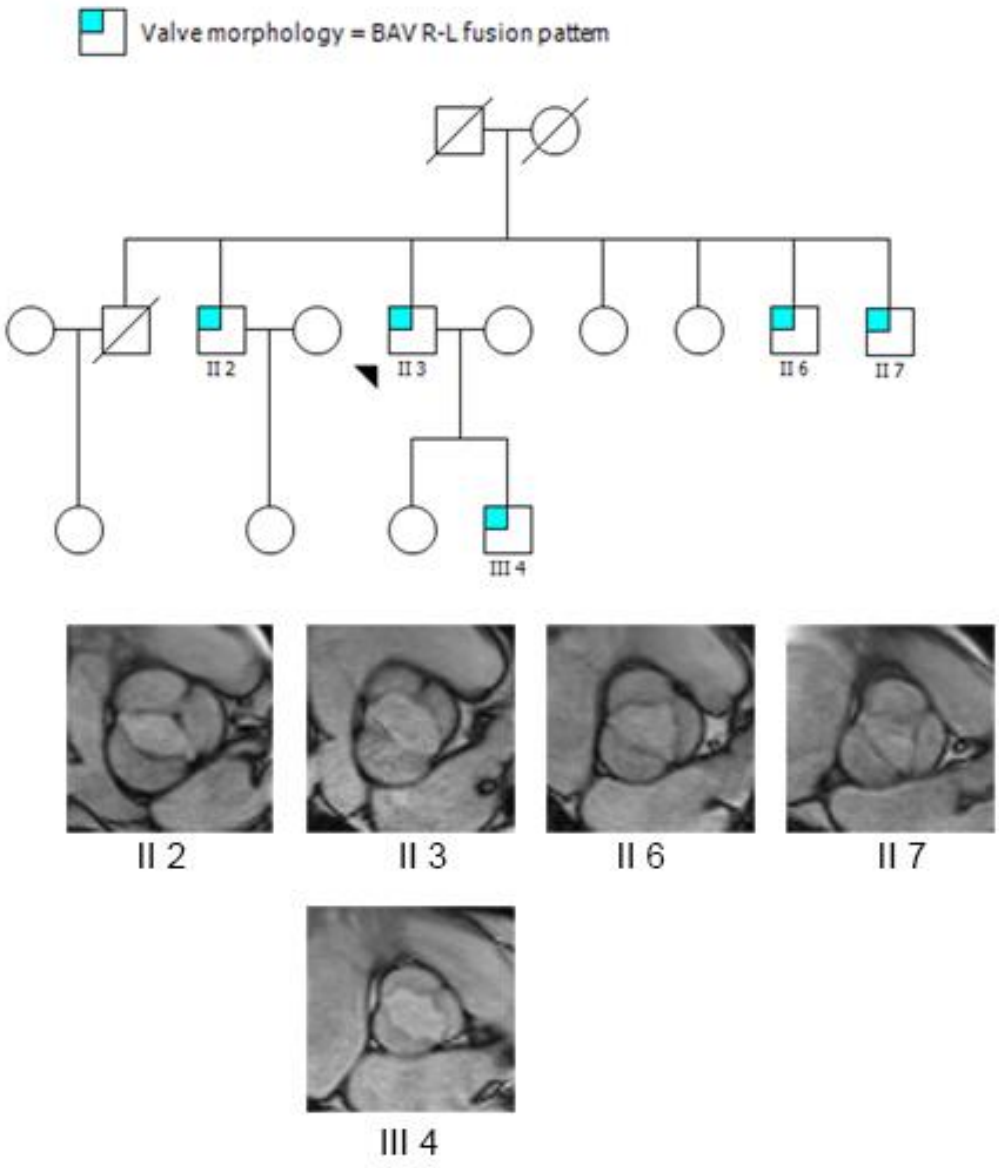

Figure 5-2: Variable degree of leaflet fusion within one family

5.4.3 The ascending aorta in family members

The ascending aorta was assessed in 117 first degree relatives undergoing advanced CMR imaging. Our index BAV patients had ascending aortic dilation in 16 cases of whom no patient had an aortic root dilation phenotype. 5/15 relatives with a bicuspid aortic valve showed concomitant aortic dilation. In contrast no relatives with a tricuspid aortic valve had ascending aortic dilation. These 101 relatives with a tricuspid aortic valve underwent

extensive CMR aortic functional assessment. For comparison we recruited 54 age-and sex matched healthy volunteers. The tricuspid aortic valve was normally functioning in all relatives. The average age was 38.7 years (range 6-90) with a mean pulse pressure 57±1.14 mmHg.

Compared to sex, age and blood-pressure matched healthy volunteers all relatives had normal aortic diameters in the descending aorta. The sinuses, the sinotubular junction (STJ) and ascending aorta (AA) were significantly smaller than in the healthy volunteers (Sinuses: healthy volunteers 16.8±2.2 vs relatives 15.5±1.9 mm, $p<0.05$; STJ: healthy volunteers 15.1±2.1 vs relatives 13.8±1.8 mm, $p<0.05$; AA: healthy volunteers 15.3±2.2 vs relatives 14.4±2.1 mm, $p<0.05$) (Table 5-1). On aortic function assessment there was no difference in arch or descending pulse wave velocity, distensibility, compliance, aortic stiffness and aortic strain in relatives compared to healthy volunteers (Figure 5-3). Further vascular parameters such as total peripheral resistance were also comparable between the groups.

Table 5-1: Demographics and aortic vascular function measures in healthy volunteers and first degree relatives with a tricuspid aortic valve

	Healthy volunteers	First degree relatives
Total number	54	101
Age (years)	39±19	39±19
Pulse pressure (mmHg)	55±7	57±11
Total peripheral resistance (pru)	1.06±0.40	1.03±0.35
Aortic diameter/BSA (mm/m^2):		
Sinuses	16.8±2.2	15.5±1.9*
Sinotubular junction	15.1±2.1	13.8±1.8*
Ascending aorta	15.3±2.2	14.4±2.1*
Proximal descending aorta	11.1±1.6	10.9±1.6
Distal descending aorta	9.9±1.6	9.3±1.7
Distensibility (1 / mmHg):		
Ascending aorta	4.84±3.28	5.29±3.64
Proximal descending aorta	4.91±2.05	5.08±2.95
Distal descending aorta	7.43±3.65	7.39±3.96
Arterial strain:		
Ascending aorta	0.22±0.13	0.24±0.16
Proximal descending aorta	0.23±0.09	0.23±0.11
Distal descending aorta	0.34±0.14	0.33±0.15
Maximum rate of systolic distension (%/ms):		
Ascending aorta	0.22±0.13	0.23±0.13
Proximal descending aorta	0.21±0.09	0.21±0.11
Distal descending aorta	0.27±0.07	0.28±0.11

Values are mean ±standard deviation; *p<0.05; BSA = body surface area

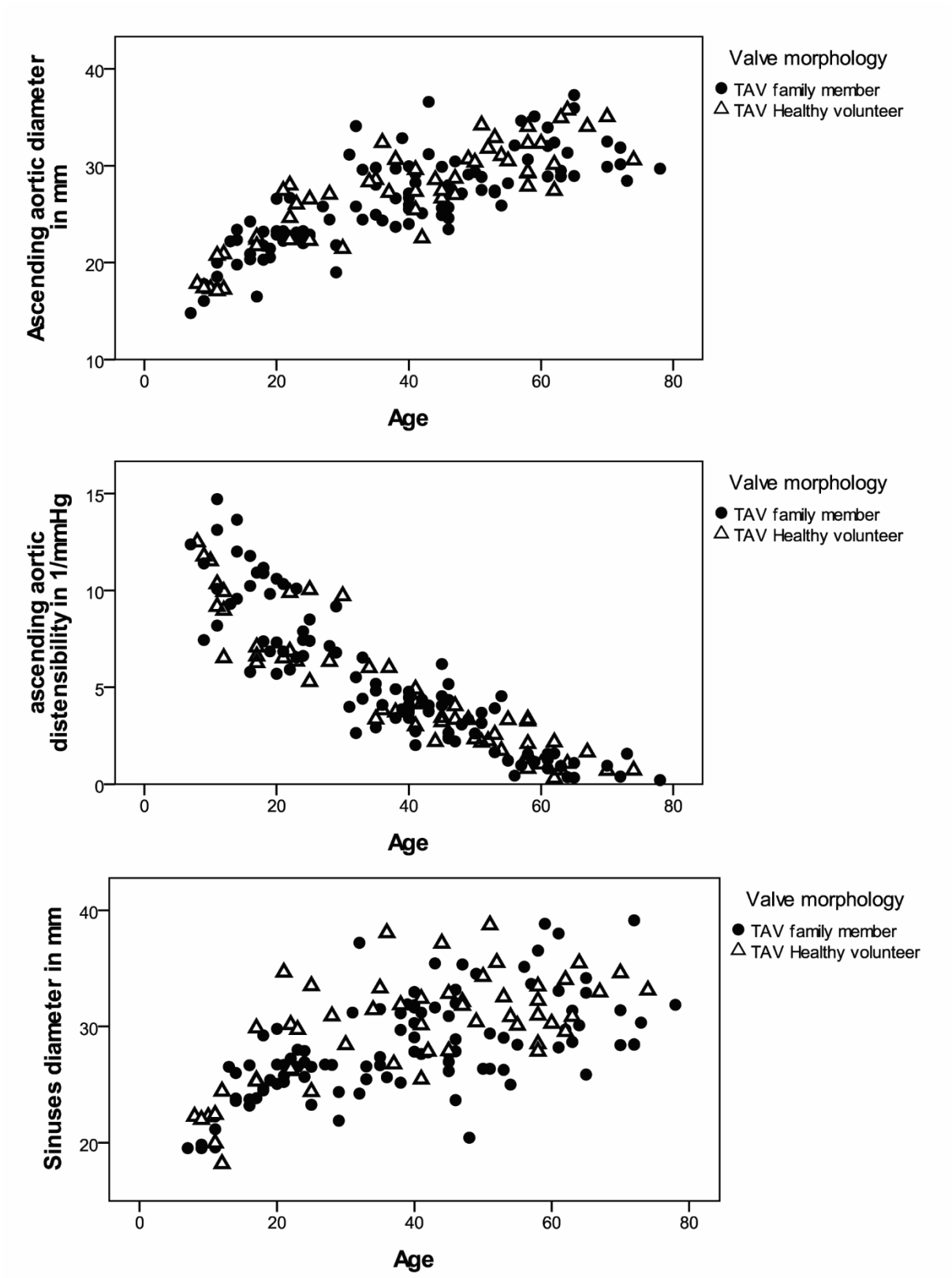

Figure 5-3: Aortic diameters, distensibility and MRSD in healthy volunteers and family members with a tricuspid aortic valve (TAV)

5.4.4 4D flow MRI assessment

All 9 family members who underwent 4D flow imaging had laminar flow on visual assessment and no eccentric flow was observed. Only one father had mildly elevated rotational flow values with otherwise normal haemodynamic parameters. Overall there was no difference in rotational flow values, flow angle and wall shear stress values (Table 5-2, Figure 5-4).

Table 5-2: Advanced haemodynamic flow parameters in healthy volunteers and first degree relatives with a tricuspid aortic valve

	Healthy Volunteers	First degree relatives
Total number	47	9
Systolic flow angle (°)	7.8±5.4	8.8±4.2
Absolute rotational flow (mm^2/s)	3.6±3.3	6.5±8.2
Mean systolic $WSS_{circavg}$ (N/m^2)	0.59±0.17	0.69±0.21
Absolute systolic in-plane (rotational) WSS (N/m^2)	0.08±0.08	0.07±0.05
Maximum systolic through-plane WSS (N/m^2)	0.73±0.20	0.86±0.26
RA-LP systolic $WSS_{circavg}$ (N/m^2)	-0.11±0.18	-0.14±0.24

Values are mean ±standard deviation; WSS = Wall shear stress

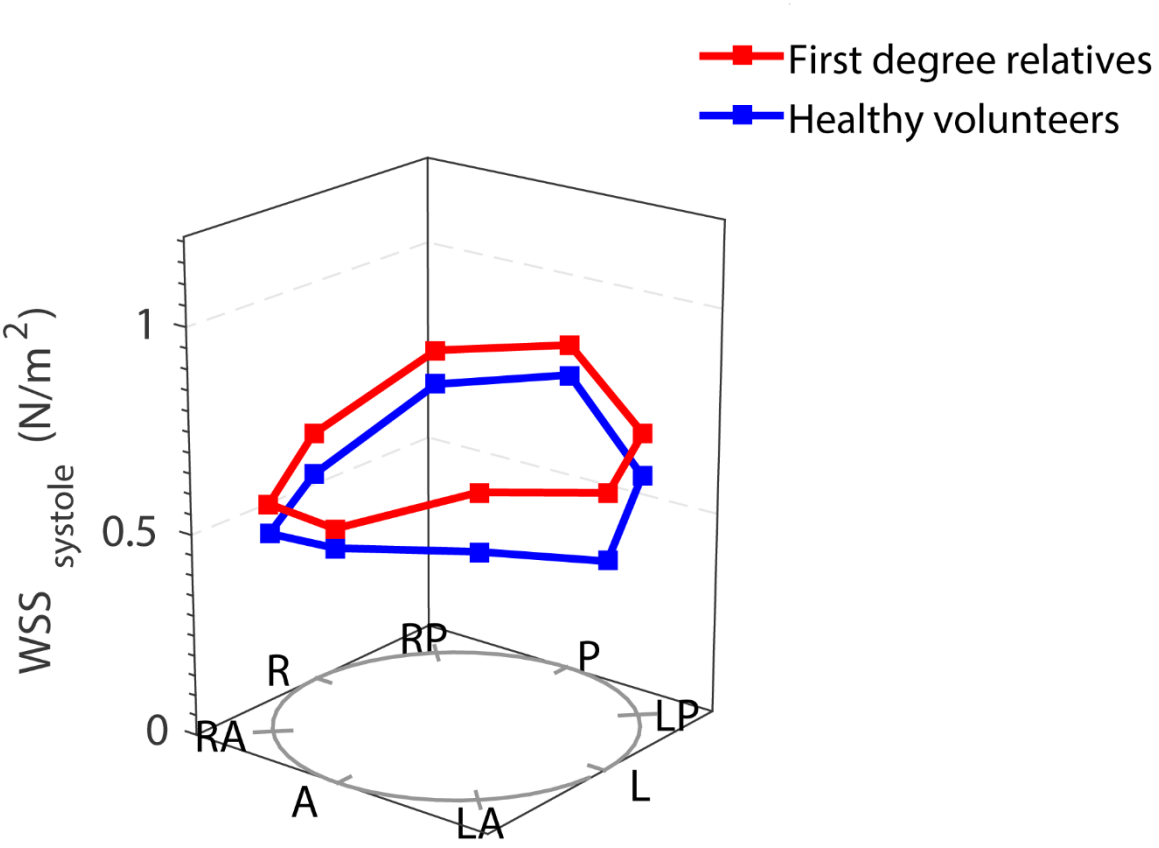

Figure 5-4: Systolic wall shear stress (WSS in relatives): The anatomical positions are shown at the bottom of the figure. A = anterior (outer curvature); LA= left anterior, L= left, LP= left posterior, P= posterior, RP= right posterior, R= right, RA= right anterior; the height of the dots indicates the WSS value

5.4.5 Circulating biomarkers

84 patients and 47 healthy also underwent peripheral blood sampling to measure MMP2 and MMP9 concentrations. Both MMP2 and MMP9 concentrations in relatives were comparable to the healthy volunteer group (Table 5-1).

5.5 DISCUSSION

5.5.1 Bicuspid aortic valve in family members

In our cohort 12% relatives were found to have a bicuspid aortic valve which is within the 9-25% reported by previous studies (6,8,9). Unlike the animal models, fusion pattern was discordant within several of our families, suggesting that these may not be distinct entities in humans. This is in line with two other recent studies showing similar discordant inheritance of BAV fusion pattern (7,94). However, BAV is clearly heritable, and it may be that genetic factors can influence the type of fusion pattern, as RN-BAV is more frequently associated with aortic stenosis in childhood (15) and RL-BAV is associated with coarctation of the aorta and the aortic root dilation phenotype (16). It may be plausible that an interplay of several unknown genes causes a bicuspid aortic valve in the majority of patients where a BAV is sporadic within the family suggesting complex autosomal recessive inheritance. In families with clear autosomal inheritance it may be that a "strong BAV gene" is inherited that causes a bicuspid aortic valve either on its own or with little help from a small number of additional genes close by.

5.5.2 Aortic dilation in family members

In this cohort, only 16/57 index patients had aortic dilation. Of the 10 families with at least one family member affected with BAV, only 2/10 index patients had aortic dilation and would have been eligible for family screening under the most recent AHA guidelines. The AHA Guidelines in 2010 suggested screening all family members for aortic dilation (30) but the 2014 guidelines only suggest screening if the index patient has an associated aortopathy

or a positive family history (11). While 5/15 relatives with a newly diagnosed BAV had aortic dilation, aortic dimensions were within normal limits in all other relatives with a tricuspid aortic valve.

Della Corte et al suggested (13,14) that the aortopathy in BAV can be subdivided into subgroups. They especially identified the aortic root phenotype with no ascending aortic dilation which mainly occurs in young males with RL-BAV and has an increased incidence of aortic regurgitation (13). Here the aortopathy is thought to have a more genetically underlying component. Embryologically this is conceivable as the aortic valve and aortic root evolve from the same cell type, whereas the ascending aorta has a separate embryonic origin (95) and haemodynamic flow abnormalities are observed higher up in the ascending aorta. This is in keeping with Binner et al's study where the majority of BAV patients had the aortic root phenotype with dilation of the aortic root alone and normal ascending aortic diameters (8). The 32% of relatives also showed root dilation with normal ascending aortic dimensions compared to HV. Interestingly, the BAV population in this study did not include any patients with the aortic root phenotype and was therefore more comparable to the recent study by Robeldo-Carmona et al which reported a very low incidence of aortic dilation among relatives (4%) (94) and Dyan et al who reported normal ascending aortic diameters in all relatives (96). These results further suggest that in the majority of BAV patients with ascending aortic dilation, the underlying pathology is driven by haemodynamic forces and not seen in relatives with normal aortic haemodynamics. However, Loscalzo et al showed a very high incidence of thoracic aortic aneurysms (TAAs) in the reported families. But all families presented to hospital due to TAAs rather than BAV (93) suggesting that an overlapping phenotype, with a similar genotype may exist, strengthening the argument towards an underlying intrinsic aortopathy. On the other hand, it may also be possible that

in this cluster of families identified from TAA clinics, the BAV was an additional genetic entity in these families with inherited TAA phenotypes rather than part of variable penetrance of the same genotype. Furthermore, a recent genetic study did not find any conclusive heritability for aortic dilation (97). Normal advanced aortic function assessment, normal haemodynamic flow assessment and normal circulating MMPs seen in this study further imply that relatives with a tricuspid aortic valve do not have any underlying inherited aortopathy.

5.5.3 Clinical significance

While BAV is heritable, a clinically significant aortopathy is rare in relatives with a tricuspid aortic valve. While one cannot rule out a subtle underlying aortopathy, no relative with a tricuspid aortic valve had an abnormally large aorta, even in the older population. This suggests that screening for a BAV alone should be sufficient and aortic assessment only becomes clinically indicated if a bicuspid aortic valve is found. If the decision for universal screening of family members for a BAV is made, one also needs to consider screening relatives of patients with partially fused cusps as two of our families showed variance in the degree of fusion pattern suggesting that partial fusion is a mild form of BAV.

This study cohort further supports the growing evidence that the aortic dilation in the ascending aortic phenotype is largely caused by haemodynamic flow abnormalities. This further suggests that in these patients, relatives with a tricuspid aortic valve need no further follow-up screening for a potentially evolving aortopathy. However, this may be different in the aortic root phenotype, which was not assessed in this thesis. Here family screening for

aortic dilation even in relatives with a tricuspid aortic valve may still be indicated as suggested by the current 2014 ESC guidelines (98).

5.5.4 Limitations

This cross-sectional study did not record any longitudinal data to assess differences in aortic growth rate in relatives. There may have been a selection bias in the recruitment of family members as these were indirectly recruited. This BAV cohort did not include any BAV patients with the aortic root phenotype which was therefore not assessed. It is difficult to assess a subtle intrinsic aortopathy. Gold standard would be histological assessment of aortic tissue which is not possible in healthy individuals. Surrogate aortic function measures are highly dependent on age (99) but we age- matched our healthy volunteers to our relatives cohort. We only assessed a small number of relatives with 4D flow MRI as a pilot study. As results of the pilot study were normal, I did not pursue this time intensive avenue further. However, subtle differences may only show in a much larger cohort.

5.5.5 Conclusion

While BAV is heritable, the fusion pattern is variable among family members. This study found no evidence of aortopathy in the relatives' cohort. These findings further point towards the importance of haemodynamic factors rather than additional haemodynamic-independent mechanisms in the aortopathy of bicuspid aortic valve patients. This suggests that further screening may not be indicated if a family member is found to have a tricuspid aortic valve. However, this may be different in the rarer aortic root phenotype BAV which

may have an underlying genetic element and where serial family screening for aortopathy may still be indicated.

6 TH CHAPTER: GENERAL CONCLUSIONS AND FUTURE WORK

6.1 BICUSPID AORTOPATHY – A CHANGING PATHOPHYSIOLOGY

At the beginning of this thesis the BAV aortopathy was believed to be intrinsic, similar to Marfan syndrome. Results in this thesis and other recent publications suggest that the flow pattern in the ascending aorta is a major contributor to the aortopathy in BAV (64,74,100,101). The proposed pathophysiology based on the results of this thesis is the following: The restricted leaflet opening of a bicuspid aortic valve, even when functioning normally, causes an asymmetrical flow jet which hits the aortic wall in the ascending portion of the aorta, leading to marked rotational (helical) flow. This abnormally high rotational (helical) flow is associated with increased ascending aortic diameters. Part of the proposed mechanism includes increased wall shear stress, which remains high in patients with BAV irrespective of ascending aortic diameter. This is in contrast to healthy volunteers where the wall shear stress decreases with increasing aortic diameters (102). To date there is a lack of prognostic follow-up data. Only one small study with 13 BAV patients showed increased aortic growth rate with increased normalised displacement, but not with increased wall shear stress (103). While numbers are small this may further support the theory that wall shear stress is instrumental in the pathophysiology of BAV aortopathy, but the dilation happens in response to the increased wall shear stress, only getting large enough to keep the wall shear stress values stable.

The differing components of wall shear stress may also play an important part – the results of this thesis as well as other current studies stipulate that in-plane (around the aortic circumference, or ‘rotational’) wall shear stress is a larger contributor to the aortic dilation in BAV than through-plane wall shear stress (parallel to the long axis of the aorta) (74,101). In-plane wall shear stress is negligible in healthy volunteers, but significantly increased in

BAV patients, even in young patients with normal ascending aortic diameters, normal valve function and resulting normal through-plane wall shear stress, suggesting that the increased wall shear stress precedes aortic dilation (74). Furthermore, in this study, the Ross group with normal ascending aortic diameters had the highest $WSS_{circavg}$ and through-plane wall shear stress. However, the in-plane wall shear stress was normal in most cases, potentially further supporting the importance of in-plane wall shear stress in the pathophysiology of aortic dilation.

While an underlying aortopathy or genetic predisposition cannot be excluded, a recent study closed the gap between the haemodynamic theory and documented histopathological changes in the ascending aorta. This study assessed 20 patients undergoing ascending aortic replacement with advanced 4D flow CMR. Histopathological analysis showed changes (such as reduced elastin) in excised aortas from BAV patients only in areas with high wall shear stress but not in areas with normal or low wall shear stress (104). This might also explain the earlier histological findings that led to the conclusion of an intrinsic aortopathy (19,25-29). The lack of aortopathy in first degree relatives with a tricuspid aortic valve as well as normal aortic function measures in our BAV cohort further suggest that an underlying intrinsic aortopathy may be very mild and not as clinically significant.

These advances have altered the widespread understanding of the pathophysiology in BAV aortopathy (105) and have contributed to the change of the most recent AHA and ESC guidelines in 2014, now suggesting aortic replacement in BAV patients similar to the normal population when the diameter reaches 5.5 cm rather than 4.5-5 cm as advised in Marfan syndrome with a clear intrinsic aortopathy (11,98). This new understanding of the haemodynamic pathophysiology may however not apply to the aortic root phenotype,

which may have a more pronounced intrinsic aortopathy. But this subtype has not been part of this thesis.

6.2 FUTURE WORK

6.2.1 Longitudinal follow-up study

I am currently undertaking a 3 year CMR follow-up study of all enrolled BAV patients who underwent 4D flow MRI during the first study visit.

I hope that by showing the causal link between abnormal flow patterns and aortic dilation, this may improve clinical management by

1) Identifying targets for new treatments such as early valve replacement in high risk groups to normalise flow patterns and reduce the risk of future aortic dilation
2) Identifying those patients who are most likely to develop progressive aortic dilation who may benefit from closer more regular CMR follow-up and/or targeted treatment
3) Identifying those patients with little or no progressive aortic dilation that require less frequent follow up of their ascending aorta with advanced imaging such as CMR and can be monitored for their valve disease using echocardiography
4) Assess whether mechanical AVR may be superior to bioprosthetic AVR in BAV patients with concomitant aortopathy in reducing aortic growth rate post-surgery

Risk assessment by cardiac imaging is well established for many other forms of cardiovascular disease, and recent advanced in CMR techniques such as 4D flow MRI make it timely to apply this approach to BAV. I believe that CMR will be able to predict progressive aortic dilation and prove useful for risk stratification of BAV aortopathy.

6.2.2 BAVCon - Genetics consortium

To further delineate the complex genetic inheritance pathways in bicuspid aortic valve disease, I have joined the BAVCon consortium as the cardiac MRI lead. The aim is to enrol 6000 BAV patients within North America and Europe. An initial 1000 patients have undergone genome wide association studies. Promising loci from this initial study are now being tested in the remaining BAV populations. This may help with understanding genetic pathways which cause a bicuspid aortic valve. It may also give further insight into disease progression of aortic stenosis, and identify genetic pre-disposition for early development of stenosis in childhood and early adulthood. Further development of this consortium will also include multi-centre imaging studies such as longitudinal assessment of patients with the very rare left-handed helical flow in a larger international cohort to delineate whether this is indeed a high risk group for rapid aortic growth.

REFERENCES

(1) Ward C. Clinical significance of the bicuspid aortic valve. Heart 2000 Jan;83(1):81-85.

(2) Fernandez B, Duran AC, Fernandez-Gallego T, Fernandez MC, Such M, Arque JM, et al. Bicuspid aortic valves with different spatial orientations of the leaflets are distinct etiological entities. J Am Coll Cardiol 2009 Dec 8;54(24):2312-2318.

(3) Michelena HI, Desjardins VA, Avierinos JF, Russo A, Nkomo VT, Sundt TM, et al. Natural history of asymptomatic patients with normally functioning or minimally dysfunctional bicuspid aortic valve in the community. Circulation 2008 May 27;117(21):2776-2784.

(4) Siu SC, Silversides CK. Bicuspid aortic valve disease. J Am Coll Cardiol 2010 Jun 22;55(25):2789-2800.

(5) Mahle WT, Sutherland JL, Frias PA. Outcome of isolated bicuspid aortic valve in childhood. J Pediatr 2010 Sep;157(3):445-449.

(6) Cripe L, Andelfinger G, Martin LJ, Shooner K, Benson DW. Bicuspid aortic valve is heritable. J Am Coll Cardiol 2004 Jul 7;44(1):138-143.

(7) Calloway TJ, Martin LJ, Zhang X, Tandon A, Benson DW, Hinton RB. Risk factors for aortic valve disease in bicuspid aortic valve: A family-based study. Am J Med Genet A 2011 May;155(5):1015-1020.

(8) Biner S, Rafique AM, Ray I, Cuk O, Siegel RJ, Tolstrup K. Aortopathy is prevalent in relatives of bicuspid aortic valve patients. J Am Coll Cardiol 2009 Jun 16;53(24):2288-2295.

(9) Hales AR, Mahle WT. Echocardiography screening of siblings of children with bicuspid aortic valve. Pediatrics 2014 May;133(5):e1212-7.

(10) Prakash SK, Bosse Y, Muehlschlegel JD, Michelena HI, Limongelli G, Della Corte A, et al. A roadmap to investigate the genetic basis of bicuspid aortic valve and its complications: insights from the International BAVCon (Bicuspid Aortic Valve Consortium). J Am Coll Cardiol 2014 Aug 26;64(8):832-839.

(11) Nishimura RA, Otto CM, Bonow RO, Carabello BA, Erwin JP,3rd, Guyton RA, et al. 2014 AHA/ACC guideline for the management of patients with valvular heart disease: a report of the American College of Cardiology/American Heart Association Task Force on Practice Guidelines. J Thorac Cardiovasc Surg 2014 Jul;148(1):e1-e132.

(12) Beaton AZ, Nguyen T, Lai WW, Chatterjee S, Ramaswamy P, Lytrivi ID, et al. Relation of coarctation of the aorta to the occurrence of ascending aortic dilation in children and young adults with bicuspid aortic valves. Am J Cardiol 2009 Jan 15;103(2):266-270.

(13) Della Corte A, Bancone C, Buonocore M, Dialetto G, Covino FE, Manduca S, et al. Pattern of ascending aortic dimensions predicts the growth rate of the aorta in patients with bicuspid aortic valve. JACC Cardiovasc Imaging 2013 Dec;6(12):1301-1310.

(14) Della Corte A, Bancone C, Quarto C, Dialetto G, Covino FE, Scardone M, et al. Predictors of ascending aortic dilatation with bicuspid aortic valve: a wide spectrum of disease expression. Eur J Cardiothorac Surg 2007 Mar;31(3):397-404; discussion 404-5.

(15) Fernandes SM, Khairy P, Sanders SP, Colan SD. Bicuspid aortic valve morphology and interventions in the young. J Am Coll Cardiol 2007 Jun 5;49(22):2211-2214.

(16) Fernandes SM, Sanders SP, Khairy P, Jenkins KJ, Gauvreau K, Lang P, et al. Morphology of bicuspid aortic valve in children and adolescents. J Am Coll Cardiol 2004 Oct 19;44(8):1648-1651.

(17) Sievers HH, Schmidtke C. A classification system for the bicuspid aortic valve from 304 surgical specimens. J Thorac Cardiovasc Surg 2007 May;133(5):1226-1233.

(18) Larson EW, Edwards WD. Risk factors for aortic dissection: a necropsy study of 161 cases. Am J Cardiol 1984 Mar 1;53(6):849-855.

(19) Braverman AC. Aortic involvement in patients with a bicuspid aortic valve. Heart 2011 Mar;97(6):506-513.

(20) Hahn RT, Roman MJ, Mogtader AH, Devereux RB. Association of aortic dilation with regurgitant, stenotic and functionally normal bicuspid aortic valves. J Am Coll Cardiol 1992 Feb;19(2):283-288.

(21) Yasuda H, Nakatani S, Stugaard M, Tsujita-Kuroda Y, Bando K, Kobayashi J, et al. Failure to prevent progressive dilation of ascending aorta by aortic valve replacement in

patients with bicuspid aortic valve: comparison with tricuspid aortic valve. Circulation 2003 Sep 9;108 Suppl 1:II291-4.

(22) Tzemos N, Lyseggen E, Silversides C, Jamorski M, Tong JH, Harvey P, et al. Endothelial function, carotid-femoral stiffness, and plasma matrix metalloproteinase-2 in men with bicuspid aortic valve and dilated aorta. J Am Coll Cardiol 2010 Feb 16;55(7):660-668.

(23) Donato Aquaro G, Ait-Ali L, Basso ML, Lombardi M, Pingitore A, Festa P. Elastic properties of aortic wall in patients with bicuspid aortic valve by magnetic resonance imaging. Am J Cardiol 2011 Jul 1;108(1):81-87.

(24) Grotenhuis HB, Ottenkamp J, Westenberg JJ, Bax JJ, Kroft LJ, de Roos A. Reduced aortic elasticity and dilatation are associated with aortic regurgitation and left ventricular hypertrophy in nonstenotic bicuspid aortic valve patients. J Am Coll Cardiol 2007 Apr 17;49(15):1660-1665.

(25) Fedak PW, Verma S, David TE, Leask RL, Weisel RD, Butany J. Clinical and pathophysiological implications of a bicuspid aortic valve. Circulation 2002 Aug 20;106(8):900-904.

(26) Fedak PW, de Sa MP, Verma S, Nili N, Kazemian P, Butany J, et al. Vascular matrix remodeling in patients with bicuspid aortic valve malformations: implications for aortic dilatation. J Thorac Cardiovasc Surg 2003 Sep;126(3):797-806.

(27) LeMaire SA, Wang X, Wilks JA, Carter SA, Wen S, Won T, et al. Matrix metalloproteinases in ascending aortic aneurysms: bicuspid versus trileaflet aortic valves. J Surg Res 2005 Jan;123(1):40-48.

(28) Wilton E, Bland M, Thompson M, Jahangiri M. Matrix metalloproteinase expression in the ascending aorta and aortic valve. Interact Cardiovasc Thorac Surg 2008 Feb;7(1):37-40.

(29) Phillippi JA, Klyachko EA, Kenny JP,4th, Eskay MA, Gorman RC, Gleason TG. Basal and oxidative stress-induced expression of metallothionein is decreased in ascending aortic aneurysms of bicuspid aortic valve patients. Circulation 2009 May 12;119(18):2498-2506.

(30) Hiratzka LF, Bakris GL, Beckman JA, Bersin RM, Carr VF, Casey D,Jr, et al. 2010 ACCF/AHA/AATS/ACR/ASA/SCA/SCAI/SIR/STS/SVM Guidelines for the Diagnosis and Management of Patients with Thoracic Aortic Disease. J Am Coll Cardiol 2010 Apr 6;55(14):e27-e129.

(31) Robicsek F, Thubrikar MJ, Cook JW, Fowler B. The congenitally bicuspid aortic valve: how does it function? Why does it fail? Ann Thorac Surg 2004 Jan;77(1):177-185.

(32) Markl M, Harloff A, Bley TA, Zaitsev M, Jung B, Weigang E, et al. Time-resolved 3D MR velocity mapping at 3T: improved navigator-gated assessment of vascular anatomy and blood flow. J Magn Reson Imaging 2007 Apr;25(4):824-831.

(33) Hope MD, Hope TA, Meadows AK, Ordovas KG, Urbania TH, Alley MT, et al. Bicuspid aortic valve: four-dimensional MR evaluation of ascending aortic systolic flow patterns. Radiology 2010 Apr;255(1):53-61.

(34) Davies PF. Hemodynamic shear stress and the endothelium in cardiovascular pathophysiology. Nat Clin Pract Cardiovasc Med 2009 Jan;6(1):16-26.

(35) Hayashi K, Naiki T. Adaptation and remodeling of vascular wall; biomechanical response to hypertension. J Mech Behav Biomed Mater 2009 Jan;2(1):3-19.

(36) Lehoux S, Tedgui A. Cellular mechanics and gene expression in blood vessels. J Biomech 2003 May;36(5):631-643.

(37) Caro CG. Discovery of the role of wall shear in atherosclerosis. Arterioscler Thromb Vasc Biol 2009 Feb;29(2):158-161.

(38) Harloff A, Strecker C, Frydrychowicz AP, Dudler P, Hetzel A, Geibel A, et al. Plaques in the descending aorta: a new risk factor for stroke? Visualization of potential embolization pathways by 4D MRI. J Magn Reson Imaging 2007 Dec;26(6):1651-1655.

(39) Harloff A, Nussbaumer A, Bauer S, Stalder AF, Frydrychowicz A, Weiller C, et al. In vivo assessment of wall shear stress in the atherosclerotic aorta using flow-sensitive 4D MRI. Magn Reson Med 2010 Jun;63(6):1529-1536.

(40) Stalder AF, Russe MF, Frydrychowicz A, Bock J, Hennig J, Markl M. Quantitative 2D and 3D phase contrast MRI: optimized analysis of blood flow and vessel wall parameters. Magn Reson Med 2008 Nov;60(5):1218-1231.

(41) Van der Velden P, Sallee D, Zaaijer E, Parks WJ, Ramamurthy S, Robbie TQ, et al. Systolic flow jet angle is an indicator of aortic dilatation for patients with bicuspid aortic valves. J Cardiovasc Magn Reson 2008;10(Suppl I):A180.

(42) Myerson SG. Valvular and hemodynamic assessment with CMR. Heart Fail Clin 2009 Jul;5(3):389-400, vi-vii.

(43) Frydrychowicz A, Arnold R, Hirtler D, Schlensak C, Stalder AF, Hennig J, et al. Multidirectional flow analysis by cardiovascular magnetic resonance in aneurysm development following repair of aortic coarctation. J Cardiovasc Magn Reson 2008 Jun 8;10(1):30.

(44) Frydrychowicz A, Bley TA, Dittrich S, Hennig J, Langer M, Markl M. Visualization of vascular hemodynamics in a case of a large patent ductus arteriosus using flow sensitive 3D CMR at 3T. J Cardiovasc Magn Reson 2007;9(3):585-587.

(45) Frydrychowicz A, Bley TA, Winterer JT, Harloff A, Langer M, Hennig J, et al. Accelerated time-resolved 3D contrast-enhanced MR angiography at 3T: clinical experience in 31 patients. MAGMA 2006 Sep;19(4):187-195.

(46) Frydrychowicz A, Harloff A, Jung B, Zaitsev M, Weigang E, Bley TA, et al. Time-resolved, 3-dimensional magnetic resonance flow analysis at 3 T: visualization of normal and pathological aortic vascular hemodynamics. J Comput Assist Tomogr 2007 Jan-Feb;31(1):9-15.

(47) Frydrychowicz A, Markl M, Harloff A, Stalder AF, Bock J, Bley TA, et al. Flow-sensitive in-vivo 4D MR imaging at 3T for the analysis of aortic hemodynamics and derived vessel wall parameters. Rofo 2007 May;179(5):463-472.

(48) Frydrychowicz A, Schlensak C, Stalder A, Russe M, Siepe M, Beyersdorf F, et al. Ascending-descending aortic bypass surgery in aortic arch coarctation: four-dimensional magnetic resonance flow analysis. J Thorac Cardiovasc Surg 2007 Jan;133(1):260-262.

(49) Frydrychowicz A, Stalder AF, Russe MF, Bock J, Bauer S, Harloff A, et al. Three-dimensional analysis of segmental wall shear stress in the aorta by flow-sensitive four-dimensional-MRI. J Magn Reson Imaging 2009 Jul;30(1):77-84.

(50) Frydrychowicz A, Weigang E, Harloff A, Beyersdorf F, Hennig J, Langer M, et al. Images in cardiovascular medicine. Time-resolved 3-dimensional magnetic resonance velocity mapping at 3 T reveals drastic changes in flow patterns in a partially thrombosed aortic arch. Circulation 2006 Mar 21;113(11):e460-1.

(51) Frydrychowicz A, Weigang E, Langer M, Markl M. Flow-sensitive 3D magnetic resonance imaging reveals complex blood flow alterations in aortic Dacron graft repair. Interact Cardiovasc Thorac Surg 2006 Aug;5(4):340-342.

(52) Markl M, Draney MT, Miller DC, Levin JM, Williamson EE, Pelc NJ, et al. Time-resolved three-dimensional magnetic resonance velocity mapping of aortic flow in healthy volunteers and patients after valve-sparing aortic root replacement. J Thorac Cardiovasc Surg 2005 Aug;130(2):456-463.

(53) Markl M, Harloff A, Foll D, Langer M, Hennig J, Frydrychowicz A. Sclerotic aortic valve: flow-sensitive 4-dimensional magnetic resonance imaging reveals 3 distinct flow-pattern changes. Circulation 2007 Sep 4;116(10):e336-7.

(54) Markl M, Schumacher R, Kuffer J, Bley TA, Hennig J. Rapid vessel prototyping: vascular modeling using 3t magnetic resonance angiography and rapid prototyping technology. MAGMA 2005 Dec;18(6):288-292.

(55) Hope TA, Markl M, Wigstrom L, Alley MT, Miller DC, Herfkens RJ. Comparison of flow patterns in ascending aortic aneurysms and volunteers using four-dimensional magnetic resonance velocity mapping. J Magn Reson Imaging 2007 Dec;26(6):1471-1479.

(56) Nistri S, Grande-Allen J, Noale M, Basso C, Siviero P, Maggi S, et al. Aortic elasticity and size in bicuspid aortic valve syndrome. Eur Heart J 2008 Feb;29(4):472-479.

(57) Buchner S, Hulsmann M, Poschenrieder F, Hamer OW, Fellner C, Kobuch R, et al. Variable phenotypes of bicuspid aortic valve disease: classification by cardiovascular magnetic resonance. Heart 2010 Aug;96(15):1233-1240.

(58) Burman ED, Keegan J, Kilner PJ. Aortic root measurement by cardiovascular magnetic resonance: specification of planes and lines of measurement and corresponding normal values. Circ Cardiovasc Imaging 2008 Sep;1(2):104-113.

(59) Haycock GB, Schwartz GJ, Wisotsky DH. Geometric method for measuring body surface area: a height-weight formula validated in infants, children, and adults. J Pediatr 1978 Jul;93(1):62-66.

(60) Pucci G, Cheriyan J, Hubsch A, Hickson SS, Gajendragadkar PR, Watson T, et al. Evaluation of the Vicorder, a novel cuff-based device for the noninvasive estimation of central blood pressure. J Hypertens 2013 Jan;31(1):77-85.

(61) Jackson CE, Shirodaria CC, Lee JM, Francis JM, Choudhury RP, Channon KM, et al. Reproducibility and accuracy of automated measurement for dynamic arterial lumen area by cardiovascular magnetic resonance. Int J Cardiovasc Imaging 2009 Dec;25(8):797-808.

(62) Kass M, Witkin A, Terzopoulos D. **Snakes: Active contour models**. Int J Comput Vision 1988;1(4):321-331.

(63) Herment A, Kachenoura N, Lefort M, Bensalah M, Dogui A, Frouin F, et al. Automated segmentation of the aorta from phase contrast MR images: validation against expert tracing in healthy volunteers and in patients with a dilated aorta. J Magn Reson Imaging 2010 Apr;31(4):881-888.

(64) Barker AJ, Markl M, Burk J, Lorenz R, Bock J, Bauer S, et al. Bicuspid aortic valve is associated with altered wall shear stress in the ascending aorta. Circ Cardiovasc Imaging 2012 Jul 1;5(4):457-466.

(65) Markl M, Wallis W, Harloff A. Reproducibility of flow and wall shear stress analysis using flow-sensitive four-dimensional MRI. J Magn Reson Imaging 2011 Apr;33(4):988-994.

(66) Lorenz R, Bock J, Barker AJ, von Knobelsdorff-Brenkenhoff F, Wallis W, Korvink JG, et al. 4D flow magnetic resonance imaging in bicuspid aortic valve disease demonstrates altered distribution of aortic blood flow helicity. Magn Reson Med 2013 May 28.

(67) Hess AT, Bissell MM, Glaze SJ, Pitcher A, Myerson SG, Neubauer S, et al. Evaluation of Circulation as a quantifying metric in 4D flow MRI. J Cardiovasc Magn Reson 2013;15(Suppl1):E36.

(68) Farthing S, Peronneau P. Flow in the thoracic aorta. Cardiovasc Res 1979 Nov;13(11):607-620.

(69) Entezari P, Schnell S, Mahadevia R, Rinewalt D, Malaisrie C, McCarthy P, et al. From unicuspid to quadricuspid: The impact of aortic valve morphology on 3D hemodynamics. J Cardiovasc Magn Reson 2013;15(Suppl1):O79.

(70) Sigovan M, Hope MD, Dyverfeldt P, Saloner D. Comparison of four-dimensional flow parameters for quantification of flow eccentricity in the ascending aorta. J Magn Reson Imaging 2011 Nov;34(5):1226-1230.

(71) Della Corte A, Bancone C, Conti CA, Votta E, Redaelli A, Del Viscovo L, et al. Restricted cusp motion in right-left type of bicuspid aortic valves: a new risk marker for aortopathy. J Thorac Cardiovasc Surg 2012 Aug;144(2):360-9, 369.e1.

(72) Burk J, Blanke P, Stankovic Z, Barker A, Russe M, Geiger J, et al. Evaluation of 3D blood flow patterns and wall shear stress in the normal and dilated thoracic aorta using flow-sensitive 4D CMR. J Cardiovasc Magn Reson 2012 Dec 13;14:84-429X-14-84.

(73) Ruddy JM, Jones JA, Stroud RE, Mukherjee R, Spinale FG, Ikonomidis JS. Differential effect of wall tension on matrix metalloproteinase promoter activation in the thoracic aorta. J Surg Res 2010 May 15;160(2):333-339.

(74) Meierhofer C, Schneider EP, Lyko C, Hutter A, Martinoff S, Markl M, et al. Wall shear stress and flow patterns in the ascending aorta in patients with bicuspid aortic valves differ significantly from tricuspid aortic valves: a prospective study. Eur Heart J Cardiovasc Imaging 2013 Aug;14(8):797-804.

(75) Geiger J, Arnold R, Herzer L, Hirtler D, Stankovic Z, Russe M, et al. Aortic wall shear stress in Marfan syndrome. Magn Reson Med Epub Nov 20th 2012 Nov 20;doi: 10.1002/mrm.24562.

(76) Hope MD, Wrenn J, Sigovan M, Foster E, Tseng EE, Saloner D. Imaging biomarkers of aortic disease: increased growth rates with eccentric systolic flow. J Am Coll Cardiol 2012 Jul 24;60(4):356-357.

(77) Yap SC, Nemes A, Meijboom FJ, Galema TW, Geleijnse ML, ten Cate FJ, et al. Abnormal aortic elastic properties in adults with congenital valvular aortic stenosis. Int J Cardiol 2008 Aug 29;128(3):336-341.

(78) Bilen E, Akcay M, Bayram NA, Kocak U, Kurt M, Tanboga IH, et al. Aortic elastic properties and left ventricular diastolic function in patients with isolated bicuspid aortic valve. J Heart Valve Dis 2012 Mar;21(2):189-194.

(79) Oulego-Erroz I, Alonso-Quintela P, Mora-Matilla M, Gautreaux Minaya S, Lapena-Lopez de Armentia S. Ascending aorta elasticity in children with isolated bicuspid aortic valve. Int J Cardiol Epub Dec 8th 2012;doi: 10.1016/j.ijcard.2012.11.080.

(80) Santarpia G, Scognamiglio G, Di Salvo G, D'Alto M, Sarubbi B, Romeo E, et al. Aortic and left ventricular remodeling in patients with bicuspid aortic valve without significant valvular dysfunction: a prospective study. Int J Cardiol 2012 Jul 26;158(3):347-352.

(81) Girdauskas E, Borger MA, Secknus MA, Girdauskas G, Kuntze T. Is aortopathy in bicuspid aortic valve disease a congenital defect or a result of abnormal hemodynamics? A critical reappraisal of a one-sided argument. Eur J Cardiothorac Surg 2011 Jun;39(6):809-814.

(82) Cohoon KP, Foley J, Dieter RS, Bakhos M, Schwartz J. The development of ascending aortic aneurysms after elective aortic valve replacement with St Jude mechanical valve prosthesis in the bicuspid patient: a pilot study. Angiology 2013 Jul;64(5):379-384.

(83) Girdauskas E, Disha K, Secknus M, Borger M, Kuntze T. Increased risk of late aortic events after isolated aortic valve replacement in patients with bicuspid aortic valve insufficiency versus stenosis. J Cardiovasc Surg (Torino) 2013 Oct;54(5):653-659.

(84) Girdauskas E, Disha K, Borger MA, Kuntze T. Long-term prognosis of ascending aortic aneurysm after aortic valve replacement for bicuspid versus tricuspid aortic valve stenosis. J Thorac Cardiovasc Surg 2014 Jan;147(1):276-282.

(85) Kim YG, Sun BJ, Park GM, Han S, Kim DH, Song JM, et al. Aortopathy and bicuspid aortic valve: haemodynamic burden is main contributor to aortic dilatation. Heart 2012 Dec;98(24):1822-1827.

(86) McKellar SH, Michelena HI, Li Z, Schaff HV, Sundt TM,3rd. Long-term risk of aortic events following aortic valve replacement in patients with bicuspid aortic valves. Am J Cardiol 2010 Dec 1;106(11):1626-1633.

(87) Charitos EI, Stierle U, Petersen M, Mohamed SA, Hanke T, Schmidtke C, et al. The fate of the bicuspid valve aortopathy after aortic valve replacement. Eur J Cardiothorac Surg 2014 Jan 30.

(88) Abdulkareem N, Soppa G, Jones S, Valencia O, Smelt J, Jahangiri M. Dilatation of the remaining aorta after aortic valve or aortic root replacement in patients with bicuspid aortic valve: a 5-year follow-up. Ann Thorac Surg 2013 Jul;96(1):43-49.

(89) von Knobelsdorff-Brenkenhoff F, Trauzeddel RF, Barker AJ, Gruettner H, Markl M, Schulz-Menger J. Blood flow characteristics in the ascending aorta after aortic valve replacement--a pilot study using 4D-flow MRI. Int J Cardiol 2014 Jan 1;170(3):426-433.

(90) Lu MT, Thadani SR, Hope MD. Quantitative Assessment of Asymmetric Aortic Dilation with Valve-related Aortic Disease. Acad Radiol 2013 Jan;20(1):10-15.

(91) Semaan E, Markl M, Malaisrie SC, Barker A, Allen B, McCarthy P, et al. Haemodynamic outcome at four-dimensional flow magnetic resonance imaging following valve-sparing aortic root replacement with tricuspid and bicuspid valve morphology. Eur J Cardiothorac Surg 2014 May;45(5):818-825.

(92) Stephens EH, Hope TA, Kari FA, Kvitting JP, Liang DH, Herfkens RJ, et al. Greater asymmetric wall shear stress in Sievers' type 1/LR compared with 0/LAT bicuspid

aortic valves after valve-sparing aortic root replacement. J Thorac Cardiovasc Surg 2015 Jul;150(1):59-68.

(93) Loscalzo ML, Goh DL, Loeys B, Kent KC, Spevak PJ, Dietz HC. Familial thoracic aortic dilation and bicommissural aortic valve: a prospective analysis of natural history and inheritance. Am J Med Genet A 2007 Sep 1;143A(17):1960-1967.

(94) Robledo-Carmona J, Rodriguez-Bailon I, Carrasco-Chinchilla F, Fernandez B, Jimenez-Navarro M, Porras-Martin C, et al. Hereditary patterns of bicuspid aortic valve in a hundred families. Int J Cardiol 2013 Oct 9;168(4):3443-3449.

(95) Krishnamurthy VK, Godby RC, Liu GR, Smith JM, Hiratzka LF, Narmoneva DA, et al. Review of molecular and mechanical interactions in the aortic valve and aorta: implications for the shared pathogenesis of aortic valve disease and aortopathy. J Cardiovasc Transl Res 2014 Dec;7(9):823-846.

(96) Dayan V, Parma G, Drever M, Straneo P, Soca G, Cura L, et al. First-degree relatives of bicuspid aortic valve patients with normal aortic dimensions do not carry an increased risk of aortic dilatation. Int J Cardiol 2014 Mar 15;172(2):518-519.

(97) Martin LJ, Hinton RB, Zhang X, Cripe LH, Benson DW. Aorta Measurements are Heritable and Influenced by Bicuspid Aortic Valve. Front Genet 2011 Sep 5;2:61.

(98) Erbel R, Aboyans V, Boileau C, Bossone E, Bartolomeo RD, Eggebrecht H, et al. 2014 ESC Guidelines on the diagnosis and treatment of aortic diseases: Document covering acute and chronic aortic diseases of the thoracic and abdominal aorta of the adult.

The Task Force for the Diagnosis and Treatment of Aortic Diseases of the European Society of Cardiology (ESC). Eur Heart J 2014 Nov 1;35(41):2873-2926.

(99) Nethononda RM, Lewandowski AJ, Stewart R, Kylinterias I, Whitworth P, Francis J, et al. Gender specific patterns of age-related decline in aortic stiffness: a cardiovascular magnetic resonance study including normal ranges. J Cardiovasc Magn Reson 2015 Feb 19;17:20-015-0126-0.

(100) Hope MD, Hope TA, Crook SE, Ordovas KG, Urbania TH, Alley MT, et al. 4D flow CMR in assessment of valve-related ascending aortic disease. JACC Cardiovasc Imaging 2011 Jul;4(7):781-787.

(101) Bissell MM, Hess AT, Biasiolli L, Glaze SJ, Loudon M, Pitcher A, et al. Aortic dilation in bicuspid aortic valve disease: flow pattern is a major contributor and differs with valve fusion type. Circ Cardiovasc Imaging 2013 Jul 1;6(4):499-507.

(102) Hope TA, Markl M, Wigstrom L, Alley MT, Miller DC, Herfkens RJ. Comparison of flow patterns in ascending aortic aneurysms and volunteers using four-dimensional magnetic resonance velocity mapping. J Magn Reson Imaging 2007 Dec;26(6):1471-1479.

(103) Hope MD, Sigovan M, Wrenn SJ, Saloner D, Dyverfeldt P. MRI hemodynamic markers of progressive bicuspid aortic valve-related aortic disease. J Magn Reson Imaging 2014 Jul;40(1):140-145.

(104) Guzzardi DG, Barker AJ, van Ooij P, Malaisrie SC, Puthumana JJ, Belke DD, et al. Valve-Related Hemodynamics Mediate Human Bicuspid Aortopathy: Insights From Wall Shear Stress Mapping. J Am Coll Cardiol 2015 Aug 25;66(8):892-900.

(105) Spinale FG, Bolger AF. Fate Versus Flow: Wall Shear Stress in the Aortopathy Associated With Bicuspid Aortic Valves. J Am Coll Cardiol 2015 Aug 25;66(8):901-904.

INDEX OF FIGURES

INDEX OF TABLES